MASTERARBEIT | MASTER'S THESIS

Titel | Title

What controls microbial activity in permafrost soils? Effects of soil organic matter and microbial community composition

verfasst von | submitted by

Cornelia Rottensteiner BSc BA

angestrebter akademischer Grad | in partial fulfilment of the requirements for the degree of

Master of Science (MSc)

Wien | Vienna, 2024

Studienkennzahl lt. Studienblatt | Degree programme code as it appears on the student record sheet:	UA 066 833
Studienrichtung lt. Studienblatt | Degree programme as it appears on the student record sheet:	Masterstudium Ecology and Ecosystems
Betreut von | Supervisor:	Univ.-Prof. Dr. Andreas Richter

Acknowledgements

I dedicate this thesis to ***my parents***, who always believe in me and whose support made this possible. I could have not done it without you. Thanks for trying to understand my research and listening to me talking about cool results or lab problems while understanding very little. Thanks for lifting me up during bad times and cheering for me during good times. I love you.

To ***Vicky***, who convinced me to do my thesis at TER and who was an awesome teacher and friend during this journey. Thank you for always telling me that I could do it.

I would especially like to thank my supervisor ***Andreas Richter***. Although it is a shame we did not get to go to Siberia, like initially planned, I loved working on this project instead. Thank you for providing me with so many great opportunities to learn and teach at TER.

Special thanks to ***Leila***, who became not only a helpful colleague, but also a true friend. Thanks for all the great talks. Your constant motivation got me through this.

Thanks to the pyrolysis team, ***Vicky, Moritz*** and ***Alberto***, for investing three years to develop a really cool new method, and to ***Ludwig***, who conquered all obstacles provided by the pyrolysis autosampler.

Thanks to ***Hannes, Leila*** and ***Joana*** for helping me with sequencing, ddPCR and the analysis of the microbial community data.

Thanks to ***Alberto***, who guided me through the model statistics, and to ***Julia***, who continuously helped me when I first started working with R.

Finally, I want to thank the whole ***TER team*** for your support and making this such a great environment to work and grow as a scientist and as a person.

Table of Contents

GENERAL INTRODUCTION

Permafrost soils

Importance of permafrost in times of global warming

The year 2023 was the warmest year on record with global mean temperature reaching 1.48 °C above pre-industrial baseline average (1850-1900) (Copernicus Climate Change Service, 2024). Global warming is on track to exceed 1.5 °C within this decade and 2 °C before 2050 (Hansen et al., 2022), threatening ecosystem stability and biodiversity, water and food security, and infrastructure and human health, among other things (Lee et al., 2023). Polar regions warm even faster than the global average, a phenomenon called Polar Amplification, caused by sea-ice loss, lower surface albedo, increased water vapor and cloud formation, changes in atmospheric and oceanic heat transport, Planck feedback (radiative response) and lapse-rate feedback (effect of vertical atmospheric temperature profile) (Pithan and Mauritsen, 2014; Goosse et al., 2018). Arctic Amplification was considered to be two to three times greater than the average worldwide temperature increase (Overland et al., 2019; Richter-Menge and Druckenmiller, 2020; Arctic Monitoring and Assessment Programme, 2021). However, a recent study found that the Arctic actually warms four times faster compared to the global average and that climate models generally underestimated Arctic Amplification (Rantanen et al., 2022).

Higher air temperatures cause permafrost to thaw. Permafrost is defined as ground remaining below the freezing point for more than two consecutive years, and is mostly frozen since glaciation in the Pleistocene (thus at least 11,000 yr old) (Muller, 1945). Globally permafrost temperature has increased by 0.29 °C from 2007 to 2016 (Biskaborn et al., 2019). Since 1850 Arctic permafrost has lost about 12 % of area; the continuous permafrost zone even got smaller by 20 %. On average 136 000 km^2 of permafrost area was lost per decade since the 1950s (Langer et al., 2022). According to the latest IPCC report, up to 99 % of permafrost area could be lost by 2100, following the high-emissions scenario (RCP8.5). Even if global warming stays below 2 °C (RCP2.6) a loss of 66 % is to be expected (Meredith et al., 2019).

Arctic lowlands are particularly prone to thawing because of their high ground ice content (Jorgenson and Osterkamp, 2005). Thawing of ice-rich permafrost leads to ground destabilization and subsidence, patterned ground, and thermokarst development, associated with changes in hydrology and biogeochemistry (Olefeldt et al., 2016; Nitzbon et al., 2021). For thousands of years permafrost has acted as a carbon sink as carbon-rich organic matter from decaying plants was preserved in a frozen state and thereby protected from microbial decomposition. With warming and thawing, microbes are now able to take up and decompose this old organic carbon, ultimately releasing part of it in the form of CO_2 or CH_4, thereby turning permafrost to a potential greenhouse gas source (Tornocai et al., 2009; Koven et al., 2011;

MacDougall et al., 2012; Schuur et al., 2015; Natali et al., 2021). According to the IPCC Sixth Assessment Report this permafrost carbon climate feedback will release additional 18 Pg CO_2-C and 2.8 Pg CH_4-C per degree of global warming until 2100 (Canadell et al., 2021).

Carbon losses from permafrost are not necessarily gradual and could intensify after initial lag time. Terrestrial permafrost is predicted to reach an irreversible tipping point at 5 °C of global warming, but cascading effects of other global tipping elements (e.g., ice sheet melt, changes in ocean circulation) could lead permafrost to tip at even lower temperatures (2 °C) (Steffen et al., 2018). According to the Global Tipping Point Report 2023 (Lenton et al., 2023), permafrost is already at risk of crossing an irreversible tipping point at the current level of global warming. Apart from this global impact, permafrost thaw also directly threatens four million people living in the Arctic. Communities and industries likely need to relocate because of permafrost thaw and thermokarst development, which will cause flooding, ground erosion, subsidence and ground collapse. Moreover, indigenous people will be affected by food and water insecurity and health related risks, due to loss of traditional hunting and transportation routes, and contamination of drinking water by changes in hydrology and mercury input from thawed permafrost (Meredith et al., 2019; Ramage et al., 2021).

Permafrost definition and distribution

Permafrost is defined as permanently (perennially) frozen soil, bedrock or deposit whose temperature stays below freezing point for more than two consecutive years. The majority of permafrost is thousands of years old, stemming from glaciations in the Pleistocene (2.58 Myr to 11,000 yr) (Muller, 1945), and has persisted through interglacials. The oldest intact permafrost that was found so far dated to 650 000 to 700 000 years (Froese et al., 2008; Murton et al., 2022). Permafrost can be found in the Arctic (Alaska, Canada, Russia, Svalbard, Iceland, Greenland), the Antarctic, and in high mountainous regions (Scandinavian Mountains, European Alps, Pyrenees, Carpathians, Tatra Mountains, Balkan Mountains, Taurus Mountains, Pontus Mountains, Caucasus Mountains, Elburz Mountain Range, Daisetsuzan Mountains and Mt. Fuji, Himalaya, Tibetan Plateau, Altai Mountains, Tien Shan, Rocky Mountains, Andes, New Zealand Alps, and East African Plateau) (Obu et al., 2019; Dobiński et al., 2023). Additionally, subsea permafrost can be found in polar continental shelfs (Kara Sea, Laptev Sea, Chukchi Sea, Bering Sea, Beaufort Sea, and circum-Antarctic), which developed when sea levels were lower (Osterkamp, 2001; Overduin et al., 2019). Furthermore, Yedoma deposits can be found in Siberia, Alaska and Northwestern Canada. This Pleistocene-age permafrost is characterized by syngenetic ice wedges and well-preserved organic matter accumulation of up to 50 m thickness, that formed through water-related and aeolian processes in a very cold climate (Strauss et al., 2017).

Four zones are commonly differentiated from high to low latitude (or altitude) depending on percentage of land area underlain by permafrost: continuous permafrost (90 - 100 % of the

surface frozen), discontinuous permafrost (50 - 90 %), sporadic permafrost (10 - 50 %), and isolated patches (0 - 10 %) (Muller, 1945; Ferrians, 1965; Brown et al., 1997; Obu et al., 2019) (Fig. 1). All zones together encompass roughly 21 million km^2 of frozen ground worldwide, although not the entire area is underlain by permafrost. Global permafrost area makes up approximately 17 million km^2 (including 2.5 million km^2 circum-Arctic subsea permafrost). Accordingly, 11 % of global land surface area and 15 % of the Northern Hemisphere are underlain by permafrost (Obu, 2021).

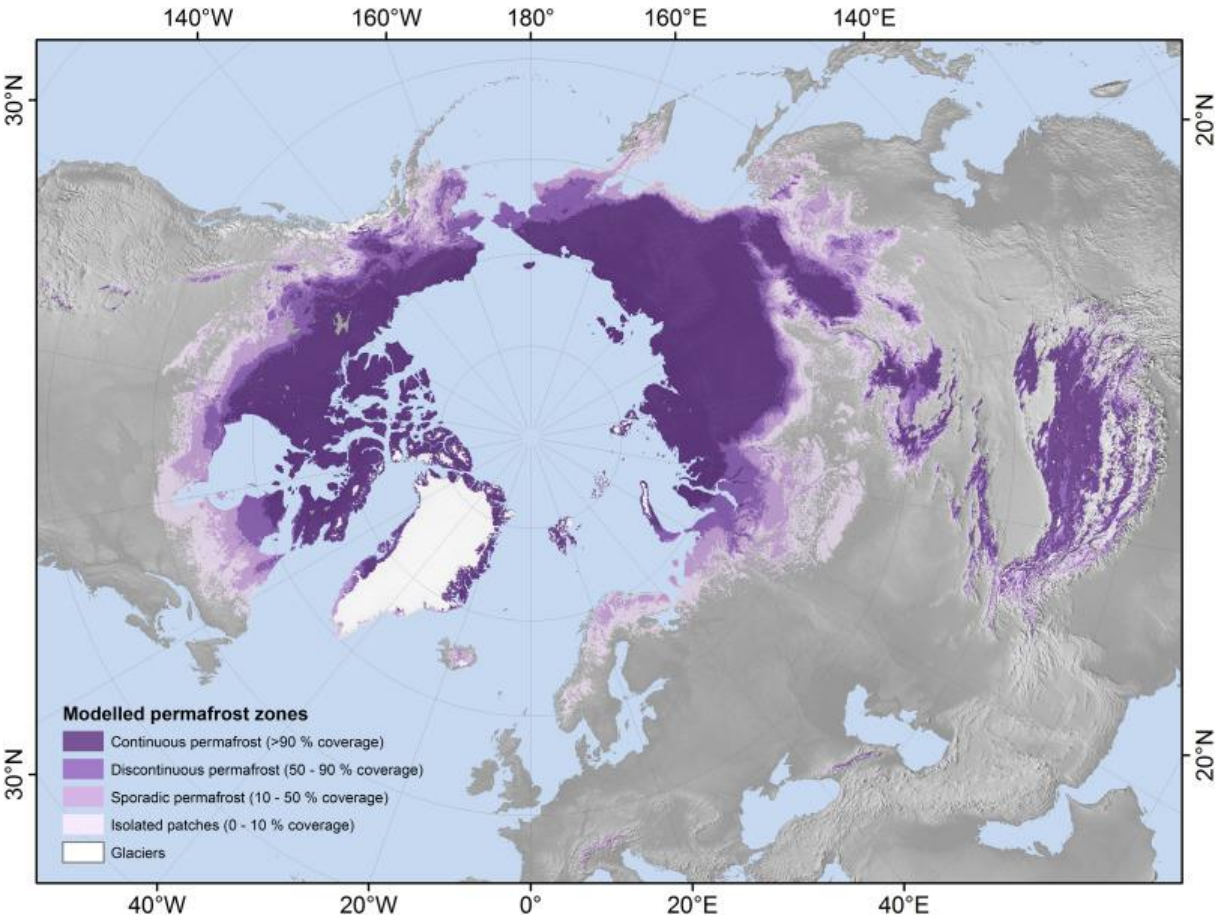

Fig. 1: **Permafrost region and zonation in the Northern Hemisphere.** Data modelled based on permafrost probability calculated as the fraction of model runs with mean annual ground temperature below 0 °C. Coverage (%) corresponds to 1 km^2 pixel underlain by permafrost. Figure from *Obu* et al*., 2019* **CC BY 4.0.**

Carbon storage in permafrost

Over millennia, limited decomposition of plant litter due to low temperatures and poor drainage, as well as repeated alluvial and aeolian deposits have caused the buildup of huge organic carbon stocks within permafrost soils (Davidson and Janssens, 2006; Hugelius et al., 2014). The northern circumpolar permafrost region stores approximately 1,300 (±200) Pg organic carbon. Thereof, 217 (±12) Pg carbon are contained in the first 30 cm depth of soil. 472 (±27) Pg are found up to the first meter and 1,035 (±150) Pg are preserved up to three meters depth. Beneath three meters depth deltaic deposits, Yedoma deposits, and perennially frozen thermokarst basin deposits are estimated to store 91 (±52), 74 (±20), and

107 (±50) Pg carbon, respectively. 63 % of the total permafrost carbon stocks (822 Pg) are perennially frozen and 37 % (485 Pg) thaw seasonally in the active layer or deeper taliks (Hugelius et al., 2014). A previous study had estimated larger carbon stocks of 1,672 Pg for the total northern permafrost region, with 88 % (1,466 Pg) being perennially frozen, and predicted 407 Pg for Yedoma deposits and 241 Pg for deltaic deposits (Tornocai et al., 2009). New estimates propose even up to 466 Pg carbon for the total Yedoma domain (Strauss et al., 2017). The IPCC (Meredith et al., 2019) states the current best estimate for terrestrial permafrost soil organic carbon stocks in the northern circumpolar region is 1,460 – 1,600 Pg C (Schuur et al., 2018). However, this does not include carbon storage in subsea or mountain permafrost. Subsea permafrost is estimated to contain approximately 560 Pg carbon in organic matter and additional 45 Pg CH_4 deposits (Sayedi et al., 2020). A recent modelling study predicted even 2,822 Pg of subsea permafrost carbon (Miesner et al., 2023). The global mountain permafrost region was estimated to hold 66.3 Pg organic carbon (Bockheim and Munroe, 2014). Though another study found that the Tibetan permafrost region alone holds 36.6 Pg carbon and states that ecosystem models had so far underestimated alpine permafrost soil organic carbon stocks (Ding et al., 2019). Nonetheless, circumarctic permafrost soils alone store more soil organic carbon than the atmosphere and about the same amount as tropical soils. When comparing to the sum of soil organic carbon within the first three meters of soil depth, permafrost alone makes up a third of global soil carbon storage (Fig. 2).

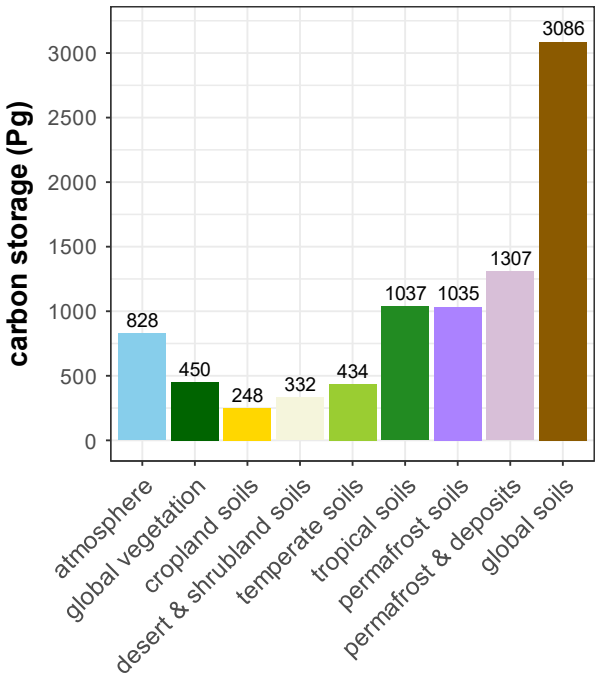

Fig. 2: **Comparison of global carbon stocks (Pg C).** Carbon stored in the atmosphere (Ciais *et al.*, 2013) and in global vegetation biomass (Erb *et al.*, 2018). Non-permafrost soil carbon stocks of 0 to 3 m depth: cropland soils, desert and sclerophyllous shrubland soils, temperate soils (grassland, deciduous & evergreen forests) and tropical soils (grasslands/savannah, deciduous & evergreen forests) based on Jobbagy and Jackson, 2000. Circumarctic permafrost soil carbon stocks for 0 to 3 m and with deep deposits (deltaic, thermokarst basins, Yedoma) below 3 m (Hugelius *et al.*, 2014). Here, global soil carbon storage is the sum of non-permafrost and permafrost soil carbon of 0 to 3 m depth.

Permafrost soil profile and cryoturbation

According to the World Soil Reference Base, permafrost- or frost-affected soils are classified as Cryosols. Other common names are Gelisols (USDA Soil Taxonomy) or Cryozems (Russian Soil Classification). They are characterized by a permanently frozen sublayer (permafrost) in the first meter, ice and irregular dynamic horizons. The parent material can be very diverse, including glacial till, aeolian, and alluvial and colluvial deposits (IUSS Working Group WRB, 2014). A major soil-forming process is the increase in soil volume upon freezing. Cryogenic processes also cause thermal cracking, ice segregation, frost heave, cryoturbation and patterned ground (Soil Survey Staff, 1999; IUSS Working Group WRB, 2014). The USDA Soil Taxonomy distinguishes three subtypes: Histels, Turbels, and Orthels. Histels are hydric soils characterized by organic carbon accumulation of greater than 30 %, water saturation and anaerobic conditions. Cryoturbation and distorted horizons are the main features of Turbels. They can also be saturated with water, accumulate organic matter on top of the permafrost and contain ice wedges. Turbels make up about half of global Gelisols. Orthels show no cryoturbation, ice wedges or organic matter accumulation and are generally drier than Turbels and Histels (Soil Survey Staff, 1999).

Permafrost soil is primarily divided into two layers: the upper active layer and the underlying perennially frozen permafrost (denoted Cf with ice or Cff if dry). The active layer consists of an organic horizon (O) and a cambic mineral soil (denoted Bw if weathering is present or Bg with gleying due to poor drainage). Occasionally one can find a humus-rich surface mineral soil (A) (Ping et al., 2015). Additionally, there is cryoturbated material of organic (Ojj) or surface mineral origin (Ajj) within the active layer, that was transported from the surface to deeper layers. The active layer is highly dynamic and thaws seasonally. Thaw depth varies regionally and annually from 15 cm to over 5 m. Active layer thickness is influenced by air temperature, slope orientation, soil type, snow cover, drainage and vegetation. The contact zone between permafrost and active layer is termed transient layer and results from fluctuations of the permafrost table (the top of the permafrost layer) between years. On a decadal to century scale an ice-rich intermediate layer can form from suspended previous surface organic layers due to permafrost aggradation. The transient and intermediate layer together build the uppermost part of the permafrost layer. Underneath, permafrost has remained frozen for centuries or millennia (French and Shur, 2010; Ping et al., 2015) (Fig. 3).

Cryoturbation is a central soil-forming process of permafrost-affected soils and refers to all vertical and lateral material displacements caused by ice segregation, thermal cracking, surface collapse and other frost-related processes. If freezing occurs at the same time downward from the surface and upward from the permafrost table, the layer between is

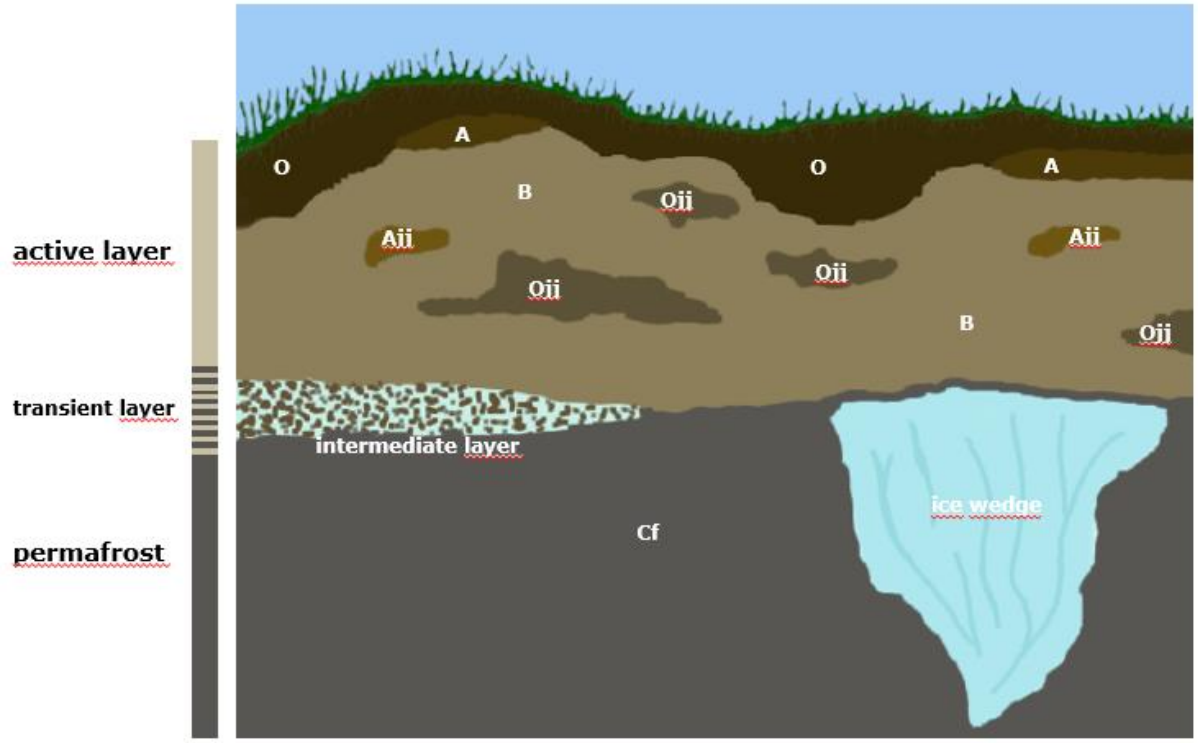

Fig. 3: **Schematic of a permafrost soil profile**. The division into active layer, transient layer and passive permafrost is shown on the left. The depicted permafrost (Cf) has an ice wedge and an intermediate layer. The active layer consists of organic (O), surface mineral (A) and mineral (B) soils. Cryoturbated matter of organic (Ojj) and surface mineral origin (Ajj) are also represented. © Cornelia Rottensteiner

subjected to high, uneven pressure conditions and gets distorted. Moreover, heave and subsidence cause downward and outward movement in the active layer, but upward and inward movement above the permafrost table, leading to a circulation of matter. The process is favored by silty parent material, frequent freeze-thaw cycles, and poor drainage. Cryoturbation causes irregular and broken horizons, bands, involutions, deformed and displaced soil material and organic matter accumulation on top of the permafrost table. This mixing of partially decomposed organic materials from the surface into the subsoil is one of the main reasons for high organic carbon content in permafrost soils (Bockheim and Tarnocai, 1998; Ping et al., 2015). Decomposition is delayed in cryoturbated organic matter, compared to the soil surface, because of unfavorable conditions, such as extended winter freeze, lower summer temperatures and higher soil moisture content. Microbial carbon and nitrogen mineralization rates were found to be considerably reduced (Kaiser et al., 2007) and a functional decoupling of organic matter and microbial community composition could explain persistence of cryoturbated carbon (Schnecker et al., 2014). Moreover, cryoturbation changes microbial community structure (Gittel et al., 2014a), decreases fungal abundance, leading to reduced protein breakdown capacity (Wild et al., 2013), and selects for Actinobacteria (Gittel et al., 2014b) and oligotrophic bacterial taxa that degrade recalcitrant organic matter (Varsadiya et al., 2021). With soil warming and deepening of the active layer cryoturbated organic matter, which is relatively fresh with a large particulate fraction, could become a highly

bioavailable fast-decomposing substrate for microorganisms (Mueller et al., 2015; Beer et al., 2022).

Ground ice, thermokarst and polygonal landscapes

Frozen ground typically contains ice in form of dispersed ground ice crystals, and ice veins, lenses or wedges, which are particularly common in lowlands and valleys due to runoff (Muller, 1945). The thawing of ice-rich permafrost and melting of ground ice leads to collapse of the land surface and characteristic landforms subsumed under the term thermokarst (permafrost degradation). Studies have so far identified 22 thermokarst landforms, for example active layer detachment slides, retrogressive thaw slumps, thermal erosion gullies, thermokarst lakes, bogs, fens, troughs and pits (Kokelj and Jorgenson, 2013). Water-filled pits and troughs are caused by the degradation of ice wedges (Kokelj and Jorgenson, 2013; Nitzbon et al., 2019). Ice wedges form with annual freeze-thaw cycles (French and Shur, 2010) and can account for 10 to 50 % of ground volume (Kanevskiy et al., 2013; Jorgenson et al., 2015, 2022). In brief, extremely low temperatures during winter cause soil to shrink irregularly, inducing stress that exceeds the soils strength to resist deformation, thus causing thermal contraction cracks in the ground. Each year these cracks fill with water in summer and refreeze in winter, which increases pressure and causes even more cracks. Over time, repeated freezing and thawing let small ice veins (less than 0.01 × 1 m) grow into large ice wedges (up to 4 × 50 m) (French and Shur, 2010). Vertical and lateral material displacement cause elevated rims above ice wedges and lowered ground between them, leading to patterned ground surfaces, often in the form of hexagonal polygons (Krantz, 1990; Fritz et al., 2016). These initial stage polygons with intact ice wedges and depressed, often water-logged, centers are termed low-center polygons (Fritz et al., 2016; Liljedahl et al., 2016). Melting of ice wedges, typically induced by active layer deepening and flooding during unusually warm and wet summers (Kanevskiy et al., 2017), leads to a transition in the surface microtopography. During initial ice wedge degradation, ground above ice wedges subsides and meltwater accumulates above the ice wedges forming isolated troughs or channels. At the same time polygon centers get increasingly drained. These flat-center polygons represent an intermediate stage of polygon succession. Continued ice wedge melting causes more meltwater, deeper troughs and a connected trough-network that leads to further drainage. In a late successional stage, the rims above melted ice wedges degrade leading to a topographic inversion of the ground to an elevated center. These landscape features with raised centers are called high-center polygons (Fritz et al., 2016; Liljedahl et al., 2016; Wolter et al., 2018) (Fig. 4). In contrast to this successional evolution of ice wedge polygons, there also exist cyclic frameworks that suggest a dynamic development with stabilization mechanisms and reversibility. In this understanding, topographic, hydrological and vegetational feedbacks can interrupt or reinforce degradation of polygon development (Jorgenson et al., 2015; Kanevskiy et al., 2017; Nitzbon et al., 2019,

2021). For instance, plant growth can reduce radiation and heat transfer and thereby stabilize the surface (Jorgenson et al., 2015) and accumulation of organic matter can form an ice-rich intermediate layer that protects ice wedges from further thaw (Kanevskiy et al., 2017). In fact, Kanevskiy *et al.* (2017) proposed that most ice wedges in the continuous permafrost zone eventually stabilize or even regrow and complete melt is rare. However, ice wedges are highly vulnerable to warming and climate change has already accelerated the rate and magnitude of their degradation (Jorgenson et al., 2006; Kokelj and Jorgenson, 2013; Wolter et al., 2018). Stronger weather extremes, such as intense summer heat and increased winter precipitation, could enhance ice wedge degradation even more (Liljedahl et al., 2016). Even small increases in active layer depth in hot summers are enough to cause ground subsidence of up to 90 cm (Farquharson et al., 2019). From 1950 to 2018 the area of ice wedge degradation increased almost tenfold from 2 % to 19 %. Degradation has also been associated with changes in trough width, water depth, thermal regime, and soil pH (Jorgenson et al., 2022). Transformation from low-center to flat-center and high-center polygons causes shifts in plant community composition (Wolter et al., 2016; Jorgenson et al., 2022) and microbial community composition and was found to change metabolic pathways and greenhouse gas fluxes (Taş et al., 2018).

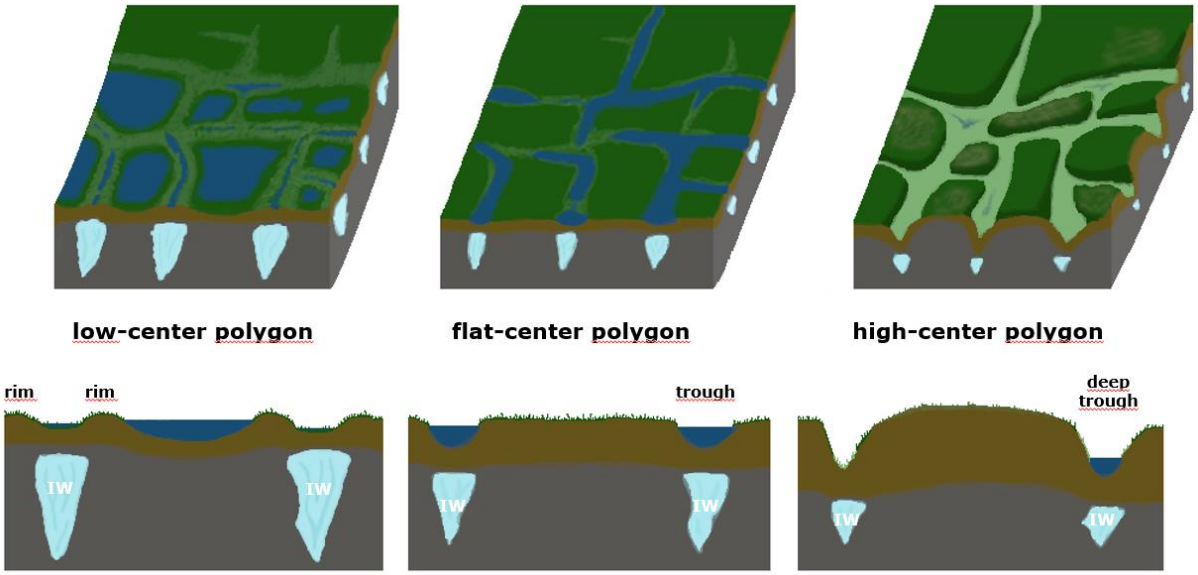

Fig. 4: **Schematic of ice wedge degradation and polygon types.** Increasing ice wedge degradation from left to right: Low-center polygons with intact ice wedges, outer rims and subsided centers, that are commonly water-filled. Flat-center polygons with slightly degraded ice wedges and outer troughs. High-center polygons with largely degraded ice wedges, deep connected and drained troughs and raised dry centers. © Cornelia Rottensteiner

Soil microbial carbon cycling

Microbial decomposition

Heterotrophic microbes are an essential part of the global carbon cycle. Without them, carbon would be drawn from the atmosphere and pile up on Earth's surface through photosynthetic fixation by plants and autotrophic microbes. Decomposition by heterotrophic microbes, and consequently the respiration of carbon to the atmosphere, is therefore crucial to keep the organic carbon cycle running (Crowther et al., 2019). However, microbes can also function as carbon stabilizers, if more carbon is invested into biomass growth than is lost via respiration, because microbial necromass can persist as soil organic matter (Liang et al., 2017; Sokol et al., 2022; Tao et al., 2023). With anthropogenic perturbations of the global carbon cycle through fossil fuel combustion and subsequent rising atmospheric carbon concentrations this microbial function to store carbon in the soil becomes increasingly important.

Heterotrophic microbes require carbon to grow and generate energy. Assimilated carbon is respired as CO_2 (at aerobic conditions) or CH_4 (at anaerobic conditions) to produce ATP or is invested into growth (i.e., cell size or cell division), and enzyme and metabolite production (Manzoni et al., 2012; Soong et al., 2020). In soil, carbon derives primarily from plant inputs via rhizodeposition (i.e., plant exudates) or above- and belowground litter (Gougoulias et al., 2014). Moreover, microbial necromass and remains make up a significant proportion of soil organic matter (Miltner et al., 2012; Liang et al., 2017). While microbes can directly take up small molecules like sugars, amino acids and organic acids, large polymers like cellulose, chitin, and proteins need to be depolymerized outside the cell (Gougoulias et al., 2014). To do this, microbes produce different extracellular enzymes, which hydrolyze or oxidize large organic compounds into their individual components. Multiple enzymes from a diverse microbial community are needed to efficiently decompose soil organic matter (Wallenstein and Weintraub, 2008) (Fig. 5).

Soil organic matter

Soil organic matter (SOM) is a "complex mixture of plant and microbial residues at various stages of decay" (Miltner et al., 2012). Plant litter contributes to the formation of soil organic matter from decaying plants and root turnover. Litter is either physically fragmented into smaller particles that form particulate organic matter (POM) (Cotrufo et al., 2015), or shredded into smaller particles by soil meso- and macrofauna and distributed through the soil profile. Soil invertebrates also transform litter chemically through ingestion, egestion and excretion (Frouz, 2018). This conversion of detritus to fecal pellets by detritivores was found to accelerate decomposition via increased lability and leaching (Joly et al., 2020). Soluble carbon compounds, i.e., dissolved organic matter (DOM), are leached and transported into the soil by water flow and can, if they are not instantly assimilated, attach to mineral surfaces and form

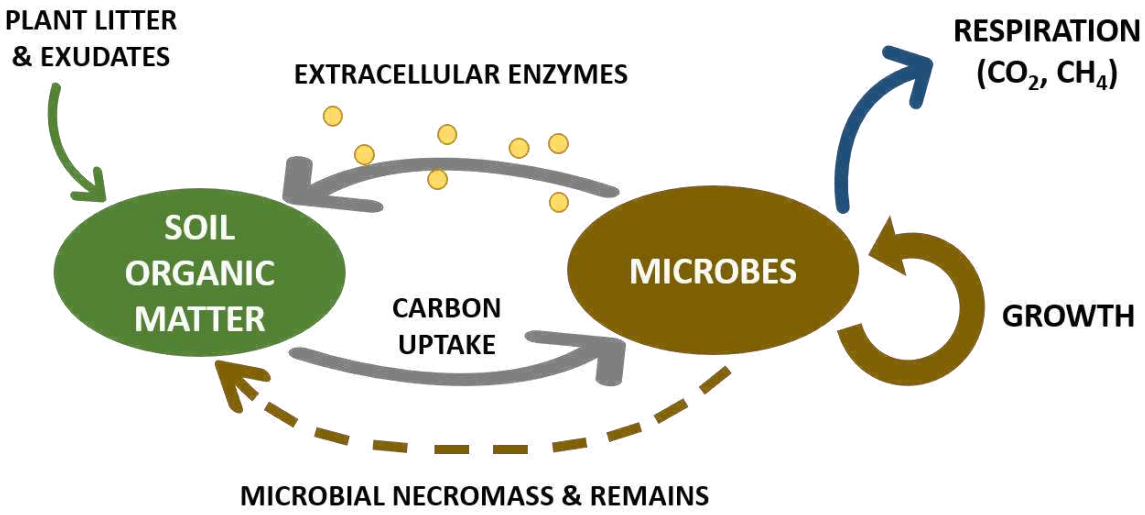

Fig. 5: **Schematic of microbial decomposition.** Soil organic matter derives from plant litter and root exudates. Microbes produce extracellular enzymes that degrade soil organic matter into smaller molecules, which can be taken up. Assimilated carbon is allocated to growth, enzyme production and respiration. When microbes die their necromass and remains contribute to soil organic matter formation. © Cornelia Rottensteiner

mineral associated organic matter (MAOM) (Cotrufo et al., 2015). Additionally, plant roots exude carbon-rich compounds (e.g., sugars, amino acids, organic acids) into the soil. These labile carbon inputs have been shown to stimulate overall decomposition of solid SOM and increase respiration rates, a process termed rhizosphere priming (Jones et al., 2009; Canarini et al., 2019; Keuper et al., 2020). Furthermore, microbes transform plant-derived carbon into biomass and their necromass contributes significantly to soil organic matter formation (Miltner et al., 2012). Adapting the concept from marine sciences, this transformation of bioavailable carbon to a persistent carbon pool via microbial biomass was termed soil microbial carbon pump (Liang, 2020). It was shown that across ecosystems on average 30 to 60 % of soil organic carbon can be derived from microbial necromass (Liang et al., 2019). To a minor extent, SOM also consists of extracellular microbial material, e.g., exuded metabolites or enzymes, or extracellular polymeric substances (EPS) (Kögel-Knabner, 2017).

Soil organic matter composition is, amongst others, influenced by soil depth (i.e., soil age), geochemistry (Rumpel and Kögel-Knabner, 2011; Mainka et al., 2022), water status (Védère et al., 2022), and vegetation and land-use type (Quideau et al., 2001; El Moujahid et al., 2017; Thai et al., 2021). Recent evidence also suggests that distinct bacterial communities form different chemical compositions of SOM (Domeignoz-Horta et al., 2021). Soil organic matter consists of various compound classes. The major compounds of plant litter are polysaccharides (cellulose, hemicellulose, pectin, starch), lignin, polyphenols, cutin, suberin, lipids, and proteins. While polysaccharides are easily degraded by microorganisms, lignin is a high molecular weight macromolecule, specific to higher plants, that is fairly resistant to decomposition and cannot be fully degraded under anoxic conditions. Chitin is the major structural component of fungi, but can also stem from insect remains. Fungal residues also

include polysaccharides, proteins, lipids, melanins, and tannins. The main component of bacterial necromass is peptidoglycan (murein), which consists of glucosamine, muramic acid, and amino acids. Yet, bacteria also contain lipids and proteins (Kögel-Knabner, 2002).

Two common methods to assess soil organic matter composition at different levels of resolution are nuclear magnetic resonance (NMR) spectroscopy and pyrolysis gas chromatography mass spectrometry (pyr-GC-MS) (Kögel-Knabner, 2002). Solid-state ^{13}C NMR reveals structural composition, but major drawbacks are its low sensitivity and low spectral resolution. Additionally, NMR requires the reduction or removal of paramagnetic material, such as Fe, usually by treatment with hydrofluoric acid (Schmidt et al., 1997). Solution-state ^{1}H NMR is able to capture distinct microbial- and plant-derived compounds, but is limited to soluble or extracted organic matter. In contrast, GC-MS is more sensitive and facilitates precise separation and quantification of compounds (Simpson and Simpson, 2012). Pyrolysis-GC-MS allows to analyze a number of different compounds, that are typically classified into the following compound classes: aromatics, carbohydrates, lignins, lipids, nitrogen-containing compounds and phenols (Vancampenhout et al., 2009). However, pyrolysis-GC-MS typically targets specific biomarkers, while NMR is non-targeted (Simpson and Simpson, 2012).

Soil microbial communities

Soils are the most biodiverse ecosystem, likely being home to 59 % of all species on Earth. About 20 % of archaea, 50 % of bacteria and 90 % of fungi can be found in soils (Anthony et al., 2023). Globally, soils hold 12 Gt carbon of fungal biomass, 7 Gt carbon of bacterial biomass and 0.5 Gt carbon of archaeal biomass (Bar-On et al., 2018). One gram of soil harbors several thousand bacterial species (Delgado-Baquerizo et al., 2018) and hundreds of fungal species (Baldrian et al., 2012; Taylor et al., 2014; Peay et al., 2016). Microorganisms, that is archaea, bacteria, fungi, microalgae, protists, and viruses, live on numerous resources, compete and cooperate with each other, or prey on one another (Weiland-Bräuer, 2021). Soil microbial communities play a crucial role in the biogeochemical cycling of the main elements of life: hydrogen, carbon, nitrogen, oxygen, sulfur and iron (Falkowski et al., 2008). While carbon mineralization is a universal feature of heterotrophic microbes, other functions are only performed by specialist groups in distinct environments (e.g., methanogenic archaea in anaerobic wetlands) (Crowther et al., 2019; Hartmann and Six, 2023). Microbial communities are strongly influenced by climate and edaphic factors, particularly soil pH (Fierer and Jackson, 2006; Rousk et al., 2010; de Vries et al., 2012; Tedersoo et al., 2014), which shapes not only their composition but also their functional potential (Bahram et al., 2018). In turn, it has also been shown that microbes can modify their environment, e.g., changing the pH via proton turnover through biochemical reactions (Ratzke and Gore, 2018). Microbial communities are also closely linked to differences in soil texture (Xia et al., 2020) and plant functional traits (de Vries et al., 2012). Moreover, resource stoichiometry, quality and diversity are important

factors that determine community structure (Chapman and Newman, 2010; Zechmeister-Boltenstern et al., 2015). Microbial richness, diversity, activity and function also vary with soil depth, corresponding to physical and chemical changes across the soil profile (Fierer et al., 2003; Naylor et al., 2022).

Microbial community structure can be analyzed by phospholipid fatty acid (PLFA) profiling, marker gene sequencing, other biomarker approaches, or metagenomics and metatranscriptomics. These methods provide different resolutions of microbial community structure and choosing one of them depends on the research question. However, they can also be complementary (Orwin et al., 2018). PLFA analysis, especially when coupled to stable isotope probing, is a powerful tool to detect shifts in the active community composition. It can also be used to estimate microbial biomass and to assess storage compounds (NLFA), necromass formation (NLFA) and potential markers for environmental stress (GLFA) (Gorka et al., 2023). However, PLFA profiling gives little insight into changes of specific microbial populations (Ramsey et al., 2006) and only performs better than metabarcoding, when differences occur in higher taxonomic groups. In contrast, metabarcoding is the best choice to detect differences on the taxon-level (Orwin et al., 2018) and can be coupled to qPCR or ddPCR (Jian et al., 2020; Alteio et al., 2021). However, metabarcoding is limited to specific marker genes: for example, specific regions of the 16S rRNA gene to target bacteria and archaea, the ITS region to target fungi and the 18S rRNA gene for eukaryotes. While the databases available for the assignment of sequences to taxa are far from being complete, they improve continuously with strong increases in available sequences. Fungal classification is particularly challenging, because of the high variability of the ITS region (George et al., 2019; Pérez-Cobas et al., 2020). Metagenomics offers an untargeted approach, that covers the entire genetic diversity in a sample. It obtains whole-genome sequences and informs not only on the taxonomic composition, but also on the functional potential (Pérez-Cobas et al., 2020). However, it is very cost and labor intensive, and depends on sequence availability in databases.

Microbial growth, respiration, and carbon use efficiency

Microorganisms drive both soil organic carbon formation and carbon losses through two processes: growth and respiration. As previously described, respiration of CO_2 leads to carbon losses from the soil to the atmosphere, while newly produced biomass (i.e., growth) and subsequent necromass formation upon the death of microbes, can lead to new soil organic matter formation. The efficiency by which organic carbon taken up is converted into new biomass is termed carbon use efficiency (CUE). It is defined as the amount of newly produced bacterial biomass (growth) per unit of consumed organic carbon (uptake), which is operationally often defined as the sum of growth and respiration (del Giorgio and Cole, 1998; Manzoni et al., 2012; Sinsabaugh et al., 2013). Accordingly, high CUE indicates efficient growth, while low CUE indicates inefficient growth and larger carbon losses through respiration.

The allocation of carbon to microbial growth or respiration depends on temperature (activation energy and metabolic rate), water availability (accessibility, osmotic adjustment, and oxygen availability), substrate quality (degree of reduction, size and regularity of substrates), nutrient limitation (stoichiometric imbalances) and microbial community composition and ecology (fungi-bacteria-ratio, growth strategies, predation) (del Giorgio and Cole, 1998; Manzoni et al., 2012; Mooshammer et al., 2014). Positive and negative effects of biotic interactions (competition, facilitation, mutualism, predation) on carbon use efficiency have been thoroughly discussed in Iven et al. (2023). Microbial biomass, growth, respiration, and carbon use efficiency show high variability throughout the year (Schnecker et al., 2023) and season was even the best predictor for microbial activity in a climate change experiment (Simon et al., 2020). Growth of heterotrophic microbes is ultimately limited by the availability of carbon (Soong et al., 2020). Given the decline in carbon content from topsoil to subsoil, carbon uptake rates decrease with soil depth. However, subsoil microbes can compensate lower carbon uptake by prolonging the turnover time of their biomass (Spohn et al., 2016). Resource quality and stoichiometry have been shown to have species-specific effects on carbon use efficiency and different responses for bacteria and fungi. While bacterial CUE is affected by nitrogen and phosphorus availability, fungal CUE is constrained by carbon (Keiblinger et al., 2010). Microbial growth was also found to be affected by soil pH, with contrasting effects for bacteria and fungi. While bacterial growth decreases with decreasing pH, fungal growth increases (Rousk et al., 2009). Moreover, it must be noted that microbes have different growth strategies (slow-growing degraders and fast-growing opportunists) with differing carbon use efficiencies (Manzoni et al., 2012) that were proposed to be two evolutionary distinct classes for growth optimization (nutrient acquiring copiotrophs vs. cell maintaining oligotrophs) (Weissman et al., 2021). Walkup *et al.* (2023) showed that bacterial growth rates are phylogenetically constraint across ecosystems and suggests that the genetic basis of bacterial growth rate is hereditary. However, Metze et al. (2023, 2024) observed that environment induced changes in bacterial activity is rather driven by shifts in the number, diversity and identity of growing taxa than in their individual growth rates.

Temperature controls microbial physiology and decomposition

Temperature is a major regulator of biochemical processes. Microorganisms and all their functions are completely dependent on the ambient temperature, as they are unable to regulate their intracellular temperature. Microbes can profit from higher temperatures by increasing enzyme rates and subsequently growth, but temperatures above a certain threshold can also cause denaturation and loss of function. Detecting a direct relationship between growth rates and temperature is sometimes challenging. On the one hand because each reaction involved in cellular growth might be differentially affected by temperature (Knapp and Huang, 2022). On the other hand, because microbial growth may not be temperature-limited

after all in soil, as soil microbes are likely more limited by carbon or energy (Soong et al., 2020). The review of Knapp and Huang (2022) provides insights into general principles of the growth-temperature relationship, pointing to temperature-dependencies of enzyme activation energies, processes involved in DNA replication, transcription and translation, membrane fluidity, as well as cellular adaptations, and ecological implications. Many of these processes followed Arrhenius' law and had similar activation energies, which led the authors to conclude that enzyme kinetics influence how temperature affects growth. According to Arrhenius (1889), process rates increase exponentially with increasing temperature, because the activation energy needed to start a reaction decreases. Arrhenius' theory builds upon the van't Hoff equation (van't Hoff, 1884), which describes the relative change of a process rate with a given change in temperature. The temperature coefficient Q_{10} is a widely used parameter in ecology, that expresses the factor by which a process rate increases with a 10 °C temperature rise: $Q_{10} = (R2 / R1) ^ (10 / (T2 – T1))$, where R1 is the measured rate at the first temperature (T1) and R2 is the measured rate at the second temperature (T2). For example, a Q_{10} of 2 translates into the doubling of a process rate with a 10 °C change in temperature (Kirschbaum, 1995).

Global temperatures rise continuously and persistently and have been shown to strongly impact soil microbial processes. Higher temperatures affect enzyme activity (Fanin et al., 2022), microbial activity, biomass, growth and growth strategy, respiration, and carbon use efficiency (Allison et al., 2010; Walker et al., 2018; Soong et al., 2021; Wang et al., 2021; Purcell et al., 2022; Propster et al., 2023), and ultimately decomposition (Kirschbaum, 1995; Fierer et al., 2005; Davidson and Janssens, 2006; Conant et al., 2011; Hopkins et al., 2012; Stuble et al., 2019). Microbial decomposition is generally temperature-dependent and constrained by physical and chemical protection of organic matter (e.g., aggregation, mineral sorption) as well as soil hydrology (e.g., water film thickness, oxygen availability, freezing) (Davidson and Janssens, 2006). Following kinetic theory, decomposition should increase with temperature, as long as there are enough substrates and enzymes available (Conant et al., 2011). Rising temperatures have been shown to increase respiration rates more than growth rates and thus decrease CUE (Sinsabaugh et al., 2013). However, the impact of increasing temperatures has been shown to be positive, negative, or neutral, often depending on associated indirect effects. Moreover, short- and long-term warming have different, sometimes contrasting, results. For instance, carbon losses were found to fluctuate over the period of a 26-year forest soil warming experiment (Melillo et al., 2017). Changes in soil respiration were found to relate to structural and functional changes within the soil microbial community. Initially, warming led to high respiration rates and a depletion of labile carbon. Thus, respiration was low in the second phase, before a community reorganization again enabled higher respiration rates, but henceforth based on the degradation of recalcitrant compounds. When this resource gets depleted as well another shift in community composition and function is to

be expected. Another study using geothermal warming found that microbial activity does not acclimate even after 50 years of warming (Walker et al., 2018). Microbial growth and respiration rates remain accelerated per unit of biomass. They decrease, however, per unit of soil, if substrate is depleted, to which microbes respond with biomass reduction, suggesting long-term effects of climate warming on microbial physiology. Microbes also react to short- (weeks), medium- (8 years) and long-term (50 years) warming by downregulating their protein biosynthesis machinery (i.e., ribosome content per cell) to liberate resources to be able to maintain these high growth rates (Söllinger et al., 2022). Warming also leads to changes in microbial community composition (Weedon et al., 2023) and microbial interactions (Burman and Bengtsson-Palme, 2021), which could alter microbial growth under climate change. Bacterial growth temperature traits have been shown to be more responsive to warming than those of respiration, or fungal growth (Cruz-Paredes et al., 2023). Moreover, temperature sensitivity (Q_{10}) of microbial growth varies between phylogenetic groups and their abundances can drive temperature sensitivities at the community level (Wang et al., 2021), supporting that community microbial growth rates depend on microbial community composition. However, this was not true when looking at taxon-specific growth, as warming did not change individual growth rates, but rather led to more actively growing taxa (Metze et al., 2024). It was also shown that temperature sensitivity of CUE cannot be explained by genomic composition across taxa, but rather depends on the physiological response to the environment (Pold et al., 2020).

Changes in decomposition under higher temperatures (Kirschbaum, 1995; Hopkins et al., 2012) also relate to warming-induced alterations of soil organic matter and edaphic factors. For instance, warming can decrease soil pH (e.g., Ji et al., 2014; Tian et al., 2023b). Lower pH was found to reduce bacterial growth and enhance fungal growth (Rousk et al., 2009), thereby indirectly changing community composition and decomposition potential. Long-term soil warming decreases soil organic matter content. Resulting changes in soil organic matter composition reduce water holding capacity, and hydrological and thermal buffering, leading to further warming and decreasing SOM (Werner et al., 2020). Warming also reduces soil water content across all seasons (Simon et al., 2020), which, on the microbial scale, causes habitat fragmentation and reduced substrate accessibility (Védère et al., 2022). Pore connectivity and diffusion of substrates determine organic matter composition in aggregates. For example, soil moisture can increase organic matter aromaticity by physically protecting complex carbon from increased decomposition rates under warmer temperatures (Cates et al., 2022). Higher temperatures change physical protection and chemical composition of soil organic matter (van den Enden et al., 2021; Cates et al., 2022) and affect sorption-desorption processes of organic matter to minerals (Conant et al., 2011). Temperature was shown to affect the organic carbon composition of bulk soil and aggregates (micro- and macro-aggregates, fractions occluded within macroaggregates, and silt and clay fractions). Warming increased the relative abundance of condensed and unsaturated hydrocarbons, tannins and amino sugars, but

decreased protein compounds (Cates et al., 2022). Warming also accelerates soil organic matter decomposition and thereby changes its composition. For instance, the ratio of alkyl to O-alkyl carbon compounds increases, because microbes preferentially take up O-alkyl compounds (i.e., carbohydrates). Moreover, plant-derived compounds, such as lipids, sugars, long-chained alkanoic acids, terpenoids and lignins are reduced by warming, while suberin and cutin compounds from roots and leaf wax coatings increase (van den Enden et al., 2021). Feng and Simpson (2008) showed that individual soil organic matter components exhibit different temperature responses. Lignins showed higher Q_{10} values than alkanes, alkanols, alkanoic acids, and steroids. Thus, the authors pointed out that Q_{10} of soil respiration does not necessarily reflect the temperature sensitivity of individual organic matter compounds. Warming has also been shown to affect decomposition of various organic matter fractions differently across the soil profile, yet induces high respiration rates in all soil depths (Soong et al., 2021).

Furthermore, organic matter composition, decomposition and microbial activity can be affected indirectly by warming-induced changes in plant biomass, community composition, litter chemistry, and rhizodeposition (Pugnaire et al., 2019). Higher temperatures have also been shown to affect soil invertebrate abundance, richness and community composition (Robinson et al., 2018; Figueroa et al., 2021), which could feedback on litter decomposition and predation on microbes, thereby changing their activity, biomass and composition. Moreover, increasing temperatures lead to a downgrading of the soil food web and a strong increase in predatory bacteria and phages (Dahl et al., 2023).

Decomposition and warming effects in permafrost soils

The Arctic is especially vulnerable to climate warming due to amplification (Rantanen et al., 2022) and large carbon stocks in permafrost soils (Hugelius et al., 2014), that could cause a positive feedback to climate change (MacDougall et al., 2012; Schuur et al., 2015). Warming and thawing of permafrost removes a major kinetic constraint of decomposition and formerly protected organic carbon becomes available to microbes (Davidson and Janssens, 2006). Global warming thus increases decomposition rates in permafrost soils, given suitable soil moisture content and oxygen availability (Aerts, 2006). Many studies have already shown that warming and permafrost thaw increase soil respiration, leading to carbon loss (e.g., Dutta et al., 2006; Biasi et al., 2008; Hicks Pries et al., 2013; Mauritz et al., 2017), also during winter (Natali et al., 2014) and in anoxic soils (Treat et al., 2015). Dry bulk density has been found to be the best predictor for carbon loss in permafrost soils, reflecting soil physical structure, oxygen availability and organic matter availability (Faucherre et al., 2018). Temperature sensitivity (Q_{10}) of permafrost soil respiration varies with soil depth (Roy Chowdhury et al., 2015; Gentsch et al., 2018) and can be controlled by organic matter bonding to minerals (Gentsch et al., 2018). While dissolved organic matter can be stabilized by mineral association,

free particulate organic matter can be quickly respired upon thawing (Beer et al., 2022). However, mineral associated organic matter makes up the dominant fraction in permafrost soils (Gentsch et al., 2015). Microbial respiration and microbial biomass are higher in organic topsoil than in mineral subsoil or cryoturbated organic matter (Kaiser et al., 2007). Enzyme activities also vary between permafrost top- and subsoil, with more hydrolytic enzymes in the topsoil and increasing oxidative enzyme activity in the subsoil, relating to changes in microbial community composition (Schnecker et al., 2015). In general, microbial abundance, microbiome structure and functional potential change throughout the permafrost soil profile (Varsadiya et al., 2021). Fungal abundances decrease with soil depth, while Actinobacteria increase with decreasing carbon content (Gittel et al., 2014a). In frozen permafrost, microbial life is only possible within small capillaries of liquid water between ice crystals or in gas-fluid inclusions within ice crystals, both being hypersaline due to concentration of the remaining liquid water during freezing (Melnikov et al., 2011). Microbial diversity and composition differs across tundra polygonal types (Taş et al., 2018). Warming and thawing restructure permafrost soil communities (Biasi et al., 2005; Feng et al., 2020) and change functional gene abundance (Yang et al., 2017). Warming of Arctic communities also leads to higher microbial growth rates. While short-term warming increases average growth rates by 36 %, long-term warming increases them by 151 % (Propster et al., 2023). Moreover, microbes change their resource preferences and favor or must rely on recalcitrant compounds at higher temperatures (Biasi et al., 2005). Warming and permafrost thaw also cause increased plant growth and changes in water table dynamics, that cause indirect effects on carbon balance (Treat et al., 2015; Mauritz et al., 2017). Warmer and longer summers together with CO_2 fertilization lead to increases in plant productivity and biomass in 20 – 40 % of Arctic tundra (Heijmans et al., 2022). Grass-like graminoid tundra is increasingly replaced by shrub and tree communities, with higher carbon fixation potential. This Arctic greening was suggested to be able to mitigate part of the permafrost carbon losses. However, there are other possible scenarios, where local conditions (e.g., drought, waterlogging, thermokarst development) could decrease plant growth (Schuur et al., 2022). Biasi et al. (2005) showed that warming-induced increases in leaf area of *Betula nana* and in plant biomass, particularly in lichens, could not compensate for carbon loss due to higher soil respiration. In addition, higher carbon sequestration in peak plant growing season were found to be counterbalanced by higher ecosystem respiration in late summer (Zona et al., 2022). Another study predicted that vegetation distribution shifts and resulting albedo and evapotranspiration feedbacks could even enhance warming (Pearson et al., 2013). Moreover, rhizosphere priming can amplify carbon losses from permafrost soils (Keuper et al., 2020). Decomposition in permafrost subsoils can also be enhanced by increased transfer of plant-derived organic carbon to deeper layers (Wild et al., 2016) and by increased root growth and rooting depth (Blume-Werry et al., 2019).

Research Objective

This study was conducted as part of the EU Horizon 2020 research project "Nunataryuk", which explores global and local impacts of thawing permafrost at the land-sea interface. The aim of its Work Package 1 was to quantify soil organic matter storage and fluxes and to assess thaw-vulnerability and thaw-effects of terrestrial permafrost. As part of this WP, our research group focused on comprehensively investigating microbial decomposition in permafrost soils under climate warming. Our study combined research into soil edaphic factors, soil organic matter, microbial communities, microbial physiology and temperature effects. These research topics are often looked at in isolation, either focusing on the microbial part or on soil geochemical properties and therefore miss their interrelations. Moreover, studies on permafrost soil microbial processes, though having received increased attention in recent years, are still scarce in comparison to other soil research areas. In particular, we have no knowledge about the specific factors that control microbial processes (i.e., growth, respiration) in permafrost soils and how these processes respond to climate warming. To our knowledge this study was the first attempt to integrate all of these aspects to get a thorough understanding on the impact of climate warming on permafrost soils and possible feedbacks. We tried to overcome the present research gap by simultaneously analyzing soil properties, soil organic matter composition, and microbial community composition and by conducting a laboratory warming experiment to determine microbial growth and microbial respiration at 4 °C (ambient) and at 14 °C (warmed) to ascertain temperature responses. To be able to give a good estimate for circumpolar lowland tundra, the heterogeneity of permafrost soils must be considered. We investigated two sites in the lowland Canadian Arctic and examined the typical soil layers (organic, mineral, cryoturbated, permafrost) within three typical landscape features emerging from different stages of ice wedge degradation (low-, flat-, and high-center polygons). The project aimed to address the following central questions:

How does permafrost heterogeneity affect microbial activity?

How do permafrost microbes respond to warming?

These research questions will be presented in forthcoming publications by PhD candidate Victoria Sophie Martin (victoria.sophie.martin@univie.ac.at). See Declaration on Data and Contributions for details on workshare within this project.

The work presented here focuses on post-hoc analysis to assess possible underlying factors that lead to the observed temperature responses of microbial growth and respiration. Given that soil organic matter (i.e., the microbial resources) and microbial communities (i.e., the acting entities of decomposition) have been implicated in microbial community growth and respiration and considering that both are affected and altered by temperature, we posed the following research questions:

- *Do soil organic matter composition and/or microbial community composition explain microbial growth and respiration patterns in permafrost soils and does this relationship change with warming?*
- *Do soil organic matter composition and/or microbial community composition explain the temperature responses of microbial growth and respiration in permafrost soils?*

To answer our research questions and obtain high-quality results, we employed a range of state-of-the-art techniques. We developed a new pyrolysis-GC-MS fingerprinting approach that facilitates an untargeted quantitative analysis of soil organic matter composition. We also combined amplicon sequencing and digital droplet PCR (ddPCR) of the 16S rRNA gene and the ITS1 region allowing for quantitative microbiome profiling of archaea, bacteria and fungi. We used principal coordinate analysis to determine compositional profiles of soil organic matter and microbial communities. Subsequently, linear mixed effect models were used to elucidate whether soil organic matter composition, microbial community composition, or soil physicochemical parameters affect or control microbial growth, microbial respiration and their temperature responses.

With this study we wanted to provide the first integrative analysis of the main drivers of microbial growth and respiration in permafrost soils and investigate possible consequences of climate warming.

MANUSCRIPT

Soil organic matter and microbial community composition explain microbial growth and respiration in permafrost soils, but not their response to temperature

Abstract

Global warming leads to permafrost thaw and makes organic carbon available to microbial decomposition, that was frozen and stored in these soils for millennia. The fate of permafrost carbon is largely dependent on how it is partitioned between microbial growth (potential carbon stabilization in soil) and microbial respiration (carbon loss to the atmosphere). Yet, our understanding of microbial growth, respiration and corresponding temperature responses in permafrost soils remains limited. Here, we investigated four soil layers (organic, mineral, cryoturbated, permafrost), within three lowland tundra polygon types (low-, flat-, high-center) from two sites (catchments) in the Canadian Arctic. We found soil organic matter composition (analyzed by pyrolysis-GC-MS fingerprinting) and the structure of the microbial communities (based on amplicon sequencing and quantitative PCR) to be distinctly different across different soil layers and polygon types. Both the structure of the microbial communities and the soil organic matter composition proved to be good predictors for mass-specific growth and respiration rates of soil microorganisms, measured after an eight-week incubation experiment at ambient (4 °C) and warmed condition (14 °C). However, the temperature responses of growth and respiration could not be explained by either the soil organic matter composition, the microbial community structure, or the physicochemical soil parameters, suggesting a rather uniform response of these microbial key processes to global warming across a wide range of lowland tundra ecosystems.

Zusammenfassung

Der Klimawandel lässt Permafrostböden auftauen, wodurch organischer Kohlenstoff, der für Jahrtausende in diesen Böden gefroren und gespeichert war, für mikrobielle Zersetzung verfügbar wird. Die Verteilung des von Mikroorganismen aufgenommen Kohlenstoffs auf mikrobielles Wachstum (mögliche Kohlenstoffstabilisierung) und mikrobielle Atmung (Kohlenstoffabgabe an die Atmosphäre) entscheidet über das Schicksal dieser alten Kohlenstoffspeicher. Unser Wissen über mikrobielles Wachstum und Atmung in Permafrostböden sowie deren Reaktion auf steigende Temperaturen ist begrenzt. In der vorliegenden Studie untersuchten wir vier Bodenschichten (organisch, mineralisch, kryoturbiert, gefroren) aus drei Landschaftstypen der Tieflandtundra (Polygone mit vertieftem, flachem, oder erhöhtem Mittelpunkt) von zwei Standorten in der Kanadischen Arktis. Wir fanden Unterschiede in der organischen Bodenzusammensetzung (analysiert durch Pyrolyse-GC-MS) und in der Struktur mikrobieller Gemeinschaften (basierend auf Amplicon-Sequenzierung und quantitativer PCR) zwischen verschiedenen Bodenschichten und Polygontypen. Sowohl die mikrobielle Gemeinschaftsstruktur als auch die Zusammensetzung der organischen Bodensubstanz erwiesen sich als gute Prädikatoren für massenspezifisches Wachstum und massenspezifische Atmung von Mikroorganismen, welche nach einem achtwöchigen Inkubationsexperiment bei 4 °C (arktische Sommertemperatur) und 14 °C (Wärmebehandlung) gemessen wurden. Hingegen konnte die Temperaturreaktion von Wachstum und Atmung weder durch die organische Bodenzusammensetzung, noch die mikrobielle Gemeinschaftsstruktur, noch durch die physikochemische Bodenparameter erklärt werden. Dies weist auf eine einheitliche Reaktion dieser mikrobiellen Schlüsselprozesse auf die globale Erwärmung in verschiedenen Tieflandtundra-Ökosystemen hin.

Introduction

The year 2023 was the warmest year on record (Copernicus Climate Change Service, 2024) and the Arctic warms about four times faster than the global average (Rantanen et al., 2022), causing extensive permafrost thaw. Since 1850 Arctic permafrost area has already shrunk by about 12 % (Langer et al., 2022) and a loss of 66 % is to be expected by 2100, even if global warming stays below 2 °C (Meredith et al., 2019). At current global warming rates, permafrost is already at risk of crossing an irreversible tipping point (Lenton et al., 2023).

Arctic lowlands are particularly affected by warming (Jorgenson and Osterkamp, 2005), as ice-rich ground is destabilized and thermokarst develops, leading to changes in hydrology and biogeochemistry (Olefeldt et al., 2016; Nitzbon et al., 2021). For millennia permafrost has acted as a carbon sink. Low temperatures and poor drainage restricted microbial decomposition and preserved organic matter from decaying plants as well as alluvial and aeolian deposits. This led to the buildup of app. 1,500 Pg organic carbon in northern circumpolar permafrost soils (Davidson and Janssens, 2006; Hugelius et al., 2014). As temperatures rise, this carbon will be accessible to microbes and can, in part, be taken up and respired to CO_2 (at aerobic conditions) or CH_4 (at anaerobic conditions) to generate ATP (Soong et al., 2020), thereby turning permafrost to a potential greenhouse gas source (Tornocai et al., 2009; Koven et al., 2011; MacDougall et al., 2012; Schuur et al., 2015; Natali et al., 2021). However, part of the carbon that microbes take up is also invested into microbial growth and can be stabilized as microbial necromass after they die (Miltner et al., 2012; Liang et al., 2017; Sokol et al., 2022; Tao et al., 2023). The partitioning of carbon into microbial growth and respiration, commonly described as carbon use efficiency (del Giorgio and Cole, 1998; Manzoni et al., 2012), therefore plays the key role in determining the fate of permafrost carbon in times of global warming.

Heterotrophic microbes are inherently limited by organic carbon and energy (Soong et al., 2020). However, organic carbon in soil is only available as a "complex mixture of plant and microbial residues at various stages of decay" (Miltner et al., 2012). Its composition is influenced, amongst other factors, by soil depth (age) and geochemistry (Rumpel and Kögel-Knabner, 2011; Mainka et al., 2022), water status (Védère et al., 2022), vegetation and land-use type (Quideau et al., 2001; El Moujahid et al., 2017; Thai et al., 2021), and microbial community composition (Domeignoz-Horta et al., 2021). Higher temperatures were found to change the physical protection and chemical composition of soil organic matter (van den Enden et al., 2021; Cates et al., 2022) and to directly affect the decomposition rate (Kirschbaum, 1995; Hopkins et al., 2012). The amount of assimilated carbon that is utilized for microbial growth depends on the quality of available soil organic matter (i.e., stoichiometry, degree of reduction, and type of chemical bonds) (del Giorgio and Cole, 1998; Manzoni et al., 2012;

Mooshammer et al., 2014). Therefore, changes in organic matter quality due to climate warming could also lead to changes in microbial growth.

One gram of soil holds thousands of bacterial taxa (Delgado-Baquerizo et al., 2018) and hundreds of fungal species (Baldrian et al., 2012; Taylor et al., 2014; Peay et al., 2016) that live on numerous resources, compete or cooperate with each other and interact with other trophic levels (Weiland-Bräuer, 2021). Apart from interactions, microbial community composition is driven by climate and edaphic factors, particularly soil pH (Fierer and Jackson, 2006; Rousk et al., 2010; de Vries et al., 2012; Tedersoo et al., 2014). Microbial communities also change with soil depth (Fierer et al., 2003; Naylor et al., 2022) and resource quality and diversity (Chapman and Newman, 2010; Zechmeister-Boltenstern et al., 2015). Resource quality also has a species-specific effect on carbon use efficiency and different responses for bacteria and fungi (Keiblinger et al., 2010). Moreover, microbes are thought to have different growth strategies (e.g., slow-growing degraders and fast-growing opportunists) with differing carbon use efficiencies (Manzoni et al., 2012) that were recently proposed to be two evolutionary distinct classes for growth optimization (nutrient acquiring copiotrophs vs. cell maintaining oligotrophs) (Weissman et al., 2021). Walkup *et al.* (2023) also showed that bacterial growth rates are phylogenetically constrained across ecosystems and suggests that the genetic basis of bacterial growth rate is hereditary. We therefore have to assume that microbial growth depends on microbial identity and varies with microbial community composition and environmental conditions. Higher temperatures change microbial community composition (Frey et al., 2008; Weedon et al., 2023) and microbial interactions (Burman and Bengtsson-Palme, 2021) and could thereby alter microbial community growth under climate change. Bacterial growth temperature traits have been shown to be more responsive to warming than fungal growth (Cruz-Paredes et al., 2023). Moreover, temperature sensitivity (Q_{10}) of microbial growth varies between taxa and their abundances can drive temperature sensitivities at the community level (Wang et al., 2021), supporting that microbial growth rates depend on microbial community composition. Moreover, microbial growth does not acclimate to warming on the short- and the long-term (Walker et al., 2018) suggesting long-term effects of climate warming on microbial physiology.

Despite the well-established fact that microbial growth is governed by soil organic matter and microbial community composition, there is no study to our knowledge, that directly addresses these relationships, especially not in permafrost soils. To close this research gap, we sampled permafrost soils from two sites in the Canadian Arctic, including three landscape types of lowland tundra (low-center, flat-center, high-center polygons) and four soil layer types (organic soil, mineral soil, cryoturbated organic matter and upper frozen permafrost) to capture the heterogeneity of permafrost soils (Siewert et al., 2021). We analyzed microbial growth, soil organic matter composition and microbial community composition in all samples. In addition, we performed a laboratory warming experiment to assess the effect of climate

warming and measured the temperature response (Q_{10}) of microbial growth (Conant et al., 2011), to answer the following research questions:

(1) Do soil organic matter composition and/or microbial community composition explain microbial growth and respiration patterns in permafrost soils and does this relationship change with warming?

(2) Do soil organic matter composition and/or microbial community composition explain the temperature responses of microbial growth and respiration in permafrost soils?

Towards this end, we analyzed microbial growth through the incorporation of $H_2{}^{18}O$ into DNA, bacterial, archaeal and fungal community composition by amplicon sequencing (16S rRNA gene and ITS1 region) and soil organic matter composition by pyrolysis-GC-MS fingerprinting. To test the effect of warming, we incubated the soils at an ambient temperature of 4 °C and an elevated temperature of 14 °C, and calculated the temperature responses (Q_{10}) of microbial growth and respiration after eight weeks of warming (see Supplementary Information). We used linear-mixed effect models to assess whether soil organic matter composition, microbial community composition, or other physicochemical soil parameters could explain the observed microbial growth, respiration and temperature responses. To our knowledge this is the first study that provides an integrative analysis of two of the main drivers of microbial growth and respiration in permafrost soils and additionally looks at possible climate change effects.

Methods

The present work is part of a larger project that investigates the effect of climate warming on permafrost microbes (see Declaration on Data and Contributions). A brief overview of the study site and warming experiment is given below. Further details on site and sampling, as well as analyses of soil physicochemical parameters, microbial biomass, growth, respiration, and temperature responses can be found in the Supplementary Information. To assess influences on microbial growth and respiration, and their temperature responses, we analyzed all field soil samples for soil organic matter composition and microbial community composition and used them as predictors in linear mixed effect models.

Study site

Two sampling campaigns were carried out in the Ivvavik National Park at the Yukon Coast (Canada): one at Ptarmigan Bay (69°29' N, 139°10' W) in 2018 and one in Komakuk Beach (69°34' N, 140°10' W) in 2019 (Fig. 6). Both sampling campaigns took place in mid-August to guarantee full thawing of the active layer. Soil samples were taken from 18 soil pits: three low-center, three flat-center, and three high-center polygons in each of the two sites. Pits of 1x1 m were excavated up to the permafrost table. Soil samples (n = 81) were

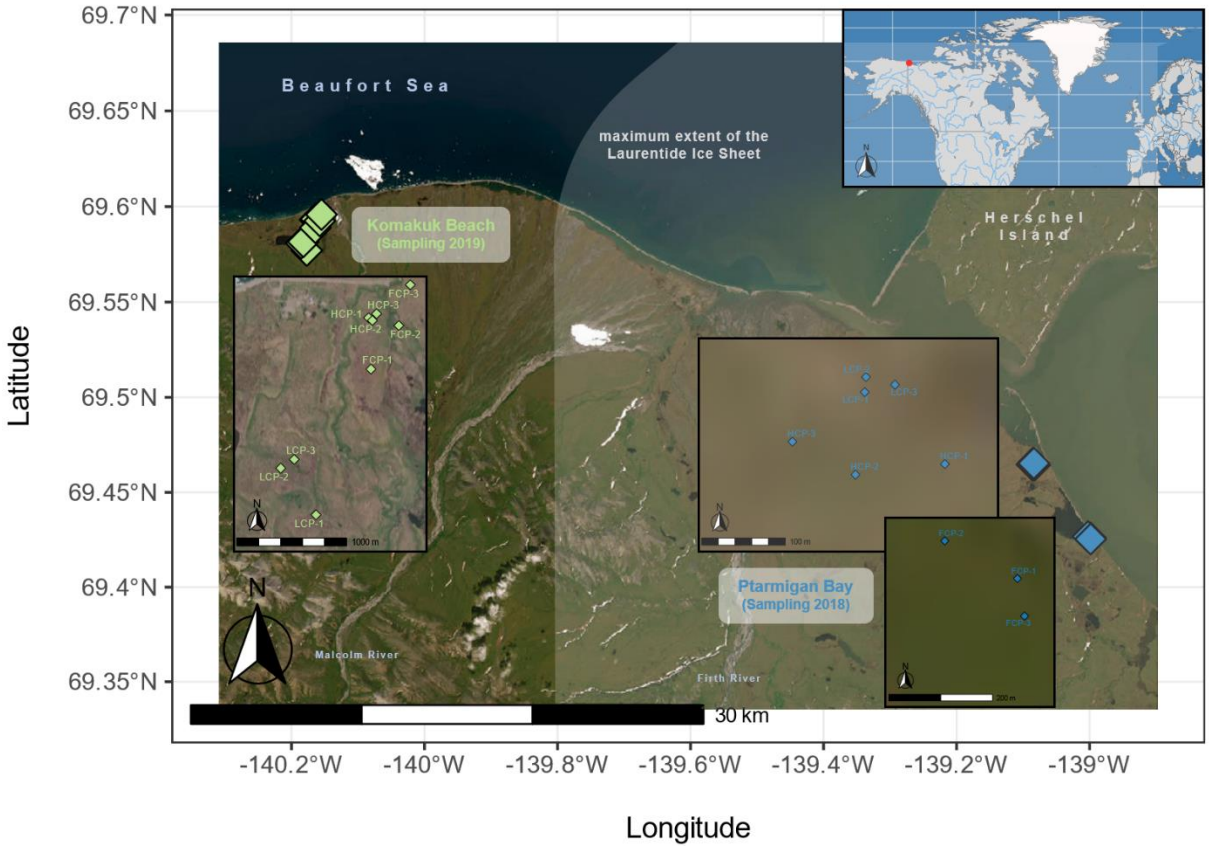

Fig. 6: The study area is located at the Yukon Coast in northwestern Canada. The locations of all soil pits are depicted as diamonds for both sampling campaigns, Ptarmigan Bay (blue) and Komakuk Beach (green). The estimated maximum extent of the Laurentide Ice Sheet is depicted in transparent grey, reaching to -139.8° W (Dyke and Prest, 1987; Fritz et al., 2012). LCP = low-center polygon, FCP = flat-center polygon, HCP = high-center polygon. © Cornelia Rottensteiner

collected from the active layer (organic soil, mineral soil, cryoturbated organic matter) and from the upper permafrost (10 cm deep with a soil corer) (S.Tab. 1). Roots were picked from the soil samples and soils stored at 4 °C until analysis.

Warming Experiment

A short-term warming experiment was performed to determine temperature responses for microbial growth and microbial respiration. In brief, each soil sample was incubated for eight weeks at two temperatures: 4 °C = "control" (representing average active layer temperature) and 14 °C = "warmed" (+10 °C elevated temperature) in incubators (TC445S, Aqua Lytic). After eight weeks of incubation, microbial biomass, microbial respiration and microbial growth were measured in each sample and temperature responses (Q_{10}) were calculated.

$$Q_{10} = \frac{\text{process rate (T+10 °C)}}{\text{process rate (T)}}$$

Microbial biomass carbon (C_{mic}) was determined by the chloroform-fumigation-extraction method (Brookes et al., 1985; Vance et al., 1987). Microbial growth rates were measured via $H_2{}^{18}O$-incorporation into microbial DNA (Spohn et al., 2016; Walker et al., 2018). Microbial respiration rates were assessed as the increase in CO_2 concentration over time, measured by gas sampling on GasBench-GC-IRMS (GasBench II, Thermo Scientific) in 2018 and by direct injection into an infrared gas analyzer (EGM-4 Environmental Gas Monitor for CO_2, PP Systems) in 2019. Mass specific growth rates (µg C g^{-1} C_{mic} h^{-1}) and mass specific respiration rates (µg C g^{-1} C_{mic} h^{-1}) were calculated by dividing each rate per unit soil (µg C g^{-1} dry soil h^{-1}) by microbial biomass carbon (µg C_{mic} g^{-1} dry soil). This approach ensures that effects from biomass differences are excluded and allows to examine physiological responses of microbial communities. See Supplementary Information for further details.

Soil organic matter composition

To characterize soil organic matter composition, we established a pyrolysis gas chromatography mass spectrometry (pyr-GC-MS) fingerprinting approach that facilitates a fast identification of compounds for many samples and allows to use the compositional information of unidentified compounds. A detailed description of the method can be found in the Supplementary Methods. In brief, finely powdered soils were pyrolyzed at 600 °C (Pyroprobe 6200 and Autosampler 6250T, CDS) and the pyrolysis products were subsequently separated and quantified on the gas chromatography time-of-flight mass spectrometry systems (Pegasus BT GC-MS, LECO, with SUPELCOWAX™ 10 Capillary GC Column, Sigma-Aldrich) and analyzed with the ChromaTOF software (version 5.51.50.068774, LECO).

Soil microbial community composition

We extracted DNA from soil that was inactivated with RNA*later* Stabilization Solution (Sigma-Aldrich) in the field and stored at -80 °C. To remove the RNA*later* from the soil samples*,* we added 1 mL sodium phosphate buffer and centrifuged the samples. The supernatant containing the RNA*later* solution was discarded, while the soil pellet containing the microorganisms and nucleic acids was retained. This cleaning procedure was repeated five times before starting with a DNA extraction kit (FastDNA™ SPIN Kit for Soil, MP Biomedicals). Negative controls were included to rule out contaminations. The DNA extracts were cleaned with OneStep PCR Inhibitor Removal (Zymo Research) and stored at -80 °C until further analysis. DNA concentrations were quantified with a PicoGreen assay (Quant-iT™ PicoGreen® dsDNA Assay Kit; Thermo Fisher Scientific) measuring fluorescence on a plate reader (Infinite M200, Tecan).

Amplicon sequencing for archaeal, bacterial and fungal communities was performed at the Joint Microbiome Facility of the Medical University of Vienna and the University of Vienna, following the two-step barcoding approach described in Pjevac *et al.* (2021). In brief, the primer pairs 515F-806R (Apprill et al., 2015; Parada et al., 2016) and ITS1F-ITS2 (White et al., 1990; Smith and Peay, 2014) were used for amplification and sequencing of the 16S SSU rRNA gene and the fungal intergenic spacer region (ITS1), respectively. Sequencing was performed in 2 × 300 cycle paired-end mode on an Illumina MiSeq sequencer using the MiSeq Reagent Kit v3 (Illumina). The raw sequencing data were extracted with FASTQ in BaseSpace (Illumina) and demultiplexed using the Python package "demultiplex" (Laros, GitHub). The R package "DADA2" (version 1.14.1, Callahan, McMurdie, et al., 2016; Callahan, Sankaran, et al., 2016) was used to infer amplicon sequence variants (ASVs). Bacterial and archaeal ASVs were classified with SINA (version 1.6.1, Pruesse, Peplies and Glöckner, 2012) and SILVA SSU database (version 138.1, Quast et al., 2013) and fungal ASVs were classified with UNITE database (version 8.2, Abarenkov et al., 2020).

For quantitative microbiome profiling we quantified 16S rRNA genes and ITS1 regions with digital droplet PCR (ddPCR) using the same primer pairs as for sequencing and ddPCR EvaGreen Supermix (Bio-Rad). Droplets were generated on a QX200TM Droplet Generator (Bio-Rad), amplified (T100 Thermal Cycler, Bio-Rad) and measured fluorometrically with a QX200 Droplet Reader (Bio-Rad). Gene copy numbers (copies g^{-1} dry soil) were calculated with the QX ONE Software (version 1.2, Bio-Rad). A detailed description can be found in the Supplementary Methods.

Data analyses

All statistical analyses were performed in R (version 4.2.2 'Innocent and Trusting', R Core Team, 2022) and RStudio (version 2022.12.0.353 'Elsbeth Geranium', RStudio Team, 2022). The significance threshold for all statistical tests was set to 0.05. Boxplots were computed with

the package "ggplot2" (Wickham, 2016) and "ggpubr" (Kassambara, 2023a). Tables were generated with the package "flextable" (Gohel and Skintzos, 2023).

Soil organic matter composition

From the pyrolysis-GC-TOF-MS analysis, we obtained chromatographic areas for individual peaks. We transformed the exported chromatographic areas to carbon (mg C g^{-1} dry soil), assuming that the total chromatographic area of a sample relates to the total C amount in the sample weight and that all organic compounds have the same response factor on the mass detector. While this is an obvious oversimplification, the procedure allows to partition carbon to different pyrolysis products, which is helpful to compare substances between treatments or other experimental units. A detailed description can be found in the supplementary methods. Compounds were assigned to the most likely origin among soil organic matter classes, i.e., (1) aromatics & phenols, (2) carbohydrates, (3) lignins, (4) lipids and (5) nitrogen compounds, based on literature (Saiz-Jimenez and De Leeuw, 1986; Hempfling and Schulten, 1990; Schulten and Schnitzer, 1997; Buurman *et al.*, 2005; Vancampenhout *et al.*, 2009; González-Pérez *et al.*, 2012; Stewart, 2012; Said *et al.*, 2015; Tolu *et al.*, 2015; Ninnes *et al.*, 2017; Shen *et al.*, 2018). If identified compounds were absent from literature, we grouped them according to their chemical similarity to other classified compounds using the US National Library of Medicine (NCBI) Medical Subject Headings (MeSH) Database (National Institutes of Health, 2023). Compounds that could not be identified were put together as (6) Unclassified. We used the "phyloseq" package (McMurdie and Holmes, 2013) to analyze the data, as it allows to assemble compound abundance, compound classification and sample information into a single data frame. We removed data below a relative abundance of 0.1 %, which mainly omitted compounds with low signal/noise and small area. Consequently, 534 compounds were used for analyses. Relative abundances were generated using the "phyloseq" function transform_sample_counts() from the "phyloseq" package (McMurdie and Holmes, 2013). To assess soil organic matter composition, we performed principal coordinate analysis (PCoA) on Bray-Curtis dissimilarity matrices based on relative abundances, using the functions distance(), ordinate() and plot_ordination() from the "phyloseq" package (McMurdie and Holmes, 2013). We used permutational multivariate analysis of variance (PERMANOVA) applying the adonis2() function of the "vegan" package (Oksanen et al., 2022) to test for compositional group differences between polygon types or soil layers. We set soil layer as the primary factor interacting with polygon type. Homogeneity of multivariate dispersions was tested with betadisper() function to check for effects of within-group variation. Multilevel pairwise comparisons were performed with the function pairwise.adonis() (Martinez Arbizu, 2020) adjusting p-values with Bonferroni correction. All permutations were set to 999.

Microbial community composition

Raw sequencing datasets of the 16S rRNA gene and the ITS1 region were pre-filtered to remove unspecific reads such as non-prokaryotic and non-fungal ASVs, respectively. Samples

with less than 500 reads were considered unsuccessful sequencing and excluded. We corrected total reads per ASV per sample from possible contaminations by subtracting the maximum read number of each ASV found in the negative extraction controls. We used the "phyloseq" package (McMurdie and Holmes, 2013) to assemble ASV abundance, taxonomy and sample information. For quantitative microbiome profiling, we normalized relative ASV abundances by multiplying with the corresponding gene or region copy numbers (copies g^{-1} dry soil) obtained from ddPCR quantifications and rounding to integers with round2() from the package "edbuildr" (Brodzik et al., 2023). We used the function transform_sample_counts() from the "phyloseq" package (McMurdie and Holmes, 2013) to filter all ASVs below 0.05 % relative abundance in each individual sample. We combined abundances (gene copy number corrected reads g^{-1} dry soil) of bacteria, archaea and fungi with the function merge_phyloseq() from the "phyloseq" package (McMurdie and Holmes, 2013) and subsequently transformed back to relative abundances. Compositional differences of this combined microbial community composition were explored by using Bray-Curtis dissimilarity matrices based on relative abundances and performing principal coordinate analyses (PCoA) with the functions distance(), ordinate() and plot_ordination() from the "phyloseq" package (McMurdie and Holmes, 2013). To test for differences among polygon types or soil layers, we performed PERMANOVA in the same manner as described above.

Linear mixed effect models

We assessed outliers in all variables using boxplots and QQ-plots, adjusting for normal or log-normal data distributions. We confirmed outliers statistically with grubbs.test() and rosnerTest() from the packages "outliers" (Komsta, 2022) and "EnvStats" (Millard, 2013), respectively. Values of Q_{10} greater than 5 (for growth) or 10 (for respiration) were considered unrealistic methodological errors and thus excluded from analysis. We used linear mixed effect models to assess whether soil organic matter composition and/or microbial community composition and/or soil parameters (C, N, P, pH, SWC) control microbial mass-specific growth, respiration, and their temperature responses (Q_{10}). We chose LMEs due to the unbalanced nature of the dataset (S.Tab. 1) and to account for hierarchical structure by including soil pit nested within site as a random effect (1 | Site / Pit). This allowed us to control for effects of nestedness, location and sampling year. We extracted the coordinates of axes 1 and 2 from the compositional PCoA plots of soil organic matter and combined microbial community composition and used them as additive predictors. Each soil parameter and axis was tested both as a single predictor and in combination. All predictor variables were centered and checked for co-correlation using the function cor_test() from the package "rstatix" (Kassambara, 2023b) with Kendall correlation coefficient, due to non-normality of data and presence of rank ties (S.Fig. 3). We also used the function vif() from the package "car" (Fox and Weisberg, 2019) to test variance inflation factors (VIFs) and excluded variables with VIFs larger than 5 (James *et al.*, 2017). We chose the best model based on the lowest AIC and BIC

as well as direct comparisons with ANOVA in case of nested models. We used the package "lme4" (Bates et al., 2015) for model computation. Significance of predictors was calculated using Type III Analysis of Variance (ANOVA) with Satterthwaite's method via the package "lmerTest" (Kuznetsova et al., 2017). We used the function resid_panel() (Goode and Rey, 2019) to generate diagnostic plots for evaluation of goodness of fit and assumptions of the models. In some cases, response variables had to be log- or sqrt-transformed to achieve homoscedasticity and normality. Conditional and marginal coefficients of determination (R^2_c and R^2_m) were calculated with the function r.squaredGLMM() from the package "MuMIn" (Bartoń, 2022).

Results

Soil organic matter composition varied across polygon types and soil layers

To relate microbial growth and respiration at different temperatures to the composition of soil organic matter, we analyzed soil organic matter composition by pyrolysis-GC-MS fingerprinting. Out of 534 total compounds, 223 were identified and grouped into common compound classes (51 aromatics & phenols, 47 carbohydrates, 16 lignins, 68 lipids and 41 nitrogen-containing compounds). Soil organic matter composition differed between the lowland tundra polygon types (PERMANOVA, $F = 5.50$, $p = 0.001$) and between the soil layers (PERMANOVA, $F = 15.05$, $p = 0.001$) (Fig. 7, S.Tab. 3). Post-hoc pairwise comparisons showed that the low-center polygons were significantly different from flat-center polygons ($p_{adj} = 0.003$) and high-center polygons ($p_{adj} = 0.006$). Organic and mineral soils were each distinct from all other soil layers (all $p_{adj} = 0.006$). There was no difference between permafrost soil and cryoturbated organic matter ($p_{adj} = 0.126$). The soil layers separated along the first PCoA axis, which explained 43.2 % of variance and was highly correlated with soil organic carbon content (Spearman's $\rho = -0.85$, $p < 0.001$), reflecting a decrease of carbon from carbon-rich organic soils over permafrost and cryoturbated organic matter to carbon-poor mineral soils (S.Tab. 2). This reflected a gradient in the level of degradation of soil organic matter, apparent upon closer examination of compound classes (S.Fig. 4, S.Fig. 5, S.Tab. 3, S.Tab. 4). Organic soils were characterized by high amounts of plant-derived carbohydrates and lignins, while mineral soils were enriched in aromatics, phenols and lipids, which are more associated with microbial necromass. Cryoturbated organic matter and permafrost soils were a mixture of organic and mineral horizons and/or in an intermediate decomposition stage.

Microbial community composition varied across polygon types and soil layers

To associate microbial community composition to microbial growth and respiration at different temperatures, we used amplicon sequencing of the 16S rRNA gene and ITS1 region to investigate the bacterial and archaeal, as well as the fungal community composition of the different polygon types and soil layers. After removal of non-prokaryotic and non-fungal sequences and samples below a read threshold of 500, we obtained a total of 676,224 reads and 4963 ASVs (4771 bacterial and 192 archaeal ASVs) of the 16S rRNA gene and 555,849 reads and 1811 ASVs of the ITS1 region. Microbial community composition differed between polygon types (PERMANOVA, $F = 5.49$, $p = 0.001$) and between soil layers (PERMANOVA, $F = 6.20$, $p = 0.001$) (Fig. 8, S.Tab. 4). However, we also observed different levels of dispersion by polygon (betadisper, $F = 6.87$, $p = 0.002$) and soil layer (betadisper, $F = 10.46$, $p < 0.001$). Post-hoc comparisons revealed distinct microbial communities for low-center polygons (all $p_{adj} = 0.003$). Microbial communities of organic soils differed from those of mineral, cryoturbated, and permafrost soils ($p_{adj} = 0.006$). Permafrost microbial communities were distinct from all other soil layers (all $p_{adj} = 0.006$). Community compositions

of mineral and cryoturbated soils were similar (p_{adj} = 0.522). We also found an interaction effect of polygon type and soil layer (PERMANOVA, F = 1.85, p = 0.001), apparent in two clusters for organic soils, one for low-center polygons and one for both flat- and high-center polygons. Microbial community differences across landscape features and throughout the soil profile were also reflected in bacterial, archaeal and fungal alpha diversity (S.Fig. 6) and composition of microbial phyla (S.Fig. 7).

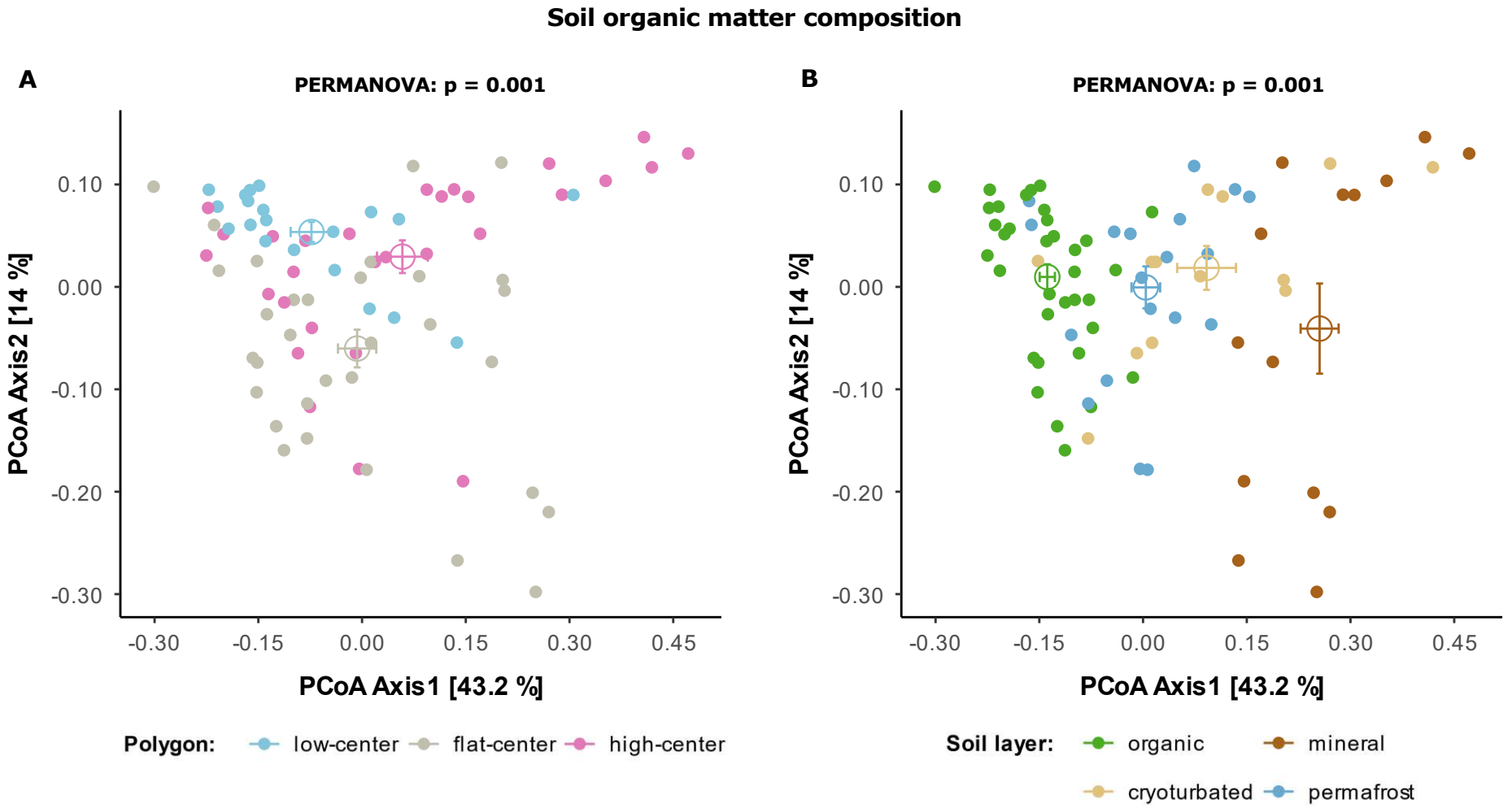

Fig. 7: **Soil organic matter composition depicted for (A) polygon types and (B) soil layers.** Principal coordinate analysis (PCoA) of Bray-Curtis dissimilarities based on relative abundance of soil organic matter compounds (N = 81). Means depicted as empty circles with standard error. Significant group differences from PERMANOVA are shown at the top. See S.Tab. 3 for detailed statistical results.

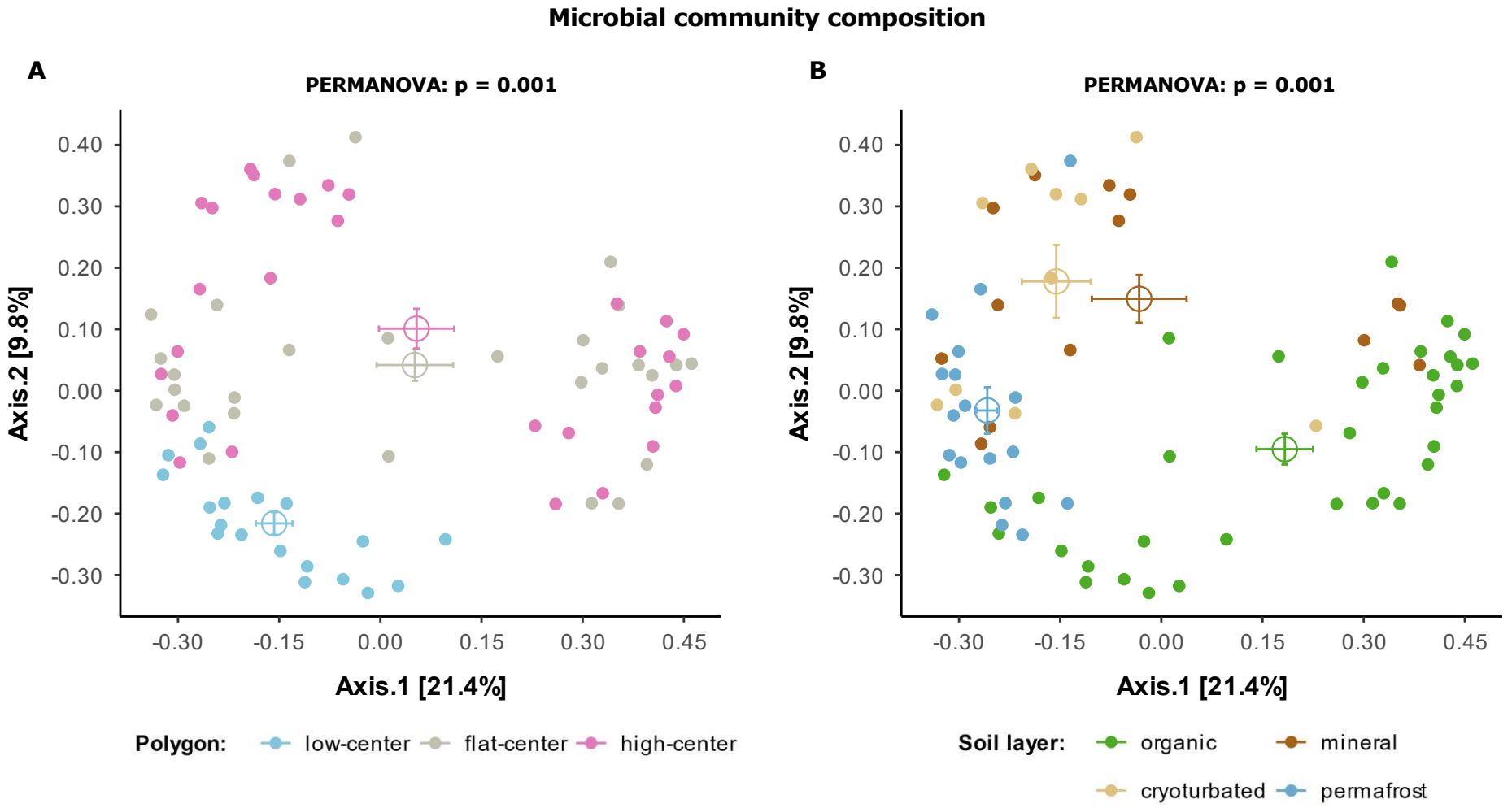

Fig. 8: **Microbial community composition depicted for (A) polygon types and (B) soil layers.** Principal coordinate analysis (PCoA) of Bray-Curtis dissimilarities based on relative abundance of ASVs (N = 76). Means depicted as empty circles with standard error. Significant group differences from PERMANOVA are shown at the top. See S.Tab. 4 for detailed statistical results.

Microbial activity

Microbial mass-specific growth and mass-specific respiration rates were determined after eight weeks of incubation at ambient temperature (4 °C) and elevated temperature (14 °C). Mass-specific growth doubled with warming, while mass-specific respiration increased fourfold (S.Fig. 1). Compositional differences in soil organic matter and microbial communities derived from PCoA axes 1 and 2 as well as soil physicochemical parameters (SWC, pH, C, N, P) were used as predictors in linear mixed effect models to explain mass-specific growth and mass-specific respiration and corresponding temperature responses.

SOM and microbial community compositions both affected microbial growth

Microbial mass-specific growth was explained by soil organic matter composition and microbial community composition both at ambient (4 °C) and at warmed (14 °C) conditions (Tab. 1, S.Tab. 5). Soil organic matter composition (Axis1: $F = 12.10$, $p < 0.001$, Axis2: $F = 2.33$, $p = 0.131$) and microbial community composition (Axis1: $F = 44.64$, $p < 0.001$, Axis2: $F = 14.58$, $p < 0.001$) together explained 56 % (R^2_m) of mass-specific growth at ambient temperature (4 °C). The total explanatory power of the model was even 73 % (R^2_c). The model fit was slightly improved by including soil nitrogen as an additional fixed effect (ANOVA, $X^2 = 6.21$, $p = 0.013$). However, including soil nitrogen only captured more variance associated with random effects, since it only improved conditional R^2 to 75 %. Soil organic carbon explained only a small proportion of variance in microbial growth (R^2_m = 8 %), while soil organic matter composition accounted for 19 %, and microbial community composition for 53 %. After eight weeks of warming at 14 °C microbial mass-specific growth was similarly controlled by soil organic matter composition (Axis1: $F = 22.71$, $p < 0.001$, Axis2: $F = 0.20$, $p = 0.658$) and microbial community composition (Axis1: $F = 58.07$, $p < 0.001$, Axis2: $F = 7.39$, $p = 0.009$) (Tab. 1, S.Tab. 6). The model explained 54 % (R^2_m) and 75 % (R^2_c) of mass-specific growth at 14 °C. Irrespective of the temperature, microbial community composition was found to have a stronger influence on microbial growth than soil organic matter composition. Models with only microbial community composition explained more of growth variance (R^2_c = 66-68 %) than models with only soil organic matter composition (R^2_c = 48-49 %). Models with soil organic matter composition (R^2_c = 48-49 %) explained more growth variance than models with soil organic carbon (R^2_c = 41-42). Models with microbial community composition coupled to soil organic carbon (R^2_c = 69-70) explained less variance than those coupled to soil organic matter composition (R^2_c = 73-75) (S.Tab. 5, S.Tab. 6).

Microbial respiration was mainly driven by microbial community composition

Microbial mass-specific respiration was predominantly controlled by microbial community composition. Yet, the effect was less pronounced than for microbial growth. At 4 °C ambient temperature microbial community composition (Axis1: $F = 20.11$, $p < 0.001$; Axis2: $F = 1.86$, $p = 0.178$) and soil organic matter composition (Axis1: $F = 1.34$, $p = 0.252$; Axis2: $F = 9.56$,

p = 0.003) together explained 28 % (R^2_m) and 29 % (R^2_c) of mass-specific respiration (Tab. 1, S.Tab. 7). The model was improved by adding soil nitrogen as an additional fixed effect (ANOVA, X^2 = 6.11, p = 0.013). This refined model explained 35 % (R^2_m) and 40 % (R^2_c) of mass-specific respiration at ambient temperature (4 °C). Adding soil nitrogen (F = 6.89, p = 0.011) reversed the importance of soil organic matter predictors. Instead of compositional change along axis 2 now axis 1 was a good predictor for microbial respiration (Axis1: F = 5.28, p = 0.025; Axis2: F = 2.69, p = 0.106). The effect of microbial community composition did not change by adding soil nitrogen (Axis1: F = 13.60, p < 0.001; Axis2: F = 0.23, p = 0.632). Soil nitrogen alone accounted for 16 % of variance in mass-specific respiration, as did microbial community composition. Soil organic matter composition only explained 7 %, while soil organic carbon explained 12 %. The best model for mass-specific respiration at warmed conditions (14 °C) was one with axis 1 of microbial community composition as a single predictor (F = 13.36, p < 0.001), explaining 14 % (R^2_m) and 34 % (R^2_c) of variance (S.Tab. 8). Models of microbial community composition in combination with soil organic carbon and a full model including microbial community composition and soil organic matter composition both improved R^2_c to 37 %, but did not provide any further explanatory power by the other predictors (Tab. 1, S.Tab. 8).

		Growth 4 °C		**Growth 14 °C**		**Respiration 4 °C**		**Respiration 14 °C**	
	R^2_m | R^2_c	0.56	0.73	0.54	0.75	0.28	0.29	0.14	0.37
Predictors	**SOM-A1**	***		***		n.s.		n.s.	
	SOM-A2	n.s.		n.s.		**		n.s.	
	MIC-A1	***		***		***		**	
	MIC-A2	***		**		n.s.		n.s.	

Tab. 1: **Linear mixed effect model results for mass specific growth and mass-specific respiration at ambient (4 °C, blue) and warmed (14 °C, orange) temperature.** Depicted is a direct comparison of the full models including soil organic matter composition (SOM) axis (A) 1 and 2 and microbial community composition (MIC) axis (A) 1 and 2 from principal coordinate analyses as predictors. All models included soil pit nested within site as random effects. Significance indicated with asterisks: *** p < 0.001, ** p < 0.01, * p < 0.05, n.s. not significant. Explanatory power of the models is depicted as marginal (m) and conditional (c) R^2 (grey). See S.Tab. 5, S.Tab. 6, S.Tab. 7, S.Tab. 8 for detailed statistical results.

Temperature responses were independent of measured variables

Neither soil organic matter composition nor microbial community composition could explain temperature responses (Q_{10}) of microbial mass-specific growth or mass-specific respiration. Temperature responses were also independent of soil water content, soil pH, soil organic carbon, soil nitrogen and soil phosphorus (S.Tab. 9, S.Tab. 10).

Discussion

Global warming leads to permafrost thaw and changes soil microbial processes, such as respiration, likely leading to positive feedbacks to climate warming (Schuur et al., 2015; Natali et al., 2021). While several studies have explored the effects of warming on microbes in the Arctic (Biasi *et al.*, 2005; Propster *et al.*, 2023) and the Subarctic (Walker et al., 2018), the specific factors that influence microbial processes (i.e., growth, respiration) and physiological adaptations to warming remain uncertain. Soil organic matter and microbial communities together are at the center of the decomposition process and the partitioning of carbon to microbial growth and microbial respiration (Manzoni et al., 2012). Substrate availability and quality as well as the community of microorganisms and their interactions change with warming (Melillo et al., 2017; Feng et al., 2020; Burman and Bengtsson-Palme, 2021; van den Enden et al., 2021; Cates et al., 2022; Weedon et al., 2023) and could thereby influence the effect of warming on permafrost soil microbial activity and determine whether carbon can be retained via microbial growth and necromass formation (Liang, 2020) or is lost to the atmosphere by microbial respiration (Schuur et al., 2015). Therefore, we here investigated soil organic matter composition and microbial community composition as potential drivers of growth and respiration at the microbial physiological level. To capture the heterogeneity of permafrost soils on the terrain scale and the soil pedon scale, we studied soils from two catchments in the Canadian Arctic, comprising three lowland tundra polygon types (low-center, flat-center, high-center polygons), and four soil layers (organic, mineral, cryoturbated, upper permafrost). To explore the effect of warming on permafrost microbes, we assessed microbial growth and microbial respiration after eight weeks of incubation at ambient temperature (4 °C) and elevated temperature (14 °C). We here report (1) to what extent soil organic matter composition and/or microbial community composition explain mass-specific growth and mass-specific respiration in permafrost soils at ambient and warmed conditions, and (2) whether soil organic matter composition and microbial community composition also explain the temperature responses of microbial growth and respiration.

Substrates and microbes explain microbial growth and respiration

Microbial growth is limited by carbon availability in soil and carbon allocation to growth and respiration depends on substrate quality, microbial community composition, and microbial interactions (Manzoni et al., 2012; Roller and Schmidt, 2015; Soong et al., 2020; Gunina and Kuzyakov, 2022; Iven et al., 2023). Our investigation of soil organic matter composition and microbial community composition revealed that both factors influence microbial activity in permafrost soils (Tab. 1). We found that microbial mass-specific growth was well explained by microbial community composition and soil organic matter composition across a wide range of permafrost soils, suggesting that both substrates and microbes control possible growth rates. Even though research consistently showed strong influences of edaphic factors

(C, N, P, pH, SWC) on microbial growth (Demoling et al., 2007; Rousk et al., 2009; Fernández-Calviño and Bååth, 2010; Manzoni et al., 2012; Silva-Sánchez et al., 2019; Cruz-Paredes et al., 2021), they did not well explain microbial mass-specific growth in our study, apart from capturing more variance in the random effects (S.Tab. 5). Soil organic carbon as the main energy source of heterotrophic microbes only explained 8 % of growth variance, while soil organic matter composition accounted for 19 %. Therefore, it is not solely the availability of carbon that controls microbial growth, but rather the composition of available substrates. Organic compound quality, particularly energy content of the substance and energy demand for degradation, determine growth efficiency (Manzoni et al., 2012). The partitioning of carbon between catabolism and anabolism depends primarily on the nominal oxidation state of carbon within low molecular weight decomposition products (Gunina and Kuzyakov, 2022). Reduced carbon compounds (e.g., aromatics, lignins, lipids) are thought to be preferentially invested into biomass production (i.e., growth), while oxidized compounds (e.g., carbohydrates, carboxylic acids) are preferentially mineralized (i.e., respiration). Moreover, the more enzymatic steps and metabolic pathways are required to decompose a compound, the more CO_2 will be respired per unit of assimilated carbon and less carbon can be invested into growth (Manzoni et al., 2012; Roller and Schmidt, 2015). Thus, a functionally diverse community is needed to efficiently degrade organic matter compounds. In fact, microbial community composition was the best predictor for mass-specific growth rates in our study, explaining 53 % of variance alone and 56 % of variance in combination with organic matter composition (Tab. 1, S.Tab. 5). Specific community compositions may facilitate growth rates by division of labor, metabolite production and improvement of the micro-scale environment, while others could inhibit growth due to competition and forced investments into defense strategies (Iven et al., 2023).

Overall, our models explained more variance of mass-specific growth than of mass-specific respiration. Our best model explained 40 % of variance in mass-specific respiration and included soil organic matter and microbial community compositions, as well as soil nitrogen (S.Tab. 7). Microbial community composition and soil nitrogen predicted an equal amount of variance. Since microorganisms need to maintain their biomass stoichiometry, soil nitrogen may become important in case of nutrient limitation causing overflow respiration (Manzoni et al., 2012; Mooshammer et al., 2014). Moreover, in contrast to mass-specific growth, part of the variation in mass-specific respiration was explained by edaphic factors (S.Tab. 7). Soil water content, soil organic carbon and soil nitrogen each explained more variance than soil organic matter composition. This relative independence of mass-specific respiration from soil organic matter composition is explainable by the fact that microbes always need to respire to generate energy, independent of which substrate they take up. Considering that 60 % of variance in mass-specific respiration remained unaccounted for, microbial respiration appears to be also dependent on other factors, which were not captured by this study.

Warming alters the controls of microbial growth and respiration

Microbial processes are temperature-dependent and should increase with temperature, as long as substrates are available (Arrhenius, 1889; Davidson and Janssens, 2006; Conant et al., 2011). We investigated the effect of warming on permafrost soil microbes by measuring temperature sensitivity as the Q_{10} of microbial growth and respiration on a mass-specific level. Higher temperatures increased mass-specific growth and mass-specific respiration in permafrost soils (S.Fig. 1). Similar effects of warming have been described in other ecosystems too (Walker et al., 2018; Tian et al., 2023a; Metze et al., 2024). We observed similar temperature sensitivities across all soil layers and polygon types (S.Fig. 1). This suggests a universal impact of global warming on microbial physiology throughout the lowland Arctic. Our results of similar Q_{10} for different polygon types are in concordance to observations that Q_{10} values of microbial growth and respiration are independent of soil moisture content (Cruz-Paredes et al., 2021). However, different Q_{10} values for microbial respiration throughout the permafrost soil profile have been reported (Song et al., 2014; Gentsch et al., 2018), which was not apparent in our study on a mass-specific level. This highlights the importance of expressing rates per unit of microbial biomass to understand the controls over physiological processes. More importantly, our results demonstrate that warming altered the factors controlling mass-specific growth and respiration (Tab. 1). The key drivers of microbial mass-specific growth, microbial community composition and organic matter composition, were similarly good predictors at higher temperatures as at ambient conditions. However, under warming mass-specific respiration lost the link to soil organic matter composition completely and also soil organic carbon and soil nitrogen lost explanatory power (S.Tab. 8). Instead, microbial community composition remained the single factor that explained most of the variance in mass-specific respiration. This unimportance of soil organic matter for mass-specific respiration may be attributed to the alleviation of temperature constraints (Davidson and Janssens, 2006). Higher temperature could reduce activation energies and thereby increase the diversity of organic matter that is accessible to microbes. This would also explain why the diversity of active microbes increases with warming (Metze et al., 2024).

Temperature responses are independent of substrate and community compositions and edaphic factors

Even though microbial community composition and organic matter composition were good predictors of mass-specific growth and mass-specific respiration, they did not explain the temperature responses of these processes (S.Tab. 9, S.Tab. 10). Temperature sensitivity of both mass-specific growth and mass-specific respiration were independent of substrate composition and community composition. Since we observed similar associations under ambient and warmed conditions, we assume that any relationship is nullified when calculating temperature responses. Moreover, physicochemical soil parameters did also not explain

temperature responses (S.Tab. 9, S.Tab. 10). This shows that temperature responses of microbial growth and respiration on a mass-specific level must be determined by other factors, that have not been assessed in our study. Considering our sampling across two sites, three landscape types and four soil layers, alongside this independence from substrates, microbial communities and physicochemical soil parameters, we can expect similar temperature responses to climate warming across other lowland permafrost ecosystems. There is at least one other study, though in boreal forests, that came to similar results, as they did not find any relationship between changes in soil organic carbon or in microbial community and the temperature sensitivity of carbon mineralization (Coucheney et al., 2013). In contrast, Sáez-Sandino et al. (2023) showed that the soil microbiome and microbial biomass were able to explain the variation in Q_{10} of microbial respiration in a global metastudy. However, this study did not look at mass-specific respiration and measured respiration after a short incubation period (10 hours) at different temperatures, which does hardly compare to our eight weeks of incubation or to field conditions.

Summary

It remains poorly understood how permafrost microbiomes will respond to global warming. This study investigated possible abiotic and biotic controls of microbial growth and respiration and their temperature responses in Arctic permafrost soils. We specifically studied the effects of soil organic matter composition, microbial community composition, and physicochemical soil parameters on two key processes in soil carbon cycling, namely microbial growth and respiration. In contrast to other studies, which often focus on one of many permafrost soils and overlook its heterogeneity at the landscape and soil profile scale, we explicitly investigated soils from three common polygon types formed by ice wedge degradation and four different soil layers, including cryoturbated organic matter and the upper frozen permafrost. Organic matter composition and microbial community composition vary across the permafrost soil profile and between polygon types. We demonstrate that soil organic matter composition and microbial community composition both were good predictors for microbial mass-specific growth and respiration rates, explaining more of the variance than physicochemical soil parameters. Soil organic matter composition was found to explain more of the variation in growth than in respiration, while microbial community composition influenced both processes equally. We observed similar associations of organic matter and microbial community composition under ambient and warmed conditions, elucidating why these variables were unable to explain the temperature responses of these processes. This suggests a rather uniform microbial response to climate warming that is not (strongly) dependent on the initial microbial community structure or soil organic matter composition.

SUPPLEMENT

Declaration on Data and Contributions

This study was part of the international EU Horizon 2020 research project "Nunataryuk" on permafrost thaw at the land-sea interface. Work Package 1 "Terrestrial Permafrost" focuses on the quantification of soil organic matter storage and fluxes and their thaw-vulnerability. It was coordinated by Gustaf Hugelius from the University of Stockholm (gustaf.hugelius@natgeo.su.se). The research group at the University of Vienna led by Andreas Richter (andreas.richter@univie.ac.at) focuses on exploring microbial activity in permafrost soils and its response to climate warming. The study presented here is largely based on data of an experiment conducted by PhD student Victoria Sophie Martin (victoria.sophie.martin@univie.ac.at). These data will be thoroughly discussed in her forthcoming publications and PhD thesis and are used here only implicitly. At this point, I would like to thank her for sharing data and for effective collaboration in this project.

The overall study design as well as the work presented here were conceived by Andreas Richter. The fieldwork was conducted by Victoria Sophie Martin, Andreas Richter, and collaborators of the University of Stockholm (Gustaf Hugelius, Willeke A'Campo, Luca Durstewitz, Julia Wagner), the Ca' Foscari University of Venice and CNR Institute of Polar Sciences (Rachele Lodi), the Vrije Universiteit Amsterdam (Niek Speetjens) and the Alfred Wegener Institute in Potsdam (George Tanski, Hugues Lantuit). Lab experiments and analyses were carried out primarily by Victoria Sophie Martin with the help of Julia Horak, Leila Jensen, Moritz Mohrlok, Carolina Urbina Malo, and Cornelia Rottensteiner with important inputs from Alberto Canarini, Hannes Schmidt and Andreas Richter. The new pyrolysis-GC-MS fingerprinting method for untargeted quantitative analysis of soil organic matter composition was jointly developed by Victoria Sophie Martin, Moritz Mohrlok, Alberto Canarini and Cornelia Rottensteiner. The lab work and data analysis of soil organic matter by pyrolysis-GC-MS was carried out by Cornelia Rottensteiner. The raw amplicon sequencing data were processed by Bela Hausmann. Quantitative microbiome profiling by ddPCR was conducted by Cornelia Rottensteiner with valuable insights from Leila Jensen and Hannes Schmidt. Microbiome data analysis was performed by Cornelia Rottensteiner. Statistical analysis with linear mixed effect models was conducted by Cornelia Rottensteiner with instructions and help from Alberto Canarini. The manuscript was written by Cornelia Rottensteiner under the supervision of Andreas Richter, with valuable suggestions by Victoria Sophie Martin, Alberto Canarini and Hannes Schmidt.

All underlying data generated by Victoria Sophie Martin that are essential for this study are briefly outlined in the Supplementary Information. Data analysis by Cornelia Rottensteiner that will be used in other publications are presented in Supplementary Results. For comprehensive details consult the forthcoming publications by Victoria Sophie Martin.

Supplementary Information

Study site

This study was conducted in the Ivvavik National Park, located on the Arctic coast of the Yukon Territory, Canada. The Yukon Coastal Plain lies within the continuous permafrost zone (Angelopoulos et al., 2020) and is characterized by static and turbic cryosols (Lacelle and Soil Classification Working Group, 2001). The landscape is structured by periglacial polygons formed by ice wedge growth and degradation (Wolter et al., 2016). The circumarctic vegetation map classifies the area as low shrub Arctic tundra (bioclimate subzone E) with mean summer temperatures of 10 – 12 °C and dense vegetation cover (80 – 100 %) comprised of mosses, sedges (*Carex sp*), tussock cottongrass (*Eriophorum vaginatum*) and dwarf-shrubs (*Ericales, Salix spp, Betula glandulosa, Rubus chamaemorus*) (Walker et al., 2005; Wolter et al., 2018).

Two sampling campaigns were carried out: one at Ptarmigan Bay (69°29' N, 139°10' W) in 2018 and one in Komakuk Beach (69°34' N, 140°10' W) in 2019. During the last glacial maximum Ptarmigan Bay was covered by the Laurentide Ice Sheet, while Komakuk Beach was not glaciated (Dyke and Prest, 1987; Fritz et al., 2012) (Fig. 6). Mean annual temperature and precipitation (1971-2000) are -10.4 °C and 204 mm at Ptarmigan Bay and -10.8 °C and 199 mm at Komakuk Beach, respectively. Under a high emissions scenario (SSP5-8.5) mean annual temperature is projected to increase to -7.0 °C and -7.4 °C by 2050 and up to -0.7 °C and -1.1 °C by the end of the century for Ptarmigan Bay and Komakuk Beach, respectively. In both sampling areas mean annual precipitation will likely increase over 50 % by the end of the century (ClimateData.ca, 2023). Both sampling campaigns took place in mid-August to guarantee deep thawing of the active layer. Soil samples were taken from 18 soil pits: three low-center, three flat-center, and three high-center polygons per site. Pits of 1x1 m were excavated up to the permafrost table. Soil samples (n = 81) were collected from the active layer (organic soil, mineral soil, cryoturbated organic matter) and from the upper permafrost (10 cm soil cores) and classified according to Schoeneberger *et al.* (2012). Stones, roots and living plant material were removed from the soil samples. All samples were stored at 4 °C until analysis.

Warming experiment

We performed a short-term warming experiment to determine temperature responses (Q_{10}) for microbial growth and microbial respiration. The temperature coefficient Q_{10} is defined as the factor by which a process rate changes when the temperature increases by ten degrees Celsius. Thus, it can be used to describe the temperature sensitivity of microbial process rates (Kirschbaum, 1995), where T is the incubation temperature of the ambient soil in °C.

$$Q_{10} = \frac{\text{process rate } (T+10\ °C)}{\text{process rate } (T)}$$

We incubated each soil sample for eight weeks at two temperatures: 4 °C = "control" (representing average active layer temperature) and 14 °C = "warmed" (+10 °C elevated temperature) in incubators (TC445S, Aqua Lytic). Subsets of each sample (between 30 and 50 g) were weighed into jars (192 mL) and placed on a fine mesh covered with ash-free cellulose filters (Whatman), to allow air circulation but preventing the soil from falling through the mesh. The jar lids had an opening (11 mm Ø) that was covered with polyethylene filter wool (Sera) preventing contamination but allowing gas exchange during the incubation period. We rewetted the soil each week with autoclaved water to maintain the initial water content throughout the incubation period. After eight weeks of incubation we measured microbial biomass, microbial respiration and microbial growth in each sample and calculated temperature responses (Q_{10}). At the end of the incubation, we measured soil parameters again, and assessed bacterial community composition (16S rRNA gene) as described in the Methods section in the main text.

Physicochemical soil parameters

All soil samples were analyzed for gravimetric water content (SWC), soil pH, total organic carbon (C), nitrogen (N), $\delta^{13}C$, $\delta^{15}N$ and total phosphorus (P). In brief, soils were dried at 80 °C for 48 h, weighed for gravimetric water content and finely ground with a ball-mill (Mixer Mill MM200, Retsch) before analyzing total C, N and P. Total soil C and N, as well as $\delta^{13}C$ and $\delta^{15}N$, were determined by EA-IRMS (EA 1110, CE-Instruments, coupled to a Finnigan DeltaPlus IRMS, Thermo Fisher Scientific). Total soil P was analyzed by estimating phosphate with the malachite green assay after ignition at 450 °C for 5 h to convert all organic P into inorganic forms and extraction with 0.5 M H_2SO_4 (1w:40V) for 16 h (D'Angelo et al., 2001). Soil pH was determined in a slurry of fresh soil and Milli-Q water (1:5, w:v) with a pH meter (Sentron SI600 with ConeFET probe, Sentron Europe B.V.).

Microbial biomass, growth, and respiration

Microbial biomass carbon (C_{mic}) was determined by chloroform-fumigation-extraction (Brookes et al., 1985; Vance et al., 1987) with some modifications. In brief, one subset of fresh soil for each sample was directly extracted with 1 M KCl (1:7.5, w:v) for 30 min on an orbital shaker and filtered through ash-free cellulose filters, while another subset was extracted in the same manner after 48 h of fumigation with chloroform in a desiccator. The extracts were stored at -20 °C until analysis of extractable organic carbon with a TOC-analyzer (TOC-V CPH/CPN/TNM-1, Shimadzu). Microbial biomass C was calculated as the difference of extractable organic C in the fumigated samples and the non-fumigated samples and divided by an extraction correction factor of 0.45 (Joergensen, 1996).

We measured microbial growth rates and microbial carbon use efficiency (CUE) via a substrate-independent method, using $H_2{}^{18}O$-incorporation into microbial DNA (Spohn et al.,

2016; Walker et al., 2018). In brief, we incubated duplicates of each soil sample (400 mg) at the respective incubation temperature (4 °C or 14 °C) in 27 mL headspace vials closed with butyl septa (Supelco Analytical, Sigma-Aldrich). One subset was labelled with $H_2{}^{18}O$ (97 at% $H_2{}^{18}O$, Campro Scientific) to reach 20 at% enrichment at 60 % soil water content. The other subset received the same volume of Milli-Q water to serve as an isotopic natural abundance control. To achieve sufficient ^{18}O-label incorporation, the incubation period for samples at 4 °C was 48 h, while samples at 14 °C were only incubated for 24 h.

Microbial respiration was measured as the increase in CO_2 concentration over time. Gas samples of 5 mL were collected with a syringe at the beginning and end of the incubation period. CO_2 concentrations were measured on GasBench-GC-IRMS (GasBench II, Thermo Scientific) in 2018 and by direct injection into an infrared gas analyzer (EGM-4 Environmental Gas Monitor for CO_2, PP Systems) in 2019. Microbial respiration rate (ng C g^{-1} dry soil h^{-1}) was calculated as the increase in CO_2 (ppm) from the start to the end of the incubation (dCO_2) per soil dry weight and incubation time (t) taking the ideal gas equation into account, where p is atmospheric pressure (101.33 kPa), n is the number of moles of the gas (molecular mass of C = 12.01 g mol^{-1}), R is the universal gas constant (8.314 J mol^{-1} K^{-1}), T is the respective incubation temperature (in Kelvin) and V is the volume of the headspace vial (in L).

$$\text{Respiration} = \frac{dCO_2}{\text{dry weight} \times t} \times \frac{p \times n}{R \times T} \times V \times 1000$$

At the end of the incubation period all samples were frozen in liquid nitrogen and stored at -80 °C. Microbial DNA was extracted with an extraction kit (FastDNA™ SPIN Kit for Soil, MP Biomedicals) and quantified fluorometrically using a PicoGreen assay (Quant-iT™ PicoGreen® dsDNA Assay Kit; Thermo Fisher Scientific). The abundance of ^{18}O and total oxygen content was determined by TC/EA-IRMS (TC/EA coupled via a ConFlo III open split system to IRMS, Delta V Advantage, Thermo Fisher Scientific).

We calculated DNA production (µg DNA g^{-1} dry soil h^{-1}) as the product of the total oxygen amount in DNA (O_{DNA}), the excess of ^{18}O abundance (at%) in the labelled sample ($^{18}O_L$) relative to the corresponding natural abundance sample ($^{18}O_{n.a.}$) divided by the ^{18}O-enrichment (at%) in the soil water ($^{18}O_{sw}$) and the average oxygen content in DNA (31.21 %).

$$DNA_{production} = O_{DNA} \times \frac{{}^{18}O_L - {}^{18}O_{n.a.}}{{}^{18}O_{sw}} \times \frac{100}{31.21}$$

Microbial growth rates (ng C g^{-1} dry soil h^{-1}) were inferred by multiplying $DNA_{production}$ with a conversion factor (f_{DNA}) that was calculated for each sample separately, representing the ratio of microbial biomass carbon (µg g^{-1} dry soil) and microbial DNA content (µg g^{-1} dry soil).

$$\text{Growth} = \frac{f_{DNA} \times DNA_{production} \times 1000}{\text{dry weight} \times t}$$

Total C uptake by the microbial community, C_{Uptake} (ng C g^{-1} dry soil h^{-1}), was estimated as the sum of carbon allocated to the production of biomass, C_{Growth} (ng C g^{-1} dry soil h^{-1}), plus the production of CO_2, $C_{Respiration}$ (ng C g^{-1} dry soil h^{-1}). Microbial carbon use efficiency (CUE) was then calculated as the quotient of growth and uptake (Manzoni et al., 2012).

$$CUE = \frac{C_{Growth}}{C_{Growth} + C_{Respiration}} = \frac{C_{Growth}}{C_{Uptake}}$$

Mass-specific growth rates, $Growth_{ms}$ (mg C g^{-1} C_{mic} h^{-1}), and mass-specific respiration rates, $Respiration_{ms}$ (µg C g^{-1} C_{mic} h^{-1}), were calculated by dividing each rate by the microbial biomass carbon, C_{mic} (g C_{mic} g^{-1} dry soil).

$$Growth_{ms} = \frac{C_{Growth}}{C_{mic}}$$

$$Respiration_{ms} = \frac{C_{Respiration}}{C_{mic}}$$

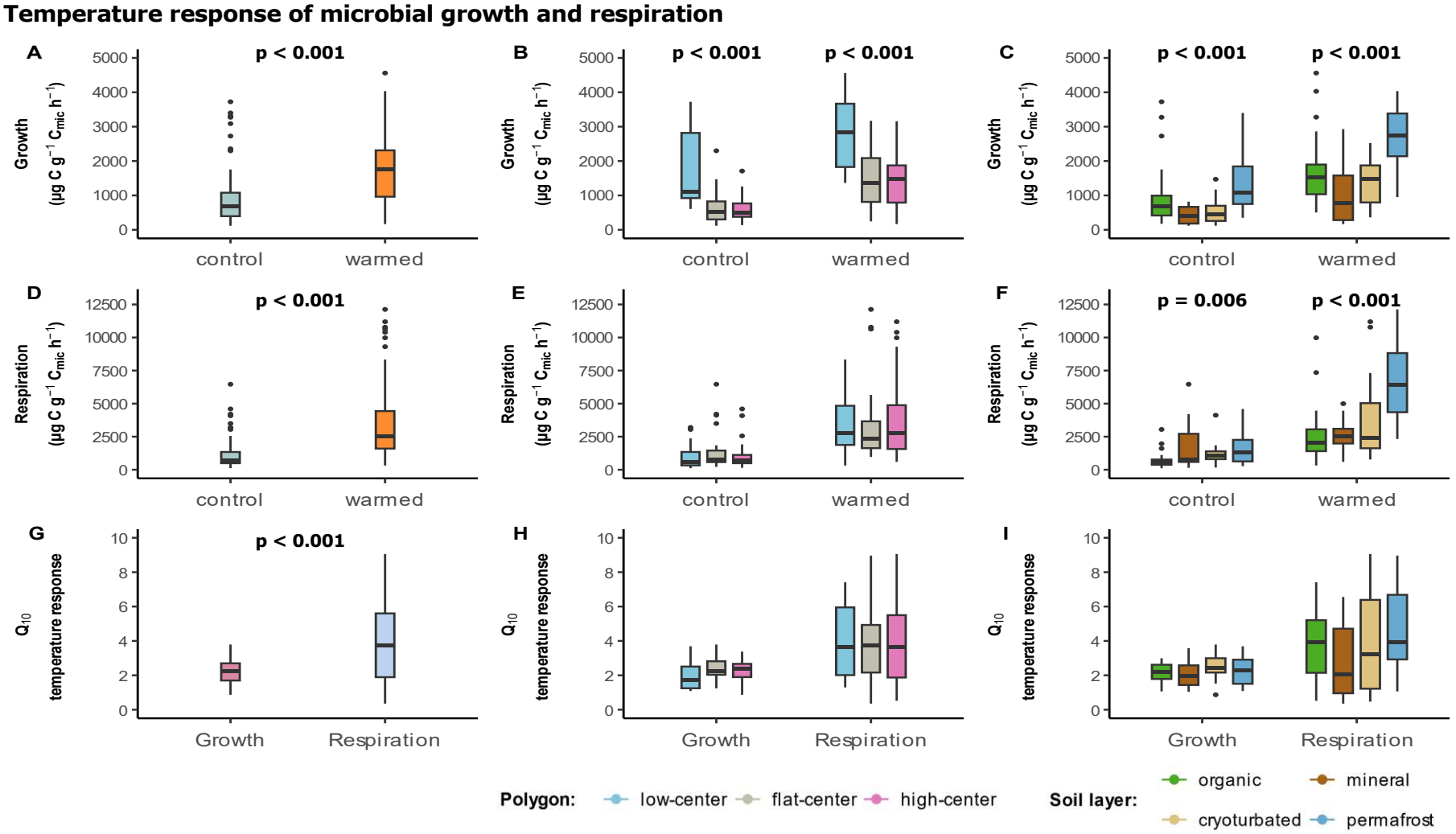

S.Fig. 1: **Microbial mass-specific growth (upper panel) and mass-specific respiration (middle panel) after eight weeks incubation at control (4 °C) and warmed (14 °C) temperature and Q_{10} temperature responses (lower panel).** Displayed are boxplots of all data (left column), polygon types (middle column) and soil layers (right column). Boxes correspond to IQR with median as bold lines, whiskers extend to 1.5 × IQR and data beyond this threshold are depicted as individual points and considered outliers. Significant group differences based on LME (B, C, E, F, G, H, I) or Wilcoxon signed rank test for paired samples (A, D) are displayed at the top.

Supplementary Methods

Sample Structure

S.Tab. 1: Categorization of samples (n = 81) to sites, polygon types and soil layers. Small sample size in some soil layers reflect natural characteristics of the polygons and thus the heterogeneity of permafrost soils.

Sample Structure (n=81)							
glaciated: 39 samples				glaciation-free: 42 samples			
	low-center 8	flat-center 17	high-center 14		low-center 12	flat-center 15	high-center 15
organic 15	4	6	5	organic 20	8	6	6
mineral 7	1	3	3	mineral 7	1	3	3
cryoturbated 7	0	4	3	cryoturbated 6	0	3	3
frozen 10	3	4	3	frozen 9	3	3	3

Pyrolysis-GC-MS fingerprinting approach for SOM composition

Soil organic matter composition was analyzed by a newly developed pyrolysis-GC-MS fingerprinting pipeline that enables a fast identification of compounds for many samples and allows to use the compositional information of unidentifiable compounds.

Two different standards were applied for quality control. We used one external standard, the IHSS Elliott Soil Humic Acid Standard IV (called Soil Standard hereafter), and a custom-made project-specific reference standard, which was a mixture of four soils representative of all soil layers, polygon types and sites (called Mixed Reference hereafter). Soil samples and standards were weighed into pyrolysis glass tubes (constricted Quartz Tubes for 6000 DISC and Autosampler, CDS Analytical). Pre-tests showed that using 0.1 mg for organic horizons and 0.2 mg for mineral soils gave optimal chromatographic results concerning peak size and resolution. All samples were analyzed in a randomized order within three runs to minimize any potential batch effect. Each run included triplicates of the Mixed Reference, one Soil Standard to check instrument performance and multiple blanks to exclude contaminations. The samples were pyrolyzed with a Pyroprobe 6200 on an Autosampler 6250T (CDS Analytics) at an initial temperature of 50 °C (5 sec) followed by a temperature ramp of 20 °C/sec and a final temperature of 600 °C (20 sec). The pyrolysis products were transferred into a GC-TOF-MS (Pegasus BT GC-MS, LECO) with a constant target flow of 1 mL helium/min at 280 °C. After each sample the pyrolysis chamber was heated to 1,000 °C for 60 seconds to clean it before the next sample. A leak check was performed for every sample. The GC (SUPELCOWAX^{TM} 10 Capillary GC Column, Sigma-Aldrich) was set to 50 °C (2 min), followed by an increase of 7 °C/min until a final temperature of 250 °C (5 min), resulting in a total GC time of 35.6 min. The MS was set to an acquisition delay of 150 sec and an acquisition rate of 10 spectra/sec with a mass range of 50 to 640 mu.

The chromatograms were analyzed with ChromaTOF software (version 5.51.50.068774, LECO). We used the Mixed Reference to construct a custom-made library to which we compared all samples. The NIST libraries *mainlib* and *replib* were used to identify peaks of one Mixed Reference. Hits were automatically assigned at a similarity greater than 800. We additionally checked all peaks in the reference sample manually by taking spectral similarity, retention time, expected and observed ion and probability into account. All identified and unidentified peaks (n = 1771) of the Mixed Reference were saved as a library. Unidentified compounds kept their initial peak number as an identifier. This library was then used to analyze all other samples. Peaks were identified by extracted ion chromatograms (XIC, 500 ppm) with a minimum peak S/N of 100 to reduce background noise. Hits were assigned at similarities greater than 700. We performed a quality check on all peaks by checking spectra similarity and retention time of the assigned hits (including both identified and unidentified compounds). Peak hits were cleared if the wrong compound was assigned.

We processed the raw data in R (version 4.2.2 'Innocent and Trusting', R Core Team, 2022) and RStudio (version 2022.12.0.353 'Elsbeth Geranium', RStudio Team, 2022). We used baseR and the packages "dplyr" (Wickham et al., 2022), "tidyverse" (Wickham et al., 2019), "phyloseq" (McMurdie and Holmes, 2013), "vegan" (Oksanen et al., 2022), "pairwiseAdonis" (Martinez Arbizu, 2020) and "ggplot2" (Wickham, 2016).

All samples were blank corrected by calculating mean areas of each compound found in the blanks of a specific run and subtracting those from the compound areas of each sample within the same run. We transformed to relative data by dividing each compound area by the total area of a sample (the sum of all blank corrected exported peak areas). We also converted area to carbon content of each peak by correcting for sample C content es in the following equation.

$$\mathrm{Peak}_{\mathrm{CARBON}} = \frac{\mathrm{Peak}_{\mathrm{AREA}} \times \mathrm{C}_{\mathrm{CONCENTRATION}}}{\mathrm{total\ Sample}_{\mathrm{AREA}}}$$

$\mathrm{Peak}_{\mathrm{CARBON}}$ represents the carbon content (mg C g^{-1} dry soil) of each peak obtained by dividing the $\mathrm{Peak}_{\mathrm{AREA}}$ with the total $\mathrm{Sample}_{\mathrm{AREA}}$ and multiplying by carbon content ($\mathrm{C}_{\mathrm{CONCENTRATION}}$ expressed in mg C g^{-1} dry soil). Here, we assume that the total chromatographic area of a sample relates to the total C amount in the sample weight, and that each compound has the same response factor. Thus, the total C was split to the relative share of each compound area in the total area of the sample.

We used the "phyloseq" package (McMurdie and Holmes, 2013) to analyze the data, as it allows to assemble compound abundance, compound classification and sample information into a single data frame. We classified the compounds to chemical categories based on the US National Library of Medicine (NCBI) Medical Subject Headings (MeSH) Database. We also assigned the most likely origin among the main soil organic matter classes: (1) aromatics & phenols, (2) carbohydrates, (3) lignins, (4) lipids and (5) nitrogen compounds, based on the literature (Saiz-Jimenez and De Leeuw, 1986; Hempfling and Schulten, 1990; Schulten and Schnitzer, 1997; Buurman *et al.*, 2005; Vancampenhout *et al.*, 2009; González-Pérez *et al.*, 2012; Stewart, 2012; Said *et al.*, 2015; Tolu *et al.*, 2015; Ninnes *et al.*, 2017; Shen *et al.*, 2018). If identified compounds were absent from literature, we grouped them according to their chemical similarity to other compounds that could be classified. Compounds that could not be identified were put together as (6) Unclassified.

We checked method performance visually in NMDS plots and statistically with permutational multivariate analysis of variance (PERMANOVA, 999 permutations) based on Bray-Curtis dissimilarities, followed by multilevel pairwise comparisons with Bonferroni correction. The technical replicates of the Soil Standard and of the Mixed Reference formed specific clusters, demonstrating the power and reproducibility of the method. Mixed References centered between all study samples, confirming good coverage of all study samples (S.Fig. 2A). Randomization of samples within and between the runs removed potential batch effects

(S.Fig. 2B). We then excluded the Soil Standards and Mixed References from further analysis. We filtered out all data below a relative abundance of 0.1 %, which mainly omitted compounds with low signal/noise and small area and increased the share of identified compounds to 42 % of total compounds. 534 compounds (226 identified, 308 unidentified) were used for final analysis.

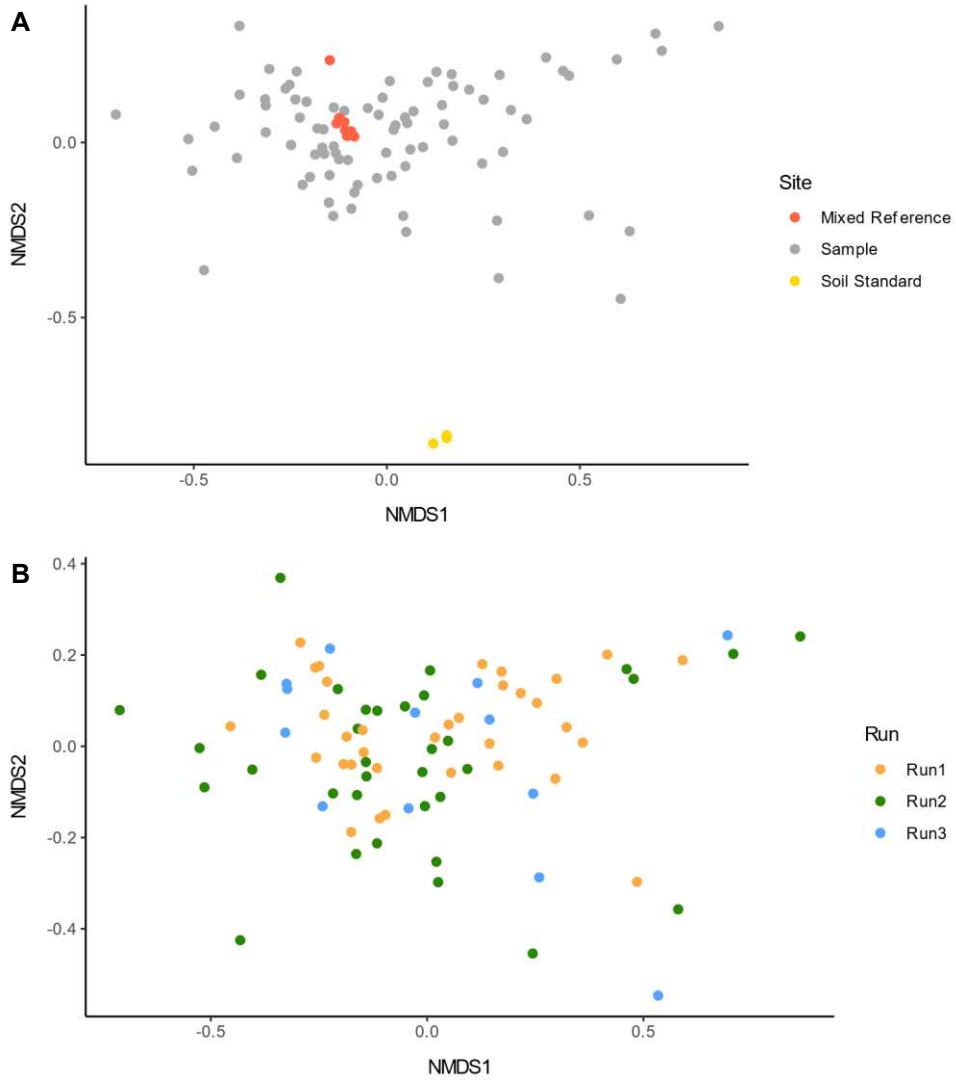

S.Fig. 2: **NMDS plots showing the performance of the pyrolysis-GC-MS method**. Stress = 0.1045. **(A)** Reproducibility is confirmed by technical replicates clustering together for both Soil Standards (yellow) and Mixed References (red). Soil Standards cluster distant to all soil samples (grey) demonstrating differences on an ecosystem scale (PERMANOVA, p_{adj} = 0.003). Replicates of the Mixed Reference Sample form a cluster amidst all soil samples, confirming that all sample types (sites, polygons, soil layers) are equally represented in the Mixed Reference. The Mixed Reference that was used as a library lies a bit offside, showing that not all peaks can be re-found. **(B)** Randomization of soil samples within the three runs on the pyrolysis-GC-MS allowed to rule out a possible batch effect (PERMANOVA, p = 0.106).

Analysis of gene copy numbers with digital droplet PCR

Digital droplet PCR (ddPCR) was used to quantify 16S rRNA genes and ITS1 regions from DNA extracts of soils. Each ddPCR reaction (22 µL) contained 1x QX200 ddPCR EvaGreen Supermix (Bio-Rad), 0.1 µmol L^{-1} of primer pairs 515F-806R (Apprill et al., 2015; Parada et al., 2016) or ITS1F-ITS2 (White et al., 1990; Smith and Peay, 2014) and 0.1 ng of template DNA for 16S rRNA gene quantification or 1 ng of template DNA for ITS1 region quantification (2 ng of template were required for extracts with very low DNA concentrations).

Reagent	Final conc.	Vol. per PCR (µl)	N. of PCRs	Total vol. (µl)
QX200 ddPCR EvaGreen Supermix (2x)	1x	11	97	1067
F primer (10 µM)	0.1 µM	0.2		19.4
R primer (10 µM)	0.1 µM	0.2		19.4
DNase free water		8.6		834.2
DNA template		2		
Total PCR volume		22		

Droplets were generated on a QX200TM Droplet Generator (Bio-Rad) and immediately subjected to PCR amplification (T100 Thermal Cycler, Bio-Rad), with the following settings.

	515F/806R	ITS1F-ITS2
1	95 °C 5 min	95 °C 5 min
2	95 °C 30 sec	95 °C 30 sec
3	57 °C 2,5 min (-1 °C each step)	60 °C 2,5 min (-1 °C each step)
	Back to step 2 (x4)	Back to step 2 (x4)
4	95 °C 30 sec	95 °C 30 sec
5	52 °C 2,5 min	55 °C 2,5 min
	Back to step 4 (x34)	*Back to step 4 (x34)*
6	4 °C 5 min	4 °C 5 min
7	90 °C 5 min	90 °C 5 min
8	4 °C hold	4 °C hold
	Add a ramp rate of 2 °C/sec to all PCR steps.	

Fluorescence intensity was measured on a QX200 Droplet Reader (Bio-Rad) and gene copy numbers were calculated using the QX ONE Software (version 1.2, Bio-Rad) following Angel and Petrova, 2020. The threshold between positive and negative droplets was set manually, yet consistently. Final ddPCR results were expressed as gene or region copy numbers g^{-1} dry soil.

Supplementary Results

Correlation of SOM and microbial community PCoA axes and soil parameters

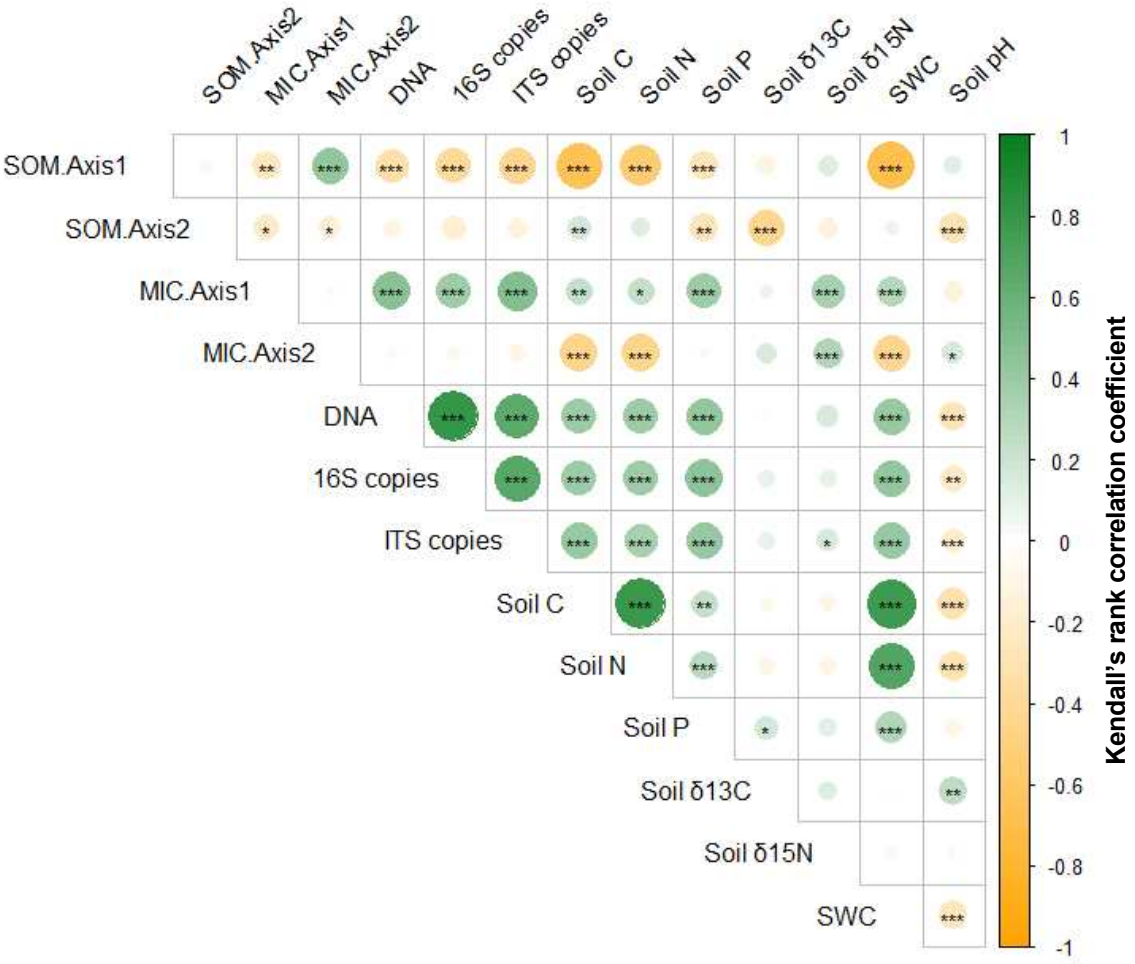

S.Fig. 3: **Correlations between PCoA-Axes 1 and 2 of soil organic matter composition (SOM), microbial community composition (MIC) and physicochemical and biological soil parameters.** Kendall's rank correlation coefficient was chosen due to non-normality and rank ties. Significant correlations are indicated with asterisks ($p < 0.001$ ***, < 0.01 **, < 0.05 *). Dot color and size indicate the strength and direction of the correlation (green = positive correlation, orange = negative correlation). DNA in µg g^{-1} dry soil; 16S rRNA gene and ITS1 region copies as copy numbers g^{-1} dry soil; Soil C, N and P in mg g^{-1} dry soil; $\delta^{13}C$ and $\delta^{15}N$ in ‰; Soil water content (SWC) in g H_2O g^{-1} dry soil.

Physicochemical and biological soil parameters

S.Tab. 2: **Physicochemical and biological soil parameters.** Mean values per gram dry soil (d. s.) with standard deviations (SD) and standard errors (SE) **(A)** for all samples **(B)** per polygon type **(C)** per soil layer. **(D)** Differences between polygon types and between soil layers, derived from LME model results [~ Polygon + Soil layer + (1|Site/Pit)] and Tukey adjusted pairwise comparisons. Letters indicate differences at $p < 0.05$, with "a" denoting the highest values. Results were generated with the packages "lme4" (Bates et al., 2015), "lmerTest" (Kuznetsova et al., 2017) and "emmeans" (Lenth, 2023).

A

Parameter	Total		
	Mean	SD	SE
water ($g\ H_2O\ g^{-1}$ d. s.)	2.3	1.6	0.2
pH (in H_2O)	5.8	0.3	0.0
C ($mg\ C\ g^{-1}$ d. s.)	240.0	133.1	14.8
N ($mg\ N\ g^{-1}$ d. s.)	12.8	7.2	0.8
P ($mg\ P\ g^{-1}$ d. s.)	0.6	0.3	0.0
$\delta^{13}C$ (‰)	-27.3	0.9	0.1
$\delta^{15}N$ (‰)	1.2	1.1	0.1
DNA ($\mu g\ DNA\ g^{-1}$ d. s.)	25.3	31.7	3.5
16S copies ($Mio\ g^{-1}$ d. s.)	2,278.3	2,349.5	261.1
ITS copies ($Mio\ g^{-1}$ d. s.)	69.9	186.4	20.7

B

Parameter	Polygon								
	low-center			flat-center			high-center		
	Mean	SD	SE	Mean	SD	SE	Mean	SD	SE
water ($g\ H_2O\ g^{-1}$ d. s.)	2.9	1.5	0.3	2.2	1.8	0.3	2.0	1.5	0.3
pH (in H_2O)	5.7	0.4	0.1	5.9	0.3	0.0	5.7	0.3	0.1
C ($mg\ C\ g^{-1}$ d. s.)	312.4	137.8	30.8	204.2	122.6	21.7	229.6	125.7	23.3
N ($mg\ N\ g^{-1}$ d. s.)	18.1	8.5	1.9	10.0	5.1	0.9	12.1	6.5	1.2
P ($mg\ P\ g^{-1}$ d. s.)	0.4	0.2	0.0	0.7	0.3	0.0	0.6	0.3	0.1
$\delta^{13}C$ (‰)	-27.9	0.6	0.1	-26.7	0.7	0.1	-27.4	0.9	0.2
$\delta^{15}N$ (‰)	0.3	0.6	0.1	1.3	1.1	0.2	1.6	1.2	0.2
DNA ($\mu g\ DNA\ g^{-1}$ d. s.)	18.3	25.4	5.7	28.2	37.4	6.6	27.0	28.8	5.4
16S copies ($Mio\ g^{-1}$ d. s.)	1,511.3	1,898.0	424.4	2,610.0	2,501.0	442.1	2,441.2	2,414.1	448.3
ITS copies ($Mio\ g^{-1}$ d. s.)	10.5	18.0	4.0	72.6	160.4	28.4	107.9	258.0	47.9

C

Parameter	Soil layer											
	organic			mineral			cryoturbated			permafrost		
	Mean	SD	SE	Mean	SD	SE	Mean	SD	SE	Mean	SD	SE
water ($g\ H_2O\ g^{-1}$ d. s.)	3.7	1.3	0.2	0.4	0.1	0.0	1.4	0.7	0.2	1.8	0.8	0.2
pH (in H_2O)	5.6	0.4	0.1	5.9	0.2	0.1	5.8	0.3	0.1	5.9	0.3	0.1
C ($mg\ C\ g^{-1}$ d. s.)	351.2	91.9	15.5	63.3	28.3	7.6	185.4	69.5	19.3	202.8	84.3	19.3
N ($mg\ N\ g^{-1}$ d. s.)	18.4	6.1	1.0	3.6	1.5	0.4	10.1	3.9	1.1	11.0	3.9	0.9
P ($mg\ P\ g^{-1}$ d. s.)	0.7	0.3	0.1	0.5	0.2	0.1	0.5	0.2	0.1	0.5	0.2	0.0
$\delta^{13}C$ (‰)	-27.3	0.9	0.2	-27.6	1.0	0.3	-27.2	0.8	0.2	-27.0	0.8	0.2
$\delta^{15}N$ (‰)	1.4	1.2	0.2	1.6	1.1	0.3	1.0	0.7	0.2	0.6	1.1	0.3
DNA ($\mu g\ DNA\ g^{-1}$ d. s.)	47.7	37.4	6.3	6.3	4.4	1.2	15.2	6.8	1.9	5.3	4.1	0.9
16S copies ($Mio\ g^{-1}$ d. s.)	3,939.2	2,627.1	444.1	476.5	334.5	89.4	1,664.0	1,057.5	293.3	966.6	832.2	190.9
ITS copies ($Mio\ g^{-1}$ d. s.)	155.7	261.4	44.2	2.4	3.2	0.9	10.3	15.1	4.2	2.5	4.8	1.1

D

Parameter	Polygon				Soil layer				
	p-value	low	flat	high	p-value	organic	mineral	cryoturbated	permafrost
water ($g\ H_2O\ g^{-1}$ d. s.)	0.603				<0.001	a	c	b	b
pH (in H_2O)	0.165				<0.001	b	a	ab	a
C ($mg\ C\ g^{-1}$ d. s.)	0.111				<0.001	a	c	b	b
N ($mg\ N\ g^{-1}$ d. s.)	0.001	a	b	b	<0.001	a	c	b	b
P ($mg\ P\ g^{-1}$ d. s.)	<0.001	b	a	a	<0.001	a	b	b	b
$\delta^{13}C$ (‰)	0.001	b	a	b	0.015	ab	b	ab	a
$\delta^{15}N$ (‰)	0.002	b	a	a	0.003	a	ab	b	b
DNA ($\mu g\ DNA\ g^{-1}$ d. s.)	<0.001	b	a	a	<0.001	a	c	b	c
16S copies ($Mio\ g^{-1}$ d. s.)	<0.001	b	a	a	<0.001	a	b	b	b
ITS copies ($Mio\ g^{-1}$ d. s.)	<0.001	b	a	a	<0.001	a	b	b	b

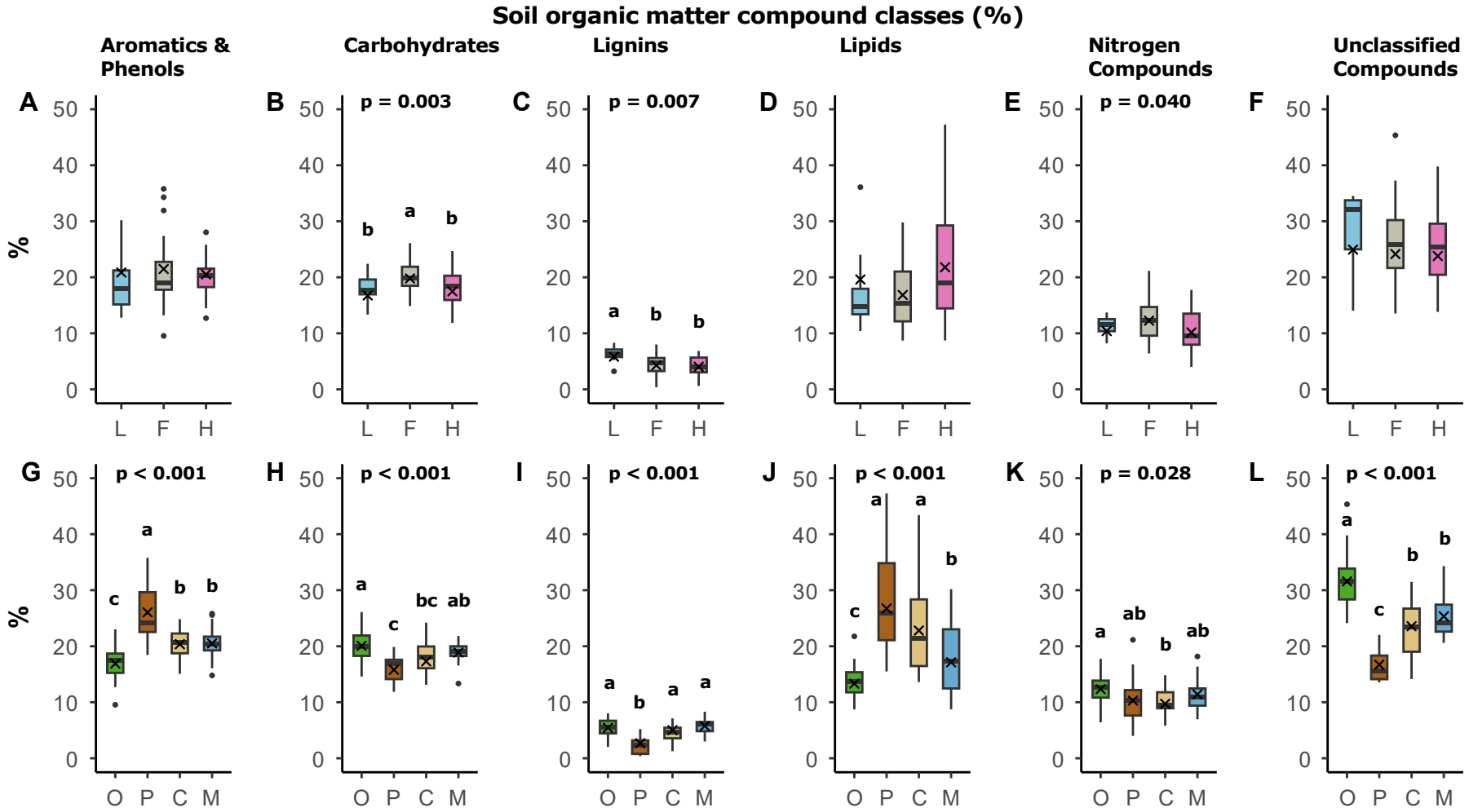

S.Fig. 4: **Soil organic matter compound classes (%) for polygon types (upper panel) and soil layer types (lower panel).** Boxplots show percentages of aromatics & phenols, carbohydrates, lignins, lipids, nitrogen compounds and unclassified compounds. Boxes correspond to IQR with median as bold lines, whiskers extend to 1.5 × IQR and data beyond this threshold are considered outliers (depicted as points). Significant group differences from LME model results [~ polygon + soil layer + (1|Site/Pit)] computed with "lme4" (Bates et al., 2015) and "lmerTest" (Kuznetsova et al., 2017) are displayed at the top. Letters indicate Tukey adjusted pairwise differences. Crosses display estimated marginal means. Pairwise comparisons were generated by the emmeans() function (Lenth, 2023). L = low-center polygon, F = flat-center polygon, H = high-center polygon, O = organic, M = mineral, C = cryoturbated, P = permafrost.

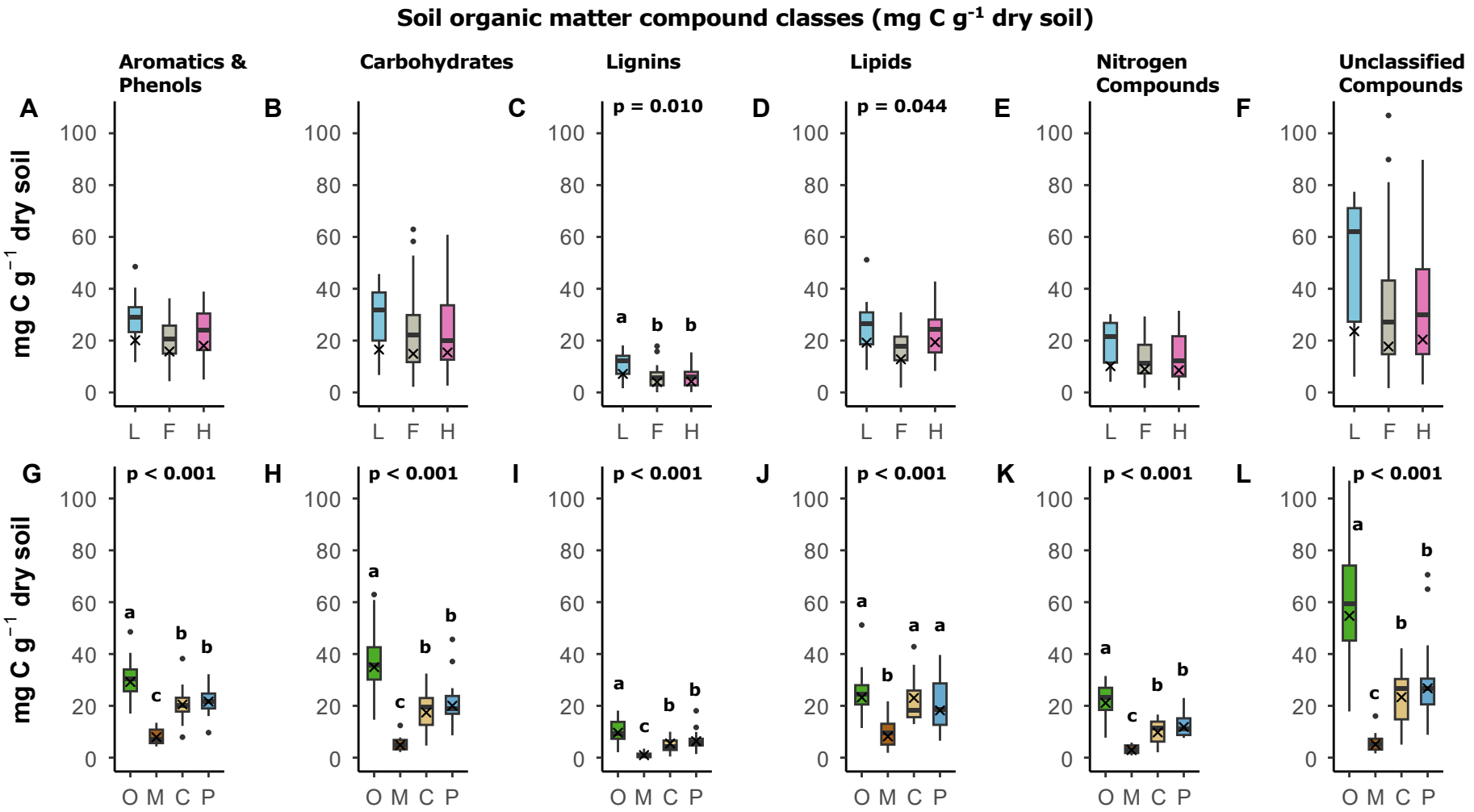

S.Fig. 5: **Absolute (mg C g^{-1} dry soil) soil organic matter compound classes for polygon types (upper panel) and soil layer types (lower panel).** Boxplots show total aromatics & phenols, carbohydrates, lignins, lipids, nitrogen compounds and unclassified compounds. Boxes correspond to IQR with median as bold lines, whiskers extend to 1.5 × IQR and data beyond this threshold are considered outliers (depicted as points). Significant group differences from LME model results [~ polygon + soil layer + (1|Site/Pit)] computed with "lme4" (Bates et al., 2015) and "lmerTest" (Kuznetsova et al., 2017) are displayed at the top. Letters indicate Tukey adjusted pairwise differences. Crosses display estimated marginal means. Pairwise comparisons were generated by the emmeans() function (Lenth, 2023). L = low-center polygon, F = flat-center polygon, H = high-center polygon, O = organic, M = mineral, C = cryoturbated, P = permafrost.

Soil organic matter composition statistics

S.Tab. 3: **Compositional differences in soil organic matter compounds between polygons and soil layers. (A)** Results of PERMANOVA. **(B)** Differences in dispersion. **(C)** Results of pairwise PERMANOVA.

A

PERMANOVA	DF	SSq	R^2	F value	p-value
Soil layer	3	1.91	0.34	15.05	0.001
Polygon	2	0.46	0.08	5.50	0.001
Interaction	5	0.23	0.04	1.08	0.318
Residuals	70	2.96	0.53		
Total	80	5.56	1.00		

B

Dispersion	DF	SSq	MSq	F value	p-value
Soil layer	3	0.03	0.01	2.87	0.042
Residuals	77	0.25	0.00		
Polygon	2	0.04	0.02	2.60	0.081
Residuals	78	0.56	0.01		

C

PERMANOVA	pairs	SSq	R^2	F value	p.adj
Polygon	low vs flat	0.37	0.11	6.30	0.003
	low vs high	0.34	0.10	5.50	0.006
	flat vs high	0.22	0.05	3.10	0.084
Soil layer	org vs min	1.60	0.41	32.29	0.006
	org vs cryo	0.55	0.21	12.17	0.006
	org vs perm	0.35	0.14	8.54	0.006
	min vs cryo	0.28	0.16	4.59	0.006
	min vs perm	0.60	0.28	11.81	0.006
	cryo vs perm	0.12	0.08	2.62	0.126

Microbial community composition statistics

S.Tab. 4: **Compositional differences in microbial communities between polygons and soil layers. (A)** Results of PERMANOVA. **(B)** Differences in dispersion. **(C)** Results of pairwise PERMANOVA.

A

PERMANOVA	DF	SSq	R^2	F value	p-value
Soil layer	3	4.90	0.18	6.20	0.001
Polygon	2	2.89	0.11	5.49	0.001
Interaction	5	2.44	0.09	1.85	0.001
Residuals	65	17.13	0.63		
Total	75	27.36	1.00		

B

Dispersion	DF	SSq	MSq	F value	p-value
Soil layer	3	0.21	0.07	10.46	<0.001
Residuals	72	0.48	0.01		
Polygon	2	0.07	0.03	6.87	0.002
Residuals	73	0.37	0.01		

C

PERMANOVA	pairs	SSq	R^2	F value	p.adj
Polygon	low vs flat	1.83	0.11	5.49	0.003
	low vs high	2.01	0.12	6.32	0.003
	flat vs high	0.57	0.03	1.61	0.264
Soil layer	org vs min	1.42	0.08	4.09	0.006
	org vs cryo	1.67	0.10	4.98	0.006
	org vs perm	2.99	0.16	9.32	0.006
	min vs cryo	0.47	0.07	1.62	0.522
	min vs perm	1.29	0.14	4.65	0.006
	cryo vs perm	0.80	0.11	3.24	0.006

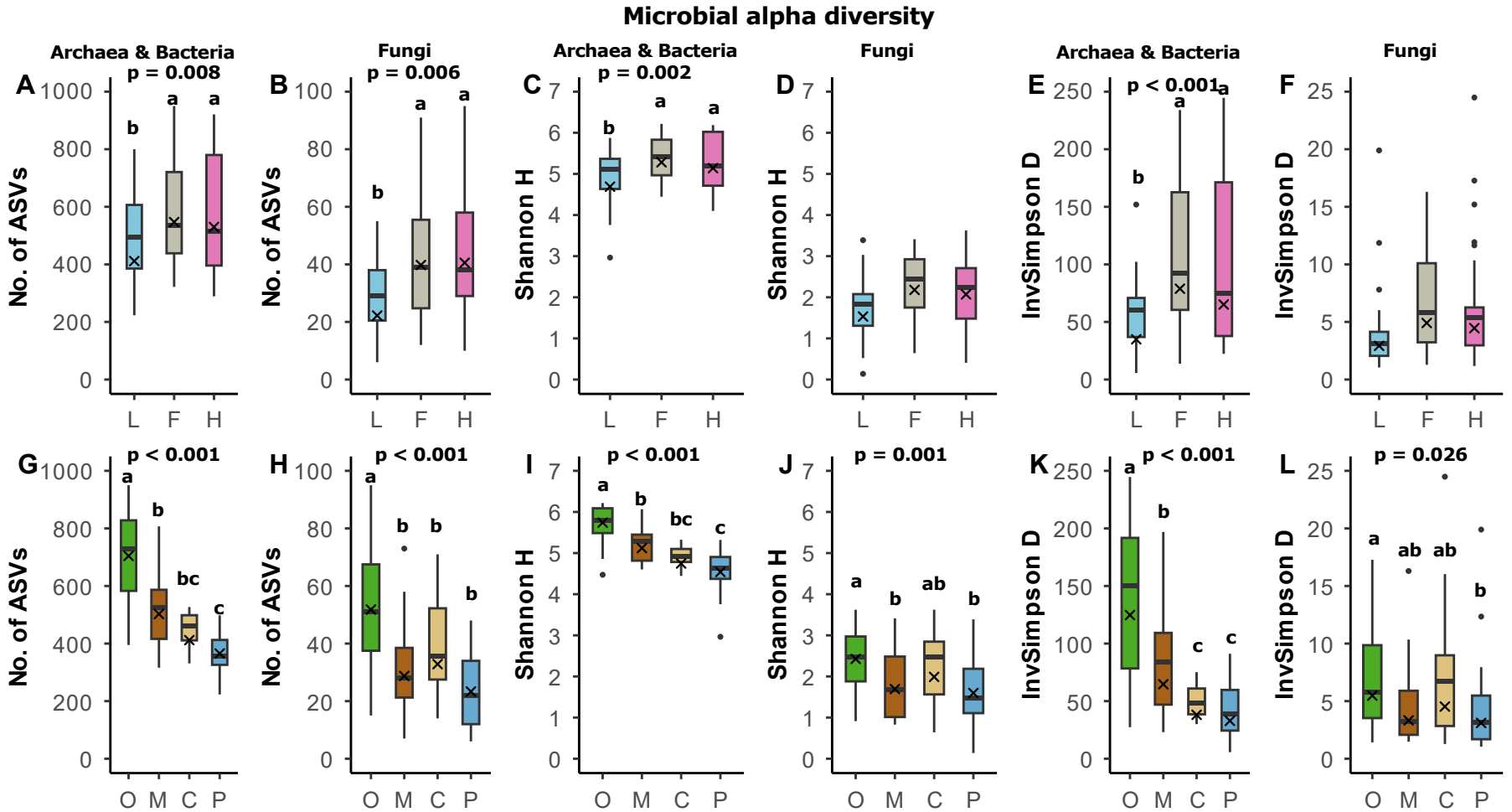

S.Fig. 6: **Microbial alpha diversity for polygon types (upper panel) and soil layers (lower panel).** Boxplots show observed ASV richness **(left),** Shannon diversity **(middle)** and Inverse Simpson diversity **(right)** for archaea, bacteria and fungi based on rarefied reads (cutoff at 2650 16S rRNA gene reads and at 543 ITS1 region reads). Indices were computed with estimate_richness() function (McMurdie and Holmes, 2013). Boxes correspond to IQR with median as bold lines, whiskers extend to 1.5 × IQR and data beyond this threshold are considered outliers (depicted as points). Significant group differences from LME model results [~ polygon + soil layer + (1|Site/Pit)] computed with "lme4" (Bates et al., 2015) and "lmerTest" (Kuznetsova et al., 2017) are displayed at the top. Letters indicate Tukey adjusted pairwise differences. Crosses display estimated marginal means. Pairwise comparisons were generated by the emmeans() function (Lenth, 2023). L = low-center polygon, F = flat-center polygon, H = high-center polygon, O = organic, M = mineral, C = cryoturbated, P = permafrost.

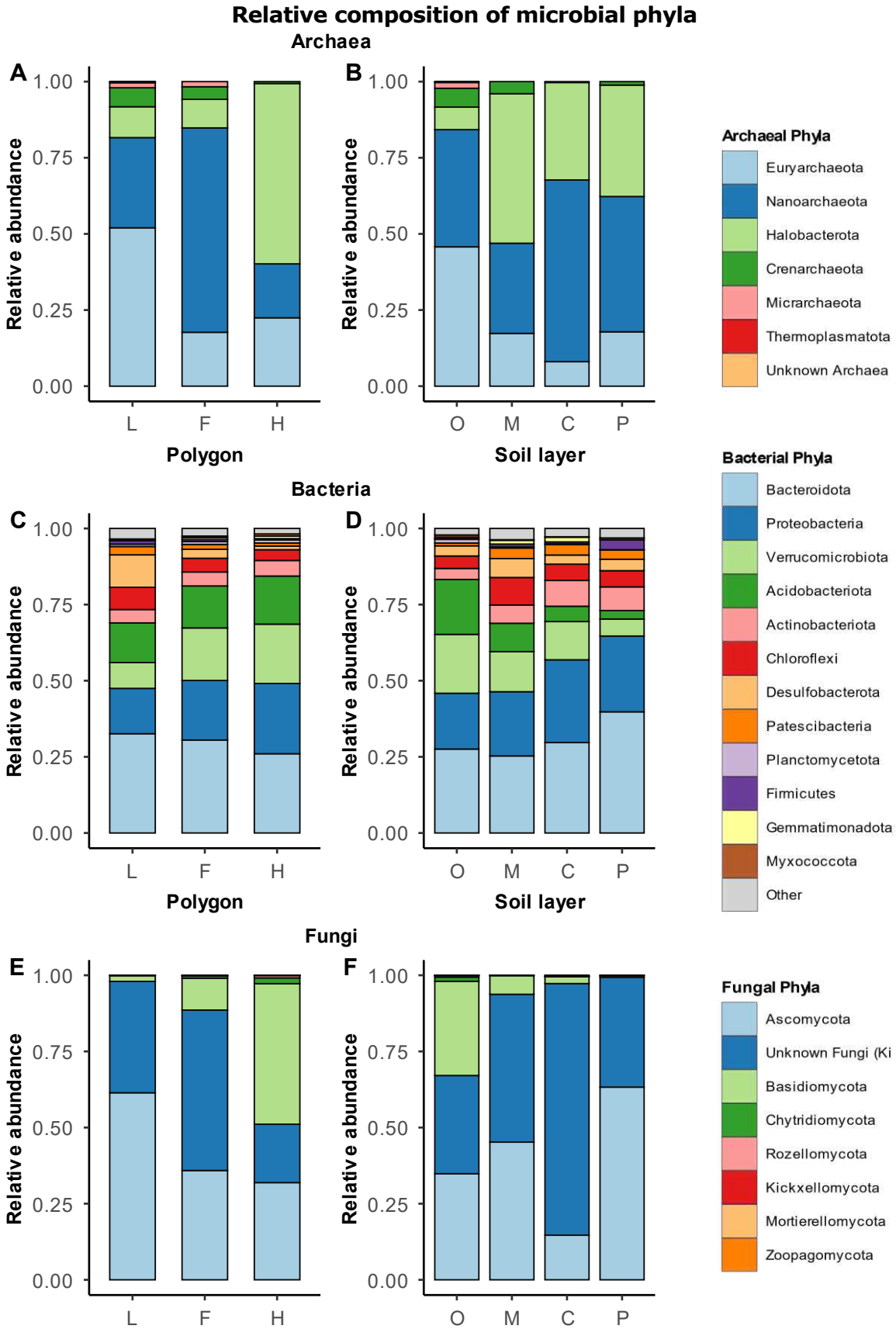

S.Fig. 7: **Relative abundances of archaea (top), bacteria (middle) and fungi (bottom) between different polygon types (left) and soil layers (right).** Data were computed with "phyloseq" (McMurdie and Holmes, 2013) and visualized with "microViz" (Barnett et al., 2021). L = low-center polygon, F = flat-center polygon, H = high-center polygon, O = organic, M = mineral, C = cryoturbated, P = permafrost.

Linear mixed effect model results

S.Tab. 5: **Linear mixed effect model results for mass-specific growth at 4 °C.** Depicted are one factor models of environmental parameters (soil water content (SWC), soil pH, soil C, N, P) and PCoA axes (SOM1, SOM2, MIC1, MIC2), a model of soil organic matter composition (SOM) with both PCoA axes, a model of microbial community composition with both PCoA axes, a model of microbial community composition and soil C (MIC.C), a model including SOM and MIC compositions (full), and an extended full model including soil N (full.N).

Model	Predictor	MSQ	DDF	F value	p-value	R^2m	R^2c	AIC	BIC	logLik	Dev.
SWC	SWC	1.24	61.39	3.01	0.088	0.03	0.42	165.38	176.76	-77.69	155.38
pH	pH	0.30	67.58	0.73	0.397	0.01	0.43	167.44	178.82	-78.72	157.44
C	C	3.69	65.90	9.08	0.004	0.08	0.42	160.45	171.83	-75.22	150.45
N	N	1.51	68.43	3.44	0.068	0.04	0.37	165.70	177.08	-77.85	155.70
P	P	2.18	61.99	5.24	0.026	0.04	0.45	163.88	175.26	-76.94	153.88
SOM1	SOM.Axis1	4.37	65.19	11.47	0.001	0.10	0.45	157.72	169.10	-73.86	147.72
SOM2	SOM.Axis2	1.91	54.76	4.76	0.033	0.05	0.48	163.93	175.32	-76.97	153.93
SOM	SOM.Axis1	6.51	67.30	17.12	<0.001	0.19	0.48	151.63	165.29	-69.82	139.63
	SOM.Axis2	3.72	28.71	9.77	0.004						
MIC1	MIC.Axis1	5.11	63.56	13.97	<0.001	0.11	0.49	155.70	167.09	-72.85	145.70
MIC2	MIC.Axis2	16.37	69.49	53.55	<0.001	0.37	0.53	131.64	143.02	-60.82	121.64
MIC	MIC.Axis1	6.94	68.00	33.34	<0.001	0.53	0.68	105.63	119.29	-46.82	93.63
	MIC.Axis2	16.14	68.36	77.51	<0.001						
MIC.C	MIC.Axis1	7.79	67.01	40.05	<0.001	0.54	0.70	102.05	117.99	-44.03	88.05
	MIC.Axis2	3.82	67.31	19.63	<0.001						
	C	1.11	67.07	5.69	0.020						
full	SOM.Axis1	2.17	66.00	12.10	<0.001	0.56	0.73	97.18	115.39	-40.59	81.18
	SOM.Axis2	0.42	66.20	2.33	0.131						
	MIC.Axis1	7.99	66.02	44.64	<0.001						
	MIC.Axis2	2.61	66.19	14.58	<0.001						
full.N	SOM.Axis1	3.15	65.04	19.01	<0.001	0.56	0.75	92.96	113.45	-37.48	74.96
	SOM.Axis2	1.13	65.27	6.81	0.011						
	MIC.Axis1	5.51	65.06	33.28	<0.001						
	MIC.Axis2	3.46	65.06	20.92	<0.001						
	N	1.03	65.14	6.23	0.015						

S.Tab. 6: **Linear mixed effect model results for mass-specific growth at 14 °C.** Depicted are one factor models of environmental parameters (soil water content (SWC), soil pH, soil C, N, P) and PCoA axes (SOM1, SOM2, MIC1, MIC2), a model of soil organic matter composition (SOM) with both PCoA axes, a model of microbial community composition with both PCoA axes, a model of microbial community composition and soil C (MIC.C), and a model including SOM and MIC compositions (full).

Model	Predictor	MSQ	DDF	F value	p-value	R^2m	R^2c	AIC	BIC	logLik	Dev.
SWC	SWC	0.88	63.10	2.49	0.120	0.02	0.38	146.63	158.02	-68.32	136.63
pH	pH	0.50	60.39	1.48	0.228	0.02	0.40	147.32	158.70	-68.66	137.32
C	C	3.52	69.06	10.37	0.002	0.09	0.41	140.17	151.55	-65.08	130.17
N	N	2.20	69.28	6.11	0.016	0.06	0.35	143.95	155.33	-66.97	133.95
P	P	0.90	66.27	2.60	0.112	0.02	0.43	146.62	158.00	-68.31	136.62
SOM1	SOM.Axis1	5.05	69.16	16.24	<0.001	0.13	0.43	134.73	146.11	-62.37	124.73
SOM2	SOM.Axis2	0.79	48.66	2.29	0.136	0.02	0.43	146.81	158.20	-68.41	136.81
SOM	SOM.Axis1	6.23	68.12	21.54	<0.001	0.18	0.49	129.78	143.44	-58.89	117.78
	SOM.Axis2	2.09	68.02	7.21	0.009						
MIC1	MIC.Axis1	4.45	66.74	14.99	<0.001	0.11	0.49	135.32	146.71	-62.66	125.32
MIC2	MIC.Axis2	10.38	69.35	42.81	<0.001	0.30	0.52	115.63	127.01	-52.81	105.63
MIC	MIC.Axis1	5.02	68.01	29.14	<0.001	0.45	0.66	92.58	106.24	-40.29	80.58
	MIC.Axis2	10.39	68.27	60.30	<0.001						
MIC.C	MIC.Axis1	5.82	67.00	36.24	<0.001	0.46	0.69	88.76	104.69	-37.38	74.76
	MIC.Axis2	2.21	67.20	13.75	<0.001						
	C	0.95	67.03	5.89	0.018						
full	SOM.Axis1	2.91	65.79	22.71	<0.001	0.54	0.75	76.17	94.38	-30.08	60.17
	SOM.Axis2	0.03	52.43	0.20	0.658						
	MIC.Axis1	7.43	65.73	58.07	<0.001						
	MIC.Axis2	0.95	54.75	7.39	0.009						

S.Tab. 7: **Linear mixed effect model results for mass-specific respiration at 4 °C.** Depicted are one factor models of environmental parameters (soil water content (SWC), soil pH, soil C, N, P) and PCoA axes (SOM1, SOM2, MIC1, MIC2), a model of soil organic matter composition (SOM) with both PCoA axes, a model of microbial community composition with both PCoA axes, a model of microbial community composition and soil C (MIC.C), a model including SOM and MIC compositions (full), and an extended full model including soil N (full.N).

Model	Predictor	MSQ	DDF	F value	p-value	R^2m	R^2c	AIC	BIC	logLik	Dev.
SWC	SWC	5.83	67.19	8.73	0.004	0.11	0.16	180.47	191.72	-85.24	170.47
pH	pH	1.53	67.97	2.10	0.152	0.03	0.09	186.82	198.06	-88.41	176.82
C	C	6.72	67.08	10.25	0.002	0.12	0.18	179.02	190.27	-84.51	169.02
N	N	9.14	67.51	14.83	<0.001	0.16	0.26	175.74	186.98	-82.87	165.74
P	P	1.72	67.30	2.36	0.129	0.03	0.08	186.32	197.57	-88.16	176.32
SOM1	SOM.Axis1	1.04	67.60	1.41	0.240	0.02	0.07	187.29	198.53	-88.65	177.29
SOM2	SOM.Axis2	2.62	67.87	3.63	0.061	0.05	0.07	184.62	195.86	-87.31	174.62
SOM	SOM.Axis1	1.51	66.58	2.13	0.149	0.07	0.11	184.70	198.19	-86.35	172.70
	SOM.Axis2	3.06	66.61	4.32	0.042						
MIC1	MIC.Axis1	8.03	67.18	12.90	<0.001	0.15	0.21	177.19	188.43	-83.59	167.19
MIC2	MIC.Axis2	1.08	67.97	1.47	0.230	0.02	0.08	187.35	198.60	-88.68	177.35
MIC	MIC.Axis1	7.51	66.29	11.87	<0.001	0.16	0.21	178.07	191.56	-83.03	166.07
	MIC.Axis2	0.97	43.79	1.54	0.221						
MIC.C	MIC.Axis1	2.52	65.01	4.03	0.049	0.19	0.22	177.05	192.79	-81.52	163.05
	MIC.Axis2	0.08	65.97	0.13	0.725						
	C	1.73	65.43	2.77	0.101						
full	SOM.Axis1	0.75	64.03	1.34	0.252	0.28	0.29	169.61	187.59	-76.80	153.61
	SOM.Axis2	5.39	64.29	9.56	0.003						
	MIC.Axis1	11.34	64.96	20.11	<0.001						
	MIC.Axis2	1.05	65.00	1.86	0.178						
full.N	SOM.Axis1	2.62	58.80	5.28	0.025	0.35	0.40	165.50	185.74	-73.75	147.50
	SOM.Axis2	1.34	58.24	2.69	0.106						
	MIC.Axis1	6.75	63.18	13.60	<0.001						
	MIC.Axis2	0.12	57.90	0.23	0.632						
	N	3.42	60.42	6.89	0.011						

S.Tab. 8: **Linear mixed effect model results for mass-specific respiration at 14 °C.** Depicted are one factor models of environmental parameters (soil water content (SWC), soil pH, soil C, N, P) and PCoA axes (SOM1, SOM2, MIC1, MIC2), a model of soil organic matter composition (SOM) with both PCoA axes, a model of microbial community composition with both PCoA axes, a model of microbial community composition and soil C (MIC.C), and a model including SOM and MIC compositions (full).

Model	Predictor	MSQ	DDF	F value	p-value	R^2m	R^2c	AIC	BIC	logLik	Dev.
SWC	SWC	4.63	63.01	8.76	0.004	0.10	0.28	157.30	168.25	-73.65	147.30
pH	pH	1.11	63.54	1.90	0.173	0.02	0.19	163.60	174.55	-76.80	153.60
C	C	3.26	63.00	5.93	0.018	0.07	0.27	159.95	170.90	-74.98	149.95
N	N	3.45	63.16	6.29	0.015	0.07	0.24	159.42	170.37	-74.71	149.42
P	P	0.93	63.10	1.59	0.212	0.02	0.20	164.02	174.97	-77.01	154.02
SOM1	SOM.Axis1	1.78	63.08	3.10	0.083	0.04	0.22	162.52	173.47	-76.26	152.52
SOM2	SOM.Axis2	0.00	63.50	0.00	0.981	0.00	0.19	165.68	176.63	-77.84	155.68
SOM	SOM.Axis1	1.87	62.01	3.22	0.078	0.04	0.22	164.41	177.55	-76.20	152.41
	SOM.Axis2	0.09	62.45	0.16	0.695						
MIC1	MIC.Axis1	6.63	63.00	13.36	<0.001	0.14	0.34	153.40	164.35	-71.70	143.40
MIC2	MIC.Axis2	0.14	63.35	0.24	0.626	0.00	0.19	165.39	176.33	-77.69	155.39
MIC	MIC.Axis1	6.54	62.00	12.99	<0.001	0.14	0.33	155.27	168.40	-71.63	143.27
	MIC.Axis2	0.05	62.29	0.10	0.754						
MIC.C	MIC.Axis1	2.54	61.11	5.09	0.028	0.15	0.37	155.80	171.13	-70.90	141.80
	MIC.Axis2	0.28	61.58	0.57	0.453						
	C	0.78	61.40	1.57	0.214						
full	SOM.Axis1	0.08	60.13	0.16	0.692	0.14	0.37	158.08	175.60	-71.04	142.08
	SOM.Axis2	0.66	60.57	1.30	0.259						
	MIC.Axis1	4.71	60.00	9.27	0.003						
	MIC.Axis2	0.02	60.42	0.04	0.838						

S.Tab. 9: **Linear mixed effect model results for temperature response (Q_{10}) of mass-specific growth.** Depicted are one factor models of environmental parameters (soil water content (SWC), soil pH, soil C, N) and PCoA axes (SOM1, SOM2, MIC1, MIC2), a model of soil organic matter composition (SOM) with both PCoA axes, a model of microbial community composition with both PCoA axes, a model of microbial community composition and soil C (MIC.C), and a model including SOM and MIC compositions (full). A model of soil P did not meet model assumptions.

Model	Predictor	MSQ	DDF	F value	p-value	R^2m	R^2c	AIC	BIC	logLik	Dev.
SWC	SWC	0.31	66.00	0.62	0.432	0.01	0.01	154.25	165.34	-72.12	144.25
pH	pH	0.46	66.00	0.91	0.344	0.01	0.01	153.96	165.05	-71.98	143.96
C	C	0.38	66.00	0.75	0.389	0.01	0.01	154.12	165.21	-72.06	144.12
N	N	0.08	66.00	0.17	0.684	0.00	0.00	154.72	165.81	-72.36	144.72
SOM1	SOM.Axis1	0.00	66.00	0.00	0.950	0.00	0.00	154.88	165.98	-72.44	144.88
SOM2	SOM.Axis2	1.60	66.00	3.30	0.074	0.05	0.05	151.57	162.67	-70.78	141.57
SOM	SOM.Axis1	0.12	65.00	0.24	0.623	0.05	0.05	153.31	166.63	-70.66	141.31
	SOM.Axis2	1.71	65.00	3.50	0.066						
MIC1	MIC.Axis1	0.83	66.00	1.68	0.200	0.02	0.02	153.18	164.28	-71.59	143.18
MIC2	MIC.Axis2	1.14	66.00	2.32	0.132	0.03	0.03	152.54	163.63	-71.27	142.54
MIC	MIC.Axis1	0.80	65.00	1.64	0.205	0.06	0.06	152.84	166.16	-70.42	140.84
	MIC.Axis2	1.11	65.00	2.27	0.136						
MIC.C	MIC.Axis1	0.97	64.00	1.97	0.165	0.06	0.06	154.42	169.95	-70.21	140.42
	MIC.Axis2	0.11	64.00	0.23	0.631						
	C	0.20	64.00	0.40	0.529						
full	SOM.Axis1	0.02	63.00	0.03	0.855	0.08	0.08	155.14	172.89	-69.57	139.14
	SOM.Axis2	0.61	63.00	1.25	0.268						
	MIC.Axis1	0.19	63.00	0.39	0.537						
	MIC.Axis2	0.48	63.00	0.98	0.326						

S.Tab. 10: **Linear mixed effect model results for temperature response (Q_{10}) of mass-specific respiration.** Depicted are one factor models of environmental parameters (soil water content (SWC), soil pH, soil C, N, P) and PCoA axes (SOM1, SOM2, MIC1, MIC2), a model of soil organic matter composition (SOM) with both PCoA axes, a model of microbial community composition with both PCoA axes, a model of microbial community composition and soil C (MIC.C), and a model including SOM and MIC compositions (full).

Model	Predictor	MSQ	DDF	F value	p-value	R^2m	R^2c	AIC	BIC	logLik	Dev.
SWC	SWC	0.44	52.00	0.92	0.342	0.01	0.39	144.05	154.43	-67.02	134.05
pH	pH	0.12	50.39	0.24	0.625	0.00	0.40	144.82	155.21	-67.41	134.82
C	C	1.17	54.84	2.51	0.119	0.03	0.38	142.40	152.79	-66.20	132.40
N	N	1.66	55.89	3.60	0.063	0.04	0.41	141.50	151.89	-65.75	131.50
P	P	1.36	55.13	3.04	0.087	0.03	0.43	142.03	152.42	-66.01	132.03
SOM1	SOM.Axis1	0.51	52.57	1.10	0.299	0.01	0.40	143.89	154.28	-66.95	133.89
SOM2	SOM.Axis2	0.31	32.00	0.63	0.434	0.01	0.35	144.38	154.76	-67.19	134.38
SOM	SOM.Axis1	0.53	51.08	1.09	0.301	0.02	0.36	145.28	157.75	-66.64	133.28
	SOM.Axis2	0.30	34.90	0.62	0.436						
MIC1	MIC.Axis1	1.35	52.82	3.11	0.084	0.03	0.45	142.15	152.54	-66.08	132.15
MIC2	MIC.Axis2	1.34	51.62	2.94	0.092	0.04	0.44	142.19	152.58	-66.10	132.19
MIC	MIC.Axis1	0.85	54.86	1.96	0.167	0.05	0.46	142.25	154.71	-65.12	130.25
	MIC.Axis2	0.86	47.26	1.99	0.165						
MIC.C	MIC.Axis1	0.82	53.62	1.87	0.177	0.05	0.47	144.17	158.71	-65.08	130.17
	MIC.Axis2	0.64	54.29	1.47	0.231						
	C	0.05	51.66	0.12	0.726						
full	SOM.Axis1	0.45	51.90	1.00	0.321	0.07	0.45	144.62	161.24	-64.31	128.62
	SOM.Axis2	0.20	41.49	0.44	0.513						
	MIC.Axis1	1.45	52.95	3.20	0.080						
	MIC.Axis2	1.19	50.21	2.62	0.112						

REFERENCES

Abarenkov, K., Zirk, A., Piirman, T., Pöhönen, R., Ivanov, F., Nilsson, R.H., Kõljalg, U., 2020. UNITE general FASTA release for eukaryotes 2. UNITE Community. doi:10.15156/BIO/786371

Aerts, R., 2006. The freezer defrosting: Global warming and litter decomposition rates in cold biomes. Journal of Ecology 94, 713–724. doi:10.1111/j.1365-2745.2006.01142.x

Allison, S.D., Wallenstein, M.D., Bradford, M.A., 2010. Soil-carbon response to warming dependent on microbial physiology. Nature Geoscience 3, 336–340. doi:10.1038/ngeo846

Alteio, L. V., Séneca, J., Canarini, A., Angel, R., Jansa, J., Guseva, K., Kaiser, C., Richter, A., Schmidt, H., 2021. A critical perspective on interpreting amplicon sequencing data in soil ecological research. Soil Biology and Biochemistry 160. doi:10.1016/j.soilbio.2021.108357

Angel, R., Petrova, E., 2020. Quantification of 16S rRNA Gene Copies Using ddPCR (EvaGreen-based assay: 338F-805R) V.2 [WWW Document]. Protocols.Io. URL https://dx.doi.org/10.17504/protocols.io.bpy6mpze

Angelopoulos, M., Overduin, P.P., Miesner, F., Grigoriev, M.N., Vasiliev, A.A., 2020. Recent advances in the study of Arctic submarine permafrost. Permafrost and Periglacial Processes 31, 442–453. doi:10.1002/ppp.2061

Anthony, M.A., Bender, S.F., van der Heijden, M.G.A., 2023. Enumerating soil biodiversity. Proceedings of the National Academy of Sciences 120, e2304663120. doi:10.1073/pnas.2304663120

Apprill, A., Mcnally, S., Parsons, R., Weber, L., 2015. Minor revision to V4 region SSU rRNA 806R gene primer greatly increases detection of SAR11 bacterioplankton. Aquatic Microbial Ecology 75, 129–137. doi:10.3354/ame01753

Arctic Monitoring and Assessment Programme, 2021. AMAP Arctic Climate Change Update 2021: Key Trends and Impacts, Arctic Monitoring and Assessment Programme (AMAP).

Arrhenius, S., 1889. Über die Reaktionsgeschwindigkeit bei der Inversion von Rohrzucker durch Säuren. Zeitschrift Für Physikalische Chemie 4U, 226–248. doi:10.1515/zpch-1889-0416

Bahram, M., Hildebrand, F., Forslund, S.K., Anderson, J.L., Soudzilovskaia, N.A., Bodegom, P.M., Bengtsson-Palme, J., Anslan, S., Coelho, L.P., Harend, H., Huerta-Cepas, J., Medema, M.H., Maltz, M.R., Mundra, S., Olsson, P.A., Pent, M., Põlme, S., Sunagawa, S., Ryberg, M., Tedersoo, L., Bork, P., 2018. Structure and function of the global topsoil microbiome. Nature 560, 233–237. doi:10.1038/s41586-018-0386-6

Baldrian, P., Kolaiřík, M., Štursová, M., Kopecký, J., Valášková, V., Větrovský, T., Žifčáková, L., Šnajdr, J., Rídl, J., Vlček, Č., Voříšková, J., 2012. Active and total microbial communities in forest soil are largely different and highly stratified during decomposition. ISME Journal 6, 248–258. doi:10.1038/ismej.2011.95

Bar-On, Y.M., Phillips, R., Milo, R., 2018. The biomass distribution on Earth. Proceedings of the National Academy of Sciences of the United States of America 115, 6506–6511. doi:10.1073/pnas.1711842115

Barnett, D.J.M., Arts, I.C.W., Penders, J., 2021. microViz: an R package for microbiome data visualization and statistics. Journal of Open Source Software 6, 3201. doi:10.21105/joss.03201

Bartoń, K., 2022. MuMIn: Multi-Model Inference. R Package, Version 1.47.1.

Bates, D., Maechler, M., Bolker, B., Walker, S., 2015. Fitting Linear Mixed-Effects Models Using lme4. Journal of Statistical Software 67, 1–48. doi:doi:10.18637/jss.v067.i01

Beer, C., Knoblauch, C., Hoyt, A.M., Hugelius, G., Palmtag, J., Mueller, C.W., Trumbore, S., 2022. Vertical pattern of organic matter decomposability in cryoturbated permafrost-affected soils. Environmental Research Letters 17. doi:10.1088/1748-9326/ac9198

Biasi, C., Meyer, H., Rusalimova, O., Hämmerle, R., Kaiser, C., Baranyi, C., Daims, H., Lashchinsky, N., Barsukov, P., Richter, A., 2008. Initial effects of experimental warming on carbon exchange rates, plant growth and microbial dynamics of a lichen-rich dwarf shrub tundra in Siberia. Plant and Soil 307, 191–205. doi:10.1007/s11104-008-9596-2

Biasi, C., Rusalimova, O., Meyer, H., Kaiser, C., Wanek, W., Barsukov, P., Junger, H., Richter, A., 2005. Temperature-dependent shift from labile to recalcitrant carbon sources of arctic heterotrophs. Rapid Communications in Mass Spectrometry 19, 1401–1408. doi:10.1002/rcm.1911

Biskaborn, B.K., Smith, S.L., Noetzli, J., Matthes, H., Vieira, G., Streletskiy, D.A., Schoeneich, P., Romanovsky, V.E., Lewkowicz, A.G., Abramov, A., Allard, M., Boike, J., Cable, W.L., Christiansen, H.H., Delaloye, R., Diekmann, B., Drozdov, D., Etzelmüller, B., Grosse, G., Guglielmin, M., Ingeman-Nielsen, T., Isaksen, K., Ishikawa, M., Johansson, M., Johannsson, H., Joo, A., Kaverin, D., Kholodov, A., Konstantinov, P., Kröger, T., Lambiel, C., Lanckman, J.P., Luo, D., Malkova, G., Meiklejohn, I., Moskalenko, N., Oliva, M., Phillips, M., Ramos, M., Sannel, A.B.K., Sergeev, D., Seybold, C., Skryabin, P., Vasiliev, A., Wu, Q., Yoshikawa, K., Zheleznyak, M., Lantuit, H., 2019. Permafrost is warming at a global scale. Nature Communications 10, 1–11. doi:10.1038/s41467-018-08240-4

Blume-Werry, G., Milbau, A., Teuber, L.M., Johansson, M., Dorrepaal, E., 2019. Dwelling in the deep – strongly increased root growth and rooting depth enhance plant interactions with thawing permafrost soil. New Phytologist 223, 1328–1339. doi:10.1111/nph.15903

Bockheim, J.G., Munroe, J.S., 2014. Organic carbon pools and genesis of alpine soils with permafrost: A review. Arctic, Antarctic, and Alpine Research 46, 987–1006. doi:10.1657/1938-4246-46.4.987

Bockheim, J.G., Tarnocai, C., 1998. Recognition of cryoturbation for classifying permafrost-affected soils. Geoderma 81, 281–293. doi:10.1016/S0016-7061(97)00115-8

Brodzik, M., Depman, C., Hodges, S., 2023. edbuildr: Automated School District Data Download and Processing.

Brookes, P.C., Landman, A., Pruden, G., Jenkinson, D.S., 1985. Chloroform fumigation and the release of soil nitrogen: A rapid direct extraction method to measure microbial biomass nitrogen in soil. Soil Biology and Biochemistry 17, 837–842. doi:10.1016/0038-0717(85)90144-0

Brown, J., Ferrians, O.J., Heginbottom, J. a., Melnikov, E.S., 1997. Circum-Arctic map of permafrost and ground-ice conditions. Circum-Pacific Map Series.

Burman, E., Bengtsson-Palme, J., 2021. Microbial Community Interactions Are Sensitive to Small Changes in Temperature. Frontiers in Microbiology 12, 1–8. doi:10.3389/fmicb.2021.672910

Buurman, P., van Bergen, P.F., Jongmans, A.G., Meijer, E.L., Duran, B., van Lagen, B., 2005. Buurman et al. 2005 Spatial and temporal variation in podzol organic matter studied by pyrolysis-gas.pdf. European Journal of Soil Science 56, 253–270. doi:10.1111/j.1365-2389.2004.00662.x

Callahan, B.J., McMurdie, P.J., Rosen, M.J., Han, A.W., Johnson, A.J.A., Holmes, S.P., 2016a. DADA2: High-resolution sample inference from Illumina amplicon data. Nature Methods 13, 581–583. doi:10.1038/nmeth.3869

Callahan, B.J., Sankaran, K., Fukuyama, J.A., McMurdie, P.J., Holmes, S.P., 2016b. Bioconductor workflow for microbiome data analysis: From raw reads to community analyses [version 1; referees: 3 approved]. F1000Research 5, 1–48. doi:10.12688/F1000RESEARCH.8986.1

Canadell, J.G., Monteiro, P.M.S., Costa, M.H., Cunha, L.C. da, Cox, P.M., Eliseev, A.V., Henson, S., Ishii, M., Jaccard, S., Koven, C., Lohila, A., Patra, P.K., Piao, S., Rogelj, J., Syampungani, S., Zaehle, S., Zickfeld, K., 2021. Global Carbon and other Biogeochemical Cycles and Feedbacks, in: Masson-Delmotte, V., Zhai, P., Pirani, A., Connors, S.L., Péan, C., Berger, S., Caud, N., Chen, Y., Goldfarb, L., Gomis, M.I., Huang, M., Leitzell, K., Lonnoy, E., Matthews, J.B.R., Maycock, T.K., Waterfield, T., Yelekçi, O., Yu, R., Zhou, B. (Eds.), Climate Change 2021: The Physical Science Basis. Contribution of Working Group I to the Sixth Assessment Report of the Intergovernmental Panel on Climate Change. Cambridge University Press, Cambridge & New York, pp. 673–816. doi:10.1017/9781009157896.007.674

Canarini, A., Kaiser, C., Merchant, A., Richter, A., Wanek, W., 2019. Root exudation of primary metabolites: Mechanisms and their roles in plant responses to environmental stimuli. Frontiers in Plant Science 10. doi:10.3389/fpls.2019.00157

Cates, A.M., Jilling, A., Tfaily, M.M., Jackson, R.D., 2022. Temperature and moisture alter organic matter composition across soil fractions. Geoderma 409, 115628. doi:10.1016/j.geoderma.2021.115628

Chapman, S.K., Newman, G.S., 2010. Biodiversity at the plant-soil interface: Microbial abundance and community structure respond to litter mixing. Oecologia 162, 763–769. doi:10.1007/s00442-009-1498-3

Ciais, P., Sabine, C., Bala, G., Bopp, L., Brovkin, V., Canadell, J., Chhabra, A., DeFries, R., Galloway, J., Heimann, M., Jones, C., Quéré, C. Le, Myneni, R.B., Piao, S., Thornton, P., 2013. Carbon and Other Biogeochemical Cycles, in: Stocker, T.F., Qin, D., Plattner, G.-K., Tignor, M., Allen, S.K., Boschung, J., Nauels, A., Xia, Y., Bex, V., Midgley, P.M. (Eds.), Climate Change 2013: The Physical Science Basis. Contribution of Working Group I to the Fifth Assessment Report of the Intergovernmental Panel on Climate Change. Cambridge University Press, Cambridge & New York, pp. 465–570. doi:10.1017/CBO9781107415324.015

ClimateData.ca, 2023. ClimateData.ca.

Conant, R.T., Ryan, M.G., Ågren, G.I., Birge, H.E., Davidson, E.A., Eliasson, P.E., Evans, S.E., Frey, S.D., Giardina, C.P., Hopkins, F.M., Hyvönen, R., Kirschbaum, M.U.F., Lavallee, J.M., Leifeld, J., Parton, W.J., Megan Steinweg, J., Wallenstein, M.D., Martin Wetterstedt, J.Å., Bradford, M.A., 2011. Temperature and soil organic matter decomposition rates - synthesis of current knowledge and a way forward. Global Change Biology 17, 3392–3404. doi:10.1111/j.1365-2486.2011.02496.x

Copernicus Climate Change Service, 2024. Global Climate Highlights 2023 [WWW Document]. The 2023 Annual Climate Summary. URL https://climate.copernicus.eu/global-climate-highlights-2023 (accessed 2.6.23).

Cotrufo, M.F., Soong, J.L., Horton, A.J., Campbell, E.E., Haddix, M.L., Wall, D.H., Parton, W.J., 2015. Formation of soil organic matter via biochemical and physical pathways of litter mass loss. Nature Geoscience 8, 776–779. doi:10.1038/ngeo2520

Coucheney, E., Strömgren, M., Lerch, T.Z., Herrmann, A.M., 2013. Long-term fertilization of a boreal Norway spruce forest increases the temperature sensitivity of soil organic carbon mineralization. Ecology and Evolution 3, 5177–5188. doi:10.1002/ece3.895

Crowther, T.W., van den Hoogen, J., Wan, J., Mayes, M.A., Keiser, A.D., Mo, L., Averill, C., Maynard, D.S., 2019. The global soil community and its influence on biogeochemistry. Science 365. doi:10.1126/science.aav0550

Cruz-Paredes, C., Tájmel, D., Rousk, J., 2023. Variation in Temperature Dependences across Europe Reveals the Climate Sensitivity of Soil Microbial Decomposers. Applied and Environmental Microbiology 89, e0209022. doi:10.1128/aem.02090-22

Cruz-Paredes, C., Tájmel, D., Rousk, J., 2021. Can moisture affect temperature dependences of microbial growth and respiration? Soil Biology and Biochemistry 156. doi:10.1016/j.soilbio.2021.108223

D'Angelo, E., Crutchfield, J., Vandiviere, M., 2001. Rapid, Sensitive, Microscale Determination of Phosphate in Water and Soil. Journal of Environmental Quality 30, 2206–2209. doi:10.2134/jeq2001.2206

Davidson, E.A., Janssens, I.A., 2006. Temperature sensitivity of soil carbon decomposition and feedbacks to climate change. Nature 440, 165–173. doi:10.1038/nature04514

de Vries, F.T., Manning, P., Tallowin, J.R.B., Mortimer, S.R., Pilgrim, E.S., Harrison, K.A., Hobbs, P.J., Quirk, H., Shipley, B., Cornelissen, J.H.C., Kattge, J., Bardgett, R.D., 2012. Abiotic drivers and plant traits explain landscape-scale patterns in soil microbial communities. Ecology Letters 15, 1230–1239. doi:10.1111/j.1461-0248.2012.01844.x

del Giorgio, P.A., Cole, J.J., 1998. Bacterial growth efficiency in natural aquatic systems. Annual Review of Ecology and Systematics 29, 503–541. doi:10.1146/annurev.ecolsys.29.1.503

Delgado-Baquerizo, M., Oliverio, A.M., Brewer, T.E., Benavent-González, A., Eldridge, D.J., Bardgett, R.D., Maestre, F.T., Singh, B.K., Fierer, N., 2018. A global atlas of the dominant bacteria found in soil. Science 359, 320–325. doi:10.1126/science.aap9516

Demoling, F., Figueroa, D., Bååth, E., 2007. Comparison of factors limiting bacterial growth in different soils. Soil Biology and Biochemistry 39, 2485–2495. doi:10.1016/j.soilbio.2007.05.002

Ding, J., Wang, T., Piao, S., Smith, P., Zhang, G., Yan, Z., Ren, S., Liu, D., Wang, S., Chen, S., Dai, F., He, J., Li, Y., Liu, Y., Mao, J., Arain, A., Tian, H., Shi, X., Yang, Y., Zeng, N., Zhao, L., 2019. The paleoclimatic footprint in the soil carbon stock of the Tibetan permafrost region. Nature Communications 10, 1–9. doi:10.1038/s41467-019-12214-5

Dobiński, W., Szafraniec, J.E., Szypuła, B., 2023. Area and borders of Antarctic and permafrost—A review and synthesis. Permafrost and Periglacial Processes 34, 37–51. doi:10.1002/ppp.2170

Domeignoz-Horta, L.A., Shinfuku, M., Junier, P., Poirier, S., Verrecchia, E., Sebag, D., DeAngelis, K.M., 2021. Direct evidence for the role of microbial community composition in the formation of soil organic matter composition and persistence. ISME Communications 1, 5–8. doi:10.1038/s43705-021-00071-7

Dutta, K., Schuur, E.A.G., Neff, J.C., Zimov, S.A., 2006. Potential carbon release from permafrost soils of Northeastern Siberia. Global Change Biology 12, 2336–2351. doi:10.1111/j.1365-2486.2006.01259.x

Dyke, A.S., Prest, V.K., 1987. Late Wisconsinan and Holocene History of the Laurentide Ice Sheet. Géographie Physique et Quarternaire 41, 237–263. doi:10.7202/032681ar

El Moujahid, L., Le Roux, X., Michalet, S., Bellvert, F., Weigelt, A., Poly, F., 2017. Effect of plant diversity on the diversity of soil organic compounds. PLoS ONE 12, 1–16. doi:10.1371/journal.pone.0170494

Erb, K.H., Kastner, T., Plutzar, C., Bais, A.L.S., Carvalhais, N., Fetzel, T., Gingrich, S., Haberl, H., Lauk, C., Niedertscheider, M., Pongratz, J., Thurner, M., Luyssaert, S., 2018. Unexpectedly large impact of forest management and grazing on global vegetation biomass. Nature 553, 73–76. doi:10.1038/nature25138

Falkowski, P.G., Fenchel, T., Delong, E.F., 2008. The microbial engines that drive earth's biogeochemical cycles. Science 320, 1034–1039. doi:10.1126/science.1153213

Fanin, N., Mooshammer, M., Sauvadet, M., Meng, C., Alvarez, G., Bernard, L., Bertrand, I., Blagodatskaya, E., Bon, L., Fontaine, S., Niu, S., Lashermes, G., Maxwell, T.L., Weintraub, M.N., Wingate, L., Moorhead, D., Nottingham, A.T., 2022. Soil enzymes in response to climate warming: Mechanisms and feedbacks. Functional Ecology 36, 1378–1395. doi:10.1111/1365-2435.14027

Farquharson, L.M., Romanovsky, V.E., Cable, W.L., Walker, D.A., Kokelj, S. V., Nicolsky, D., 2019. Climate Change Drives Widespread and Rapid Thermokarst Development in Very Cold Permafrost in the Canadian High Arctic. Geophysical Research Letters 46, 6681–6689. doi:10.1029/2019GL082187

Faucherre, S., Jørgensen, C.J., Blok, D., Weiss, N., Siewert, M.B., Bang-Andreasen, T., Hugelius, G., Kuhry, P., Elberling, B., 2018. Short and Long-Term Controls on Active Layer and Permafrost Carbon Turnover Across the Arctic. Journal of Geophysical Research: Biogeosciences 123, 372–390. doi:10.1002/2017JG004069

Feng, J., Wang, C., Lei, J., Yang, Y., Yan, Q., Zhou, X., Tao, X., Ning, D., Yuan, M.M., Qin, Y., Shi, Z.J., Guo, X., He, Z., Van Nostrand, J.D., Wu, L., Bracho-Garillo, R.G., Penton, C.R., Cole, J.R., Konstantinidis, K.T., Luo, Y., Schuur, E.A.G., Tiedje, J.M., Zhou, J., 2020. Warming-induced permafrost thaw exacerbates tundra soil carbon decomposition mediated by microbial community. Microbiome 8, 1–12. doi:10.1186/s40168-019-0778-3

Feng, X., Simpson, M.J., 2008. Temperature responses of individual soil organic matter components. Journal of Geophysical Research: Biogeosciences 113, 1–14. doi:10.1029/2008JG000743

Fernández-Calviño, D., Bååth, E., 2010. Growth response of the bacterial community to pH in soils differing in pH. FEMS Microbiology Ecology 73, 149–156. doi:10.1111/j.1574-6941.2010.00873.x

Ferrians, O.J.J., 1965. Permafrost Map of Alaska: U.S. Geological Survey Miscellaneous Geologic Investigations Map 445.

Fierer, N., Craine, J.M., Mclauchlan, K., Schimel, J.P., 2005. Litter quality and the temperature sensitivity of decomposition. Ecology 86, 320–326. doi:10.1890/04-1254

Fierer, N., Jackson, R.B., 2006. The diversity and biogeography of soil bacterial communities. Proceedings of the National Academy of Sciences of the United States of America 103, 626–631. doi:10.1073/pnas.0507535103

Fierer, N., Schimel, J.P., Holden, P.A., 2003. Variations in microbial community composition through two soil depth profiles. Soil Biology and Biochemistry 35, 167–176. doi:10.1016/S0038-0717(02)00251-1

Figueroa, L.L., Maran, A., Pelini, S.L., 2021. Increasing temperatures reduce invertebrate abundance and slow decomposition. PLoS ONE 16, 1–14. doi:10.1371/journal.pone.0259045

Fox, J., Weisberg, S., 2019. An {R} Companion to Applied Regression, Third Edition., Third. ed. Sage, Thousand Oaks, CA.

French, H., Shur, Y., 2010. The principles of cryostratigraphy. Earth-Science Reviews 101, 190–206. doi:10.1016/j.earscirev.2010.04.002

Frey, S.D., Drijber, R., Smith, H., Melillo, J., 2008. Microbial biomass, functional capacity, and community structure after 12 years of soil warming. Soil Biology and Biochemistry 40, 2904–2907. doi:10.1016/j.soilbio.2008.07.020

Fritz, M., Wetterich, S., Schirrmeister, L., Meyer, H., Lantuit, H., Preusser, F., Pollard, W.H., 2012. Eastern Beringia and beyond: Late Wisconsinan and Holocene landscape dynamics along the Yukon Coastal Plain, Canada. Palaeogeography, Palaeoclimatology, Palaeoecology 319–320, 28–45. doi:10.1016/j.palaeo.2011.12.015

Fritz, M., Wolter, J., Rudaya, N., Palagushkina, O., Nazarova, L., Obu, J., Rethemeyer, J., Lantuit, H., Wetterich, S., 2016. Holocene ice-wedge polygon development in northern Yukon permafrost peatlands (Canada). Quaternary Science Reviews 147, 279–297. doi:10.1016/j.quascirev.2016.02.008

Froese, D.G., Westgate, J.A., Reyes, A. V., Enkin, R.J., Preece, S.J., 2008. Ancient permafrost and a future, warmer arctic. Science 321, 1648. doi:10.1126/science.1157525

Frouz, J., 2018. Effects of soil macro- and mesofauna on litter decomposition and soil organic matter stabilization. Geoderma 332, 161–172. doi:10.1016/j.geoderma.2017.08.039

Gentsch, N., Mikutta, R., Alves, R.J.E., Barta, J., Čapek, P., Gittel, A., Hugelius, G., Kuhry, P., Lashchinskiy, N., Palmtag, J., Richter, A., Šantrůčková, H., Schnecker, J., Shibistova, O., Urich, T., Wild, B., Guggenberger, G., 2015. Storage and transformation of organic matter fractions in cryoturbated permafrost soils across the Siberian Arctic. Biogeosciences 12, 4525–4542. doi:10.5194/bg-12-4525-2015

Gentsch, N., Wild, B., Mikutta, R., Čapek, P., Diáková, K., Schrumpf, M., Turner, S., Minnich, C., Schaarschmidt, F., Shibistova, O., Schnecker, J., Urich, T., Gittel, A., Šantrůčková, H., Bárta, J., Lashchinskiy, N., Fuß, R., Richter, A., Guggenberger, G., 2018. Temperature response of permafrost soil carbon is attenuated by mineral protection. Global Change Biology 24, 3401–3415. doi:10.1111/gcb.14316

George, P.B.L., Creer, S., Griffiths, R.I., Emmett, B.A., Robinson, D.A., Jones, D.L., 2019. Primer and Database Choice Affect Fungal Functional but Not Biological Diversity Findings in a National Soil Survey. Frontiers in Environmental Science 7. doi:10.3389/fenvs.2019.00173

Gittel, A., Bárta, J., Kohoutová, I., Mikutta, R., Owens, S., Gilbert, J., Schnecker, J., Wild, B., Hannisdal, B., Maerz, J., Lashchinskiy, N., Čapek, P., Šantrůčková, H., Gentsch, N., Shibistova, O., Guggenberger, G., Richter, A., Torsvik, V.L., Schleper, C., Urich, T., 2014a. Distinct microbial communities associated with buried soils in the siberian tundra. ISME Journal 8, 841–853. doi:10.1038/ismej.2013.219

Gittel, A., Bárta, J., Kohoutová, I., Schnecker, J., Wild, B., Čapek, P., Kaiser, C., Torsvik, V.L., Richter, A., Schleper, C., Urich, T., 2014b. Site- and horizon-specific patterns of microbial community structure and enzyme activities in permafrost-affected soils of Greenland. Frontiers in Microbiology 5, 1–14. doi:10.3389/fmicb.2014.00541

Gohel, D., Skintzos, P., 2023. flextable: Functions for Tabular Reporting.

González-Pérez, M., Buurman, P., Vidal-Torrado, P., Martin-Neto, L., 2012. Pyrolysis-Gas Chromatography/Mass Spectrometry Characterization of Humic Acids in Coastal Spodosols from Southeastern Brazil.pdf. Soil Science Society of America Journal 76, 961–971. doi:10.2136/sssaj 2011.0178

Goode, K., Rey, K., 2019. ggResidpanel: Panels and Interactive Versions of Diagnostic Plots using "ggplot2."

Goosse, H., Kay, J.E., Armour, K.C., Bodas-Salcedo, A., Chepfer, H., Docquier, D., Jonko, A., Kushner, P.J., Lecomte, O., Massonnet, F., Park, H.S., Pithan, F., Svensson, G., Vancoppenolle, M., 2018. Quantifying climate feedbacks in polar regions. Nature Communications 9. doi:10.1038/s41467-018-04173-0

Gorka, S., Darcy, S., Horak, J., Imai, B., Mohrlok, M., Salas, E., Richter, A., Schmidt, H., Wanek, W., Kaiser, C., Canarini, A., 2023. Beyond PLFA: Concurrent extraction of neutral and glycolipid fatty acids provides new insights into soil microbial communities. Soil Biology and Biochemistry 187, 109205. doi:10.1016/j.soilbio.2023.109205

Gougoulias, C., Clark, J.M., Shaw, L.J., 2014. The role of soil microbes in the global carbon cycle: Tracking the below-ground microbial processing of plant-derived carbon for manipulating carbon dynamics in agricultural systems. Journal of the Science of Food and Agriculture 94, 2362–2371. doi:10.1002/jsfa.6577

Gunina, A., Kuzyakov, Y., 2022. From energy to (soil organic) matter. Global Change Biology 28, 2169–2182. doi:10.1111/gcb.16071

Hansen, J.E., Sato, M., Simons, L., Nazarenko, L.S., von Schuckmann, K., Loeb, N.G., Osman, M.B., Kharecha, P., Jin, Q., Tselioudis, G., Lacis, A., Ruedy, R., Russell, G., Cao, J., Li, J., 2022. Global warming in the pipeline 3.

Hartmann, M., Six, J., 2023. Soil structure and microbiome functions in agroecosystems. Nature Reviews Earth and Environment 4, 4–18. doi:10.1038/s43017-022-00366-w

Heijmans, M.M.P.D., Magnússon, R., Lara, M.J., Frost, G. V., Myers-Smith, I.H., van Huissteden, J., Jorgenson, M.T., Fedorov, A.N., Epstein, H.E., Lawrence, D.M., Limpens, J., 2022. Tundra vegetation change and impacts on permafrost. Nature Reviews Earth and Environment 3, 68–84. doi:10.1038/s43017-021-00233-0

Hempfling, R., Schulten, H.R., 1990. Chemical characterization of the organic matter in forest soils by Curie point pyrolysis-GC/MS and pyrolysis-field ionization mass spectrometry. Organic Geochemistry 15, 131–145. doi:10.1016/0146-6380(90)90078-E

Hicks Pries, C.E., Schuur, E.A.G., Crummer, K.G., 2013. Thawing permafrost increases old soil and autotrophic respiration in tundra: Partitioning ecosystem respiration using δ13C and δ14C. Global Change Biology 19, 649–661. doi:10.1111/gcb.12058

Hopkins, F.M., Torn, M.S., Trumbore, S.E., 2012. Warming accelerates decomposition of decades-old carbon in forest soils. Proceedings of the National Academy of Sciences of the United States of America 109. doi:10.1073/pnas.1120603109

Hugelius, G., Strauss, J., Zubrzycki, S., Harden, J.W., Schuur, E.A.G., Ping, C.L., Schirrmeister, L., Grosse, G., Michaelson, G.J., Koven, C.D., O'Donnell, J.A., Elberling, B., Mishra, U., Camill, P., Yu, Z., Palmtag, J., Kuhry, P., 2014. Estimated stocks of circumpolar permafrost carbon with quantified uncertainty ranges and identified data gaps. Biogeosciences 11, 6573–6593. doi:10.5194/bg-11-6573-2014

IUSS Working Group WRB, 2014. World Reference Base for Soil Resources. International soil classification system for naming soils and creating legends for soil maps, Update 201. ed, World Soil Resources Report No. 106. FAO, Rome. doi:10.1007/978-3-319-24409-9_25

Iven, H., Walker, T.W.N., Anthony, M., 2023. Biotic Interactions in Soil are Underestimated Drivers of Microbial Carbon Use Efficiency. Current Microbiology 80, 1–14. doi:10.1007/s00284-022-02979-2

James, G., Witten, D., Hastie, T., Tibshirani, R., 2017. An Introduction to Statistical Learning - with applications in R, Springer Texts in Statistics. Springer New York, New York, Heidelberg, Dordrecht, London. doi:10.1007/978-1-4614-7138-7

Ji, C.-J., Yang, Y.H., Han, W.X., He, Y.F., Smith, J., Smith, P., 2014. Climatic and Edaphic Controls on Soil pH in Alpine Grasslands on the Tibetan Plateau, China: A Quantitative Analysis. Pedosphere 24, 39–44. doi:10.1016/S1002-0160(13)60078-8

Jian, C., Luukkonen, P., Yki-Järvinen, H., Salonen, A., Korpela, K., 2020. Quantitative PCR provides a simple and accessible method for quantitative microbiota profiling. PLoS ONE 15, 1–10. doi:10.1371/journal.pone.0227285

Jobbagy, E.G., Jackson, R.B., 2000. The Vertical Distribution of Soil Organic Carbon and Its Relation to Climate and Vegetation. Ecological Applications 10, 423. doi:10.2307/2641104

Joergensen, R.G., 1996. The fumigation-extraction method to estimate soil microbial biomass: Calibration of the kEC value. Soil Biology and Biochemistry 28, 25–31. doi:10.1016/0038-0717(95)00102-6

Joly, F.X., Coq, S., Coulis, M., David, J.F., Hättenschwiler, S., Mueller, C.W., Prater, I., Subke, J.A., 2020. Detritivore conversion of litter into faeces accelerates organic matter turnover. Communications Biology 3, 1–9. doi:10.1038/s42003-020-01392-4

Jones, D.L., Nguyen, C., Finlay, R.D., 2009. Carbon flow in the rhizosphere: Carbon trading at the soil-root interface. Plant and Soil 321, 5–33. doi:10.1007/s11104-009-9925-0

Jorgenson, M.T., Kanevskiy, M., Shur, Y., Moskalenko, N., Brown, D.R.N., Wickland, K., Striegl, R., Koch, J., 2015. Role of ground ice dynamics and ecological feedbacks in recent ice wedge degradation and stabilization. Journal of Geophysical Research: Earth Surface 120, 2280–2297. doi:doi:10.1002/2015JF003602

Jorgenson, M.T., Kanevskiy, M.Z., Jorgenson, J.C., Liljedahl, A., Shur, Y., Epstein, H., Kent, K., Griffin, C.G., Daanen, R., Boldenow, M., Orndahl, K., Witharana, C., Jones, B.M., 2022. Rapid transformation of tundra ecosystems from ice-wedge degradation. Global and Planetary Change 216, 103921. doi:10.1016/j.gloplacha.2022.103921

Jorgenson, M.T., Osterkamp, T.E., 2005. Response of boreal ecosystems to varying modes of permafrost degradation. Canadian Journal of Forest Research 35, 2100–2111. doi:10.1139/x05-153

Jorgenson, M.T., Shur, Y.L., Pullman, E.R., 2006. Abrupt increase in permafrost degradation in Arctic Alaska. Geophysical Research Letters 33, 2–5. doi:10.1029/2005GL024960

Kaiser, C., Meyer, H., Biasi, C., Rusalimova, O., Barsukov, P., Richter, A., 2007. Conservation of soil organic matter through cryoturbation in arctic soils in Siberia. Journal of Geophysical Research: Biogeosciences 112, 1–8. doi:10.1029/2006JG000258

Kanevskiy, M., Shur, Y., Jorgenson, M.T., Ping, C.L., Michaelson, G.J., Fortier, D., Stephani, E., Dillon, M., Tumskoy, V., 2013. Ground ice in the upper permafrost of the Beaufort Sea coast of Alaska. Cold Regions Science and Technology 85, 56–70. doi:10.1016/j.coldregions.2012.08.002

Kanevskiy, M., Shur, Y., Jorgenson, T., Brown, D.R.N., Moskalenko, N., Brown, J., Walker, D.A., Raynolds, M.K., Buchhorn, M., 2017. Degradation and stabilization of ice wedges: Implications for assessing risk of thermokarst in northern Alaska. Geomorphology 297, 20–42. doi:10.1016/j.geomorph.2017.09.001

Kassambara, A., 2023a. ggpubr: "ggplot2" Based Publication Ready Plots.

Kassambara, A., 2023b. rstatix: Pipe-Friendly Framework for Basic Statistical Tests. R Package, Version 0.7.2.

Keiblinger, K.M., Hall, E.K., Wanek, W., Szukics, U., Hämmerle, I., Ellersdorfer, G., Böck, S., Strauss, J., Sterflinger, K., Richter, A., Zechmeister-Boltenstern, S., 2010. The effect of resource quantity and resource stoichiometry on microbial carbon-use-efficiency. FEMS Microbiology Ecology 73, 430–440. doi:10.1111/j.1574-6941.2010.00912.x

Keuper, F., Wild, B., Kummu, M., Beer, C., Blume-Werry, G., Fontaine, S., Gavazov, K., Gentsch, N., Guggenberger, G., Hugelius, G., Jalava, M., Koven, C., Krab, E.J., Kuhry, P., Monteux, S., Richter, A., Shahzad, T., Weedon, J.T., Dorrepaal, E., 2020. Carbon loss from northern circumpolar permafrost soils amplified by rhizosphere priming. Nature Geoscience 13, 560–565. doi:10.1038/s41561-020-0607-0

Kirschbaum, M.U.F., 1995. The temperature dependence of soil organic matter decomposition, and the effect of global warming on soil organic C storage. Soil Biology and Biochemistry 27, 753–760. doi:10.1016/0038-0717(94)00242-S

Knapp, B.D., Huang, K.C., 2022. The Effects of Temperature on Cellular Physiology. Annual Review of Biophysics 51, 499–526. doi:10.1146/annurev-biophys-112221-074832

Kögel-Knabner, I., 2017. The macromolecular organic composition of plant and microbial residues as inputs to soil organic matter: Fourteen years on. Soil Biology and Biochemistry 105, A3–A8. doi:10.1016/j.soilbio.2016.08.011

Kögel-Knabner, I., 2002. The macromolecular organic composition of plant and microbial residues as inputs to soil organic matter. Soil Biology and Biochemistry 34, 139–162. doi:10.1016/S0038-0717(01)00158-4

Kokelj, S. V., Jorgenson, M.T., 2013. Advances in thermokarst research. Permafrost and Periglacial Processes 24, 108–119. doi:10.1002/ppp.1779

Komsta, L., 2022. outliers: Tests for Outliers.

Koven, C.D., Ringeval, B., Friedlingstein, P., Ciais, P., Cadule, P., Khvorostyanov, D., Krinner, G., Tarnocai, C., 2011. Permafrost carbon-climate feedbacks accelerate global warming. Proceedings of the National Academy of Sciences of the United States of America 108, 14769–14774. doi:10.1073/pnas.1103910108

Krantz, W.B., 1990. Self-organization manifest as patterned ground in recurrently frozen soils. Earth Science Reviews 29, 117–130. doi:10.1016/0012-8252(0)90031-P

Kuznetsova, A., Brockhoff, P.B., Christensen, R.H.B., 2017. lmerTest Package: Tests in Linear Mixed Effects Models. Journal of Statistical Software 82, 1–26. doi:doi.org/10.18637/jss.v082.i13

Lacelle, B., Soil Classification Working Group, 2001. Soils of Canada.

Langer, M., Nitzbon, J., Groenke, B., Assmann, L.M., Schneider von Deimling, T., Stuenzi, S.M., Westermann, S., 2022. Prepint: The evolution of Arctic permafrost over the last three centuries. EGUsphere 2022, 1–27.

Laros, J.F.J., n.d. Demultiplex: FASTA/FASTQ demultiplexer.

LECO, n.d. ChromaTOF. Version 5.51.50.068774.

Lee, H., Calvin, K., Dasgupta, D., Krinner, G., Mukherji, A., Thorne, P., Trisos, C., Romero, J., Aldunce, P., Barrett, K., Blanco, G., Cheung, W.W.L., Connors, S.L., Denton, F., Diongue-Niang, A., Dodman, D., Garschagen, M., Geden, O., Hayward, B., Jones, C., Jotzo, F., Krug, T., Lasco, R., Lee, J.-Y., Masson-Delmotte, V., Meinshausen, M., Mintenbeck, K., Mokssit, A., Otto, F.E.L., Pathak, M., Pirani, A., Poloczanska, E., Pörtner, H.-O., Revi, A., Roberts, D.C., Roy, J., Ruane, A.C., Skea, J., Shukla, P.R., Slade, R., Slangen, A., Sokona, Y., Sörensson, A.A., Tignor, M., van Vuuren, D., Wei, Y.-M., Winkler, H., Zhai, P., Zommers, Z., 2023. Climate Change 2023: Synthesis Report. A Report of the Intergovernmental Panel on Climate Change. Contribution of Working Groups I, II and III to the Sixth Assessment Report of the Intergovernmental Panel on Climate Change, IPCC. IPCC, Geneva.

Lenth, R. V., 2023. emmeans: Estimated Marginal Means, aka Least-Squares Means.

Lenton, T.M., Armstrong McKay, D.I., Loriani, S., Abrams, J.F., Lade, S.J., Donges, J.F., Milkoreit, M., Powell, T., Smith, S.R., Zimm, C., Buxton, J.E., Bailey, E., Laybourn, L., Ghadiali, A., Dyke, J.G., 2023. The Global Tipping Points Report. Exeter.

Liang, C., 2020. Soil microbial carbon pump: Mechanism and appraisal. Soil Ecology Letters 2, 241–254. doi:10.1007/s42832-020-0052-4

Liang, C., Amelung, W., Lehmann, J., Kästner, M., 2019. Quantitative assessment of microbial necromass contribution to soil organic matter. Global Change Biology 25, 3578–3590. doi:10.1111/GCB.14781

Liang, C., Schimel, J.P., Jastrow, J.D., 2017. The importance of anabolism in microbial control over soil carbon storage. Nature Microbiology 2. doi:10.1038/nmicrobiol.2017.105

Liljedahl, A.K., Boike, J., Daanen, R.P., Fedorov, A.N., Frost, G. V., Grosse, G., Hinzman, L.D., Iijma, Y., Jorgenson, J.C., Matveyeva, N., Necsoiu, M., Raynolds, M.K., Romanovsky, V.E., Schulla, J., Tape, K.D., Walker, D.A., Wilson, C.J., Yabuki, H., Zona, D., 2016. Pan-Arctic ice-wedge degradation in warming permafrost and its influence on tundra hydrology. Nature Geoscience 9, 312–318. doi:10.1038/ngeo2674

MacDougall, A.H., Avis, C.A., Weaver, A.J., 2012. Significant contribution to climate warming from the permafrost carbon feedback. Nature Geoscience 5, 719–721. doi:10.1038/ngeo1573

Mainka, M., Summerauer, L., Wasner, D., Garland, G., Griepentrog, M., Berhe, A.A., Doetterl, S., 2022. Soil geochemistry as a driver of soil organic matter composition: Insights from a soil chronosequence. Biogeosciences 19, 1675–1689. doi:10.5194/bg-19-1675-2022

Manzoni, S., Taylor, P., Richter, A., Porporato, A., Ågren, G.I., 2012. Environmental and stoichiometric controls on microbial carbon-use efficiency in soils. New Phytologist 196, 79–91. doi:10.1111/j.1469-8137.2012.04225.x

Martinez Arbizu, P., 2020. pairwiseAdonis: Pairwise multilevel comparison using adonis. R Package, Version 0.4, GitHub Repository.

Mauritz, M., Bracho, R., Celis, G., Hutchings, J., Natali, S.M., Pegoraro, E., Salmon, V.G., Schädel, C., Webb, E.E., Schuur, E.A.G., 2017. Nonlinear CO2 flux response to 7 years of experimentally induced permafrost thaw. Global Change Biology 23, 3646–3666. doi:10.1111/gcb.13661

McMurdie, P.J., Holmes, S., 2013. phyloseq: An R Package for Reproducible Interactive Analysis and Graphics of Microbiome Census Data. PLoS ONE 8, e61217. doi:10.1371/journal.pone.0061217

Melillo, J.M., Frey, S.D., DeAngelis, K.M., Werner, W.J., Bernard, M.J., Bowles, F.P., Pold, G., Knorr, M.A., Grandy, A.S., 2017. Long-term pattern and magnitude of soil carbon feedback to the climate system in a warming world. Science 358, 101–105. doi:10.1126/science.aan2874

Melnikov, V.P., Rogov, V. V., Kurchatova, A.N., Brouchkov, A. V., Griva, G.I., 2011. Permafrost microbiology: Distribution of microorganizms in frozen ground. Earth's Cryosphere 15, 75–78.

Meredith, M., Sommerkorn, M., Cassotta, S., Derksen, C., Ekaykin, A., Hollowed, A., Kofinas, G., Mackintosh, A., Melbourne-Thomas, J., Muelbert, M.M.C., Ottersen, G., Pritchard, H., Schuur, E.A.G., 2019. Polar Regions, in: Pörtner, H.-O., Roberts, D.C., Masson-Delmotte, V., Zhai, P., Tignor, M., Poloczanska, E., Mintenbeck, K., Alegría, A., Nicolai, M., Okem, A., Petzold, J., Rama, B., Weyer, N.M. (Eds.), IPCC Special Report on the Ocean and Cryosphere in a Changing Climate. Cambridge & New York, pp. 203–320. doi:10.1017/9781009157964.005

Metze, D., Schnecker, J., Canarini, A., Fuchslueger, L., Koch, B.J., Stone, B.W., Hungate, B.A., Hausmann, B., Schmidt, H., Schaumberger, A., Bahn, M., Kaiser, C., Richter, A., 2023. Microbial growth under drought is confined to distinct taxa and modified by potential future climate conditions. Nature Communications 14, 1–12. doi:10.1038/s41467-023-41524-y

Metze, D., Schnecker, J., Le, C., Carlan, N. De, Bhattarai, B., Verbruggen, E., Ostonen, I., Janssens, I.A., Sigurdsson, B.D., Hausmann, B., Kaiser, C., Richter, A., 2024. Soil warming increases the number of growing bacterial taxa but not their growth rates 6295. doi:10.1126/sciadv.adk6295

Miesner, F., Overduin, P.P., Grosse, G., Strauss, J., Langer, M., Westermann, S., Schneider von Deimling, T., Brovkin, V., Arndt, S., 2023. Subsea permafrost organic carbon stocks are large and of dominantly low reactivity. Scientific Reports 13, 1–12. doi:10.1038/s41598-023-36471-z

Millard, S.P., 2013. EnvStats: An R Package for Environmental Statistics. Springer, New York.

Miltner, A., Bombach, P., Schmidt-Brücken, B., Kästner, M., 2012. SOM genesis: Microbial biomass as a significant source. Biogeochemistry 111, 41–55. doi:10.1007/s10533-011-9658-z

Mooshammer, M., Wanek, W., Zechmeister-Boltenstern, S., Richter, A., 2014. Stoichiometric imbalances between terrestrial decomposer communities and their resources: Mechanisms and implications of microbial adaptations to their resources. Frontiers in Microbiology 5, 1–10. doi:10.3389/fmicb.2014.00022

Mueller, C.W., Rethemeyer, J., Kao-Kniffin, J., Löppmann, S., Hinkel, K.M., Bockheim, J.G., 2015. Large amounts of labile organic carbon in permafrost soils of northern Alaska. Global Change Biology 21, 2804–2817. doi:10.1111/gcb.12876

Muller, S.W., 1945. Permafrost or permanently frozen ground and related engineering problems, Special Report, Strategic Engeneering Study. Washington D.C.

Murton, J.B., Opel, T., Toms, P., Blinov, A., Fuchs, M., Wood, J., Gärtner, A., Merchel, S., Rugel, G., Savvinov, G., Wetterich, S., 2022. A multimethod dating study of ancient permafrost, Batagay megaslump, east Siberia. Quaternary Research (United States) 105, 1–22. doi:10.1017/qua.2021.27

Natali, S.M., Holdren, J.P., Rogers, B.M., Treharne, R., Duffy, P.B., Pomerance, R., MacDonald, E., 2021. Permafrost carbon feedbacks threaten global climate goals. Proceedings of the National Academy of Sciences of the United States of America 118, 1–3. doi:10.1073/pnas.2100163118

Natali, S.M., Schuur, E.A.G., Webb, E.E., Pries, C.E.H., Crummer, K.G., 2014. Permafrost degradation stimulates carbon loss from experimentally warmed tundra. Ecology 95, 602–608. doi:10.1890/13-0602.1

National Institutes of Health, U.S.D. of H. and H.S., 2023. Medical Subject Headings (MeSH), National Library of Medicine [WWW Document]. URL www.ncbi.nlm.nih.gov/mesh (accessed 7.1.23).

Naylor, D., McClure, R., Jansson, J., 2022. Trends in Microbial Community Composition and Function by Soil Depth. Microorganisms 10. doi:10.3390/microorganisms10030540

Ninnes, S., Tolu, J., Meyer-Jacob, C., Mighall, T.M., Bindler, R., 2017. Investigating molecular changes in organic matter composition in two Holocene lake-sediment records from central Sweden using pyrolysis-GC/MS. Journal of Geophysical Research: Biogeosciences 122, 1423–1438. doi:10.1002/2016JG003715

Nitzbon, J., Langer, M., Martin, L.C.P., Westermann, S., Schneider Von Deimling, T., Boike, J., 2021. Effects of multi-scale heterogeneity on the simulated evolution of ice-rich permafrost lowlands under a warming climate. Cryosphere 15, 1399–1422. doi:10.5194/tc-15-1399-2021

Nitzbon, J., Langer, M., Westermann, S., Martin, L., Aas, K.S., Boike, J., 2019. Pathways of ice-wedge degradation in polygonal tundra under different hydrological conditions. Cryosphere 13, 1089–1123. doi:10.5194/tc-13-1089-2019

Obu, J., 2021. How Much of the Earth's Surface is Underlain by Permafrost? Journal of Geophysical Research: Earth Surface 126, 1–5. doi:10.1029/2021JF006123

Obu, J., Westermann, S., Bartsch, A., Berdnikov, N., Christiansen, H.H., Dashtseren, A., Delaloye, R., Elberling, B., Etzelmüller, B., Kholodov, A., Khomutov, A., Kääb, A., Leibman, M.O., Lewkowicz, A.G., Panda, S.K., Romanovsky, V., Way, R.G., Westergaard-Nielsen, A., Wu, T., Yamkhin, J., Zou, D., 2019. Northern Hemisphere permafrost map based on TTOP modelling for 2000–2016 at 1 km2 scale. Earth-Science Reviews 193, 299–316. doi:10.1016/j.earscirev.2019.04.023

Oksanen, J., Simpson, G., Blanchet, F., Kindt, R., Legendre, P., Minchin, P., O'Hara, R., Solymos, P., Stevens, M., Szoecs, E., Wagner, H., Barbour, M., Bedward, M., Bolker, B., Borcard, D., Carvalho, G., Chirico, M., De Caceres, M., Durand, S., Evangelista, H., FitzJohn, R., Friendly, M., Furneaux, B., Hannigan, G., Hill, M., Lahti, L., McGlinn, D., Ouellette, M., Ribeiro Cunha, E., Smith, T., Stier, A., Ter Braak, C., Weedon, J., 2022. vegan: Community Ecology Package. R Package, Version 2.6-4.

Olefeldt, D., Goswami, S., Grosse, G., Hayes, D., Hugelius, G., Kuhry, P., Mcguire, A.D., Romanovsky, V.E., Sannel, A.B.K., Schuur, E.A.G., Turetsky, M.R., 2016. Circumpolar distribution and carbon storage of thermokarst landscapes. Nature Communications 7, 1–11. doi:10.1038/ncomms13043

Orwin, K.H., Dickie, I.A., Holdaway, R., Wood, J.R., 2018. A comparison of the ability of PLFA and 16S rRNA gene metabarcoding to resolve soil community change and predict ecosystem functions. Soil Biology and Biochemistry 117, 27–35. doi:10.1016/j.soilbio.2017.10.036

Osterkamp, T.E., 2001. Sub-sea Permafrost, in: Steele, J.H., Thorpe, S.A., Turekian, K.K. (Eds.), Encyclopedia of Ocean Sciences. Academic Press, San Diego, pp. 2902–2912. doi:10.1006/rwos.2001.0008

Overduin, P.P., Schneider von Deimling, T., Miesner, F., Grigoriev, M.N., Ruppel, C., Vasiliev, A., Lantuit, H., Juhls, B., Westermann, S., 2019. Submarine Permafrost Map in the Arctic Modeled Using 1-D Transient Heat Flux (SuPerMAP). Journal of Geophysical Research: Oceans 124, 3490–3507. doi:10.1029/2018JC014675

Overland, J.E., Hanna, E., Hanssen-Bauer, I., Kim, S.-J., Walsh, J.E., Wang, M., Bhatt, U.S., Thoman, R.L., Ballinger, T.J., 2019. Surface Air Temperature, in: Richter-Menge, J., Druckenmiller, M.L., Jeffries, M. (Eds.), Arctic Report Card 2019. pp. 5–10. doi:10.1007/978-94-007-5784-4_38

Parada, A.E., Needham, D.M., Fuhrman, J.A., 2016. Every base matters: Assessing small subunit rRNA primers for marine microbiomes with mock communities, time series and global field samples. Environmental Microbiology 18, 1403–1414. doi:10.1111/1462-2920.13023

Pearson, R.G., Phillips, S.J., Loranty, M.M., Beck, P.S.A., Damoulas, T., Knight, S.J., Goetz, S.J., 2013. Shifts in Arctic vegetation and associated feedbacks under climate change. Nature Climate Change 3, 673–677. doi:10.1038/nclimate1858

Peay, K.G., Kennedy, P.G., Talbot, J.M., 2016. Dimensions of biodiversity in the Earth mycobiome. Nature Reviews Microbiology 14, 434–447. doi:10.1038/nrmicro.2016.59

Pérez-Cobas, A.E., Gomez-Valero, L., Buchrieser, C., 2020. Metagenomic approaches in microbial ecology: An update on whole-genome and marker gene sequencing analyses. Microbial Genomics 6, 1–22. doi:10.1099/mgen.0.000409

Ping, C.L., Jastrow, J.D., Jorgenson, M.T., Michaelson, G.J., Shur, Y.L., 2015. Permafrost soils and carbon cycling. Soil 1, 147–171. doi:10.5194/soil-1-147-2015

Pithan, F., Mauritsen, T., 2014. Arctic amplification dominated by temperature feedbacks in contemporary climate models. Nature Geoscience 7, 181–184. doi:10.1038/ngeo2071

Pjevac, P., Hausmann, B., Schwarz, J., Kohl, G., Herbold, C.W., Loy, A., Berry, D., 2021. An Economical and Flexible Dual Barcoding, Two-Step PCR Approach for Highly Multiplexed Amplicon Sequencing. Frontiers in Microbiology 12. doi:10.3389/fmicb.2021.669776

Pold, G., Domeignoz-Horta, L.A., Morrison, E.W., Frey, S.D., Sistla, S.A., Deangelis, K.M., 2020. Carbon use efficiency and its temperature sensitivity covary in soil bacteria. MBio 11, 1–16. doi:10.1128/mBio.02293-19

Propster, J.R., Schwartz, E., Hayer, M., Miller, S., Monsaint-Queeney, V., Koch, B.J., Morrissey, E.M., Mack, M.C., Hungate, B.A., 2023. Distinct Growth Responses of Tundra Soil Bacteria to Short-Term and Long-Term Warming. Applied and Environmental Microbiology 89, e0154322. doi:10.1128/aem.01543-22

Pruesse, E., Peplies, J., Glöckner, F.O., 2012. SINA: Accurate high-throughput multiple sequence alignment of ribosomal RNA genes. Bioinformatics 28, 1823–1829. doi:10.1093/bioinformatics/bts252

Pugnaire, F.I., Morillo, J.A., Peñuelas, J., Reich, P.B., Bardgett, R.D., Gaxiola, A., Wardle, D.A., Van Der Putten, W.H., 2019. Climate change effects on plant-soil feedbacks and consequences for biodiversity and functioning of terrestrial ecosystems. Science Advances 5, 1–11. doi:10.1126/sciadv.aaz1834

Purcell, A.M., Hayer, M., Koch, B.J., Mau, R.L., Blazewicz, S.J., Dijkstra, P., Mack, M.C., Marks, J.C., Morrissey, E.M., Pett-Ridge, J., Rubin, R.L., Schwartz, E., van Gestel, N.C., Hungate, B.A., 2022. Decreased growth of wild soil microbes after 15 years of transplant-induced warming in a montane meadow. Global Change Biology 28, 128–139. doi:10.1111/gcb.15911

Quast, C., Pruesse, E., Yilmaz, P., Gerken, J., Schweer, T., Yarza, P., Peplies, J., Glöckner, F.O., 2013. The SILVA ribosomal RNA gene database project: Improved data processing and web-based tools. Nucleic Acids Research 41, 590–596. doi:10.1093/nar/gks1219

Quideau, S.A., Chadwick, O.A., Benesi, A., Graham, R.C., Anderson, M.A., 2001. A direct link between forest vegetation type and soil organic matter composition. Geoderma 104, 41–60. doi:10.1016/S0016-7061(01)00055-6

R Core Team, 2022. R: A language and environment for statistical computing. Version 4.2.2 "Innocent and Trusting."

Ramage, J., Jungsberg, L., Wang, S., Westermann, S., Lantuit, H., Heleniak, T., 2021. Population living on permafrost in the Arctic. Population and Environment 43, 22–38. doi:10.1007/s11111-020-00370-6

Ramsey, P.W., Rillig, M.C., Feris, K.P., Holben, W.E., Gannon, J.E., 2006. Choice of methods for soil microbial community analysis: PLFA maximizes power compared to CLPP and PCR-based approaches. Pedobiologia 50, 275–280. doi:10.1016/j.pedobi.2006.03.003

Rantanen, M., Karpechko, A.Y., Lipponen, A., Nordling, K., Hyvärinen, O., Ruosteenoja, K., Vihma, T., Laaksonen, A., 2022. The Arctic has warmed nearly four times faster than the globe since 1979. Communications Earth and Environment 3, 1–10. doi:10.1038/s43247-022-00498-3

Ratzke, C., Gore, J., 2018. Modifying and reacting to the environmental pH can drive bacterial interactions. PLOS Biology 16, e2004248.

Richter-Menge, J., Druckenmiller, M.L., 2020. The Arctic [in "State of the Climate in 2019"], in: Blunden, J., Arndt, D.S. (Eds.), Bulletin of the American Meteorological Society. pp. 239–285. doi:https://doi.org/10.1175/BAMS-D-20-0086.1

Robinson, S.I., McLaughlin, Ó.B., Marteinsdóttir, B., O'Gorman, E.J., 2018. Soil temperature effects on the structure and diversity of plant and invertebrate communities in a natural warming experiment. Journal of Animal Ecology 87, 634–646. doi:10.1111/1365-2656.12798

Roller, B.R.K., Schmidt, T.M., 2015. The physiology and ecological implications of efficient growth. ISME Journal 9, 1481–1487. doi:10.1038/ismej.2014.235

Rousk, J., Bååth, E., Brookes, P.C., Lauber, C.L., Lozupone, C., Caporaso, J.G., Knight, R., Fierer, N., 2010. Soil bacterial and fungal communities across a pH gradient in an arable soil. ISME Journal 4, 1340–1351. doi:10.1038/ismej.2010.58

Rousk, J., Brookes, P.C., Bååth, E., 2009. Contrasting soil pH effects on fungal and bacterial growth suggest functional redundancy in carbon mineralization. Applied and Environmental Microbiology 75, 1589–1596. doi:10.1128/AEM.02775-08

Roy Chowdhury, T., Herndon, E.M., Phelps, T.J., Elias, D.A., Gu, B., Liang, L., Wullschleger, S.D., Graham, D.E., 2015. Stoichiometry and temperature sensitivity of methanogenesis and CO2 production from saturated polygonal tundra in Barrow, Alaska. Global Change Biology 21, 722–737. doi:10.1111/gcb.12762

RStudio Team, 2022. RStudio: Integrated Development Environment for R. Version 2022.12.0.353 'Elsbeth Geranium.'

Rumpel, C., Kögel-Knabner, I., 2011. Deep soil organic matter-a key but poorly understood component of terrestrial C cycle. Plant and Soil 338, 143–158. doi:10.1007/s11104-010-0391-5

Sáez-Sandino, T., García-Palacios, P., Maestre, F.T., Plaza, C., Guirado, E., Singh, B.K., Wang, J., Cano-Díaz, C., Eisenhauer, N., Gallardo, A., Delgado-Baquerizo, M., 2023. The soil microbiome governs the response of microbial respiration to warming across the globe. Nature Climate Change 13, 1382–1387. doi:10.1038/s41558-023-01868-1

Said, M., John, G., Mhilu, C., Manyele, S., 2015. The Study of Kinetic Properties and Analytical Pyrolysis of Coconut Shells. Journal of Renewable Energy 2015, 1–8. doi:10.1155/2015/307329

Saiz-Jimenez, C., De Leeuw, J.W., 1986. Chemical characterization of soil organic matter fractions by analytical pyrolysis-gas chromatography-mass spectrometry. Journal of Analytical and Applied Pyrolysis 9, 99–119. doi:10.1016/0165-2370(86)85002-1

Sayedi, S.S., Abbott, B.W., Thornton, B.F., Frederick, J.M., Vonk, J.E., Overduin, P., Schädel, C., Schuur, E.A.G., Bourbonnais, A., Demidov, N., Gavrilov, A., He, S., Hugelius, G., Jakobsson, M., Jones, M.C., Joung, D.J., Kraev, G., Macdonald, R.W., David McGuire, A., Mu, C., O'Regan, M., Schreiner, K.M., Stranne, C., Pizhankova, E., Vasiliev, A., Westermann, S., Zarnetske, J.P., Zhang, T., Ghandehari, M., Baeumler, S., Brown, B.C., Frei, R.J., 2020. Subsea permafrost carbon stocks and climate change sensitivity estimated by expert assessment. Environmental Research Letters 15. doi:10.1088/1748-9326/abcc29

Schmidt, M.W.I., Knicker, H., Hatcher, P.G., Kögel-Knabner, I., 1997. Improvement of 13C and 15N CPMAS NMR spectra of bulk soils, particle size fractions and organic material by treatment with 10% hydrofluoric acid. European Journal of Soil Science 48, 319–328. doi:10.1111/j.1365-2389.1997.tb00552.x

Schnecker, J., Baldaszti, L., Gündler, P., Pleitner, M., Sandén, T., Simon, E., Spiegel, F., Spiegel, H., Urbina Malo, C., Zechmeister-Boltenstern, S., Richter, A., 2023. Seasonal dynamics of soil microbial growth, respiration, biomass, and carbon use efficiency in temperate soils. Geoderma 440. doi:10.1016/j.geoderma.2023.116693

Schnecker, J., Wild, B., Hofhansl, F., Alves, R.J.E., Bárta, J., Čapek, P., Fuchslueger, L., Gentsch, N., Gittel, A., Guggenberger, G., Hofer, A., Kienzl, S., Knoltsch, A., Lashchinskiy, N., Mikutta, R., Šantrůčková, H., Shibistova, O., Takriti, M., Urich, T., Weltin, G., Richter, A., 2014. Effects of soil organic matter properties and microbial community composition on enzyme activities in cryoturbated arctic soils. PLoS ONE 9. doi:10.1371/journal.pone.0094076

Schnecker, J., Wild, B., Takriti, M., Eloy Alves, R.J., Gentsch, N., Gittel, A., Hofer, A., Klaus, K., Knoltsch, A., Lashchinskiy, N., Mikutta, R., Richter, A., 2015. Microbial community composition shapes enzyme patterns in topsoil and subsoil horizons along a latitudinal transect in Western Siberia. Soil Biology and Biochemistry 83, 106–115. doi:10.1016/j.soilbio.2015.01.016

Schoeneberger, P.J., Wysocki, D.A., Benham, E.C., Soil Survey Staff, 2012. Field book for describing and sampling soils, Version 3.0, Natural Resources Conservation Service, National Soil Survey Center, U.S. Department of Agriculture. Lincoln, NE.

Schulten, H.R., Schnitzer, M., 1997. The chemistry of soil organic nitrogen: A review. Biology and Fertility of Soils 26, 1–15. doi:10.1007/s003740050335

Schuur, E.A.G., Abbott, B.W., Commane, R., Ernakovich, J., Euskirchen, E., Hugelius, G., Grosse, G., Jones, M., Koven, C., Leshyk, V., Lawrence, D., Loranty, M.M., Mauritz, M., Olefeldt, D., Natali, S., Rodenhizer, H., Salmon, V., Schädel, C., Strauss, J., Treat, C., Turetsky, M., 2022. Permafrost and Climate Change: Carbon Cycle Feedbacks From the Warming Arctic. Annual Review of Environment and Resources 47, 343–371. doi:10.1146/annurev-environ-012220-011847

Schuur, E.A.G., McGuire, A.D., Schädel, C., Grosse, G., Harden, J.W., Hayes, D.J., Hugelius, G., Koven, C.D., Kuhry, P., Lawrence, D.M., Natali, S.M., Olefeldt, D., Romanovsky, V.E., Schaefer, K., Turetsky, M.R., Treat, C.C., Vonk, J.E., 2015. Climate change and the permafrost carbon feedback. Nature 520, 171–179. doi:10.1038/nature14338

Schuur, T., McGuire, A.D., Romanovsky, V., Schädel, C., Mack, M., 2018. SOCCR2 Chapter 11: Arctic and Boreal Carbon. Second State of the Carbon Cycle Report. Second State of the Carbon Cycle Report (SOCCR2): A Sustained Assessment Report 428–468.

Shen, Q., Suarez-Abelenda, M., Camps-Arbestain, M., Calvelo Pereira, R., McNally, S.R., Kelliher, F., 2018. Data on the organic matter characteristics of New Zealand soils under different land uses. Data in Brief 21, 620–638. doi:10.1016/j.dib.2018.10.016

Siewert, M.B., Lantuit, H., Richter, A., Hugelius, G., 2021. Permafrost Causes Unique Fine-Scale Spatial Variability Across Tundra Soils. Global Biogeochemical Cycles 35, 1–19. doi:10.1029/2020GB006659

Silva-Sánchez, A., Soares, M., Rousk, J., 2019. Testing the dependence of microbial growth and carbon use efficiency on nitrogen availability, pH, and organic matter quality. Soil Biology and Biochemistry 134, 25–35. doi:10.1016/j.soilbio.2019.03.008

Simon, E., Canarini, A., Martin, V., Séneca, J., Böckle, T., Reinthaler, D., Pötsch, E.M., Piepho, H.P., Bahn, M., Wanek, W., Richter, A., 2020. Microbial growth and carbon use efficiency show seasonal responses in a multifactorial climate change experiment. Communications Biology 3. doi:10.1038/s42003-020-01317-1

Simpson, M.J., Simpson, A.J., 2012. The Chemical Ecology of Soil Organic Matter Molecular Constituents. Journal of Chemical Ecology 38, 768–784. doi:10.1007/s10886-012-0122-x

Sinsabaugh, R.L., Manzoni, S., Moorhead, D.L., Richter, A., 2013. Carbon use efficiency of microbial communities: Stoichiometry, methodology and modelling. Ecology Letters 16, 930–939. doi:10.1111/ele.12113

Smith, D.P., Peay, K.G., 2014. Sequence depth, not PCR replication, improves ecological inference from next generation DNA sequencing. PLoS ONE 9. doi:10.1371/journal.pone.0090234

Soil Survey Staff, 1999. USDA Soil Taxonomy. A Basic System of Soil Classification for Making and Interpreting Soil Surveys, Second Edi. ed, Agriculture Handbook. US Government Printing Office, Washington D.C. doi:10.1007/BF01574372

Sokol, N.W., Slessarev, E., Marschmann, G.L., Nicolas, A., Blazewicz, S.J., Brodie, E.L., Firestone, M.K., Foley, M.M., Hestrin, R., Hungate, B.A., Koch, B.J., Stone, B.W., Sullivan, M.B., Zablocki, O., Trubl, G., McFarlane, K., Stuart, R., Nuccio, E., Weber, P., Jiao, Y., Zavarin, M., Kimbrel, J., Morrison, K., Adhikari, D., Bhattacharaya, A., Nico, P., Tang, J., Didonato, N., Paša-Tolić, L., Greenlon, A., Sieradzki, E.T., Dijkstra, P., Schwartz, E., Sachdeva, R., Banfield, J., Pett-Ridge, J., 2022. Life and death in the soil microbiome: how ecological processes influence biogeochemistry. Nature Reviews Microbiology 20, 415–430. doi:10.1038/s41579-022-00695-z

Söllinger, A., Séneca, J., Dahl, M.B., Motleleng, L.L., Prommer, J., Verbruggen, E., Sigurdsson, B.D., Janssens, I., Peñuelas, J., Urich, T., Richter, A., Tveit, A.T., 2022. Down-regulation of the bacterial protein biosynthesis machinery in response to weeks, years, and decades of soil warming. Science Advances 8. doi:10.1126/sciadv.abm3230

Song, C., Wang, X., Miao, Y., Wang, J., Mao, R., Song, Y., 2014. Effects of permafrost thaw on carbon emissions under aerobic and anaerobic environments in the Great Hing'an Mountains, China. Science of the Total Environment 487, 604–610. doi:10.1016/j.scitotenv.2013.09.083

Soong, J.L., Castanha, C., Hicks Pries, C.E., Ofiti, N., Porras, R.C., Riley, W.J., Schmidt, M.W.I., Torn, M.S., 2021. Five years of whole-soil warming led to loss of subsoil carbon stocks and increased CO2 efflux. Science Advances 7, 1–8. doi:10.1126/sciadv.abd1343

Soong, J.L., Fuchslueger, L., Marañon-Jimenez, S., Torn, M.S., Janssens, I.A., Penuelas, J., Richter, A., 2020. Microbial carbon limitation: The need for integrating microorganisms into our understanding of ecosystem carbon cycling. Global Change Biology 26, 1953–1961. doi:10.1111/gcb.14962

Spohn, M., Klaus, K., Wanek, W., Richter, A., 2016. Microbial carbon use efficiency and biomass turnover times depending on soil depth - Implications for carbon cycling. Soil Biology and Biochemistry 96, 74–81. doi:10.1016/j.soilbio.2016.01.016

Steffen, W., Rockström, J., Richardson, K., Lenton, T.M., Folke, C., Liverman, D., Summerhayes, C.P., Barnosky, A.D., Cornell, S.E., Crucifix, M., Donges, J.F., Fetzer, I., Lade, S.J., Scheffer, M., Winkelmann, R., Schellnhuber, H.J., 2018. Trajectories of the Earth System in the Anthropocene. Proceedings of the National Academy of Sciences of the United States of America 115, 8252–8259. doi:10.1073/pnas.1810141115

Stewart, C.E., 2012. Evaluation of angiosperm and fern contributions to soil organic matter using two methods of pyrolysis-gas chromatography-mass spectrometry. Plant and Soil 351, 31–46. doi:10.1007/s11104-011-0927-3

Strauss, J., Schirrmeister, L., Grosse, G., Fortier, D., Hugelius, G., Knoblauch, C., Romanovsky, V., Schädel, C., Schneider von Deimling, T., Schuur, E.A.G., Shmelev, D., Ulrich, M., Veremeeva, A., 2017. Deep Yedoma permafrost: A synthesis of depositional characteristics and carbon vulnerability. Earth-Science Reviews 172, 75–86. doi:10.1016/j.earscirev.2017.07.007

Stuble, K.L., Ma, S., Liang, J., Luo, Y., Classen, A.T., Souza, L., 2019. Long-term impacts of warming drive decomposition and accelerate the turnover of labile, not recalcitrant, carbon. Ecosphere 10. doi:10.1002/ecs2.2715

Tao, F., Huang, Y., Hungate, B.A., Manzoni, S., Frey, S.D., Schmidt, M.W.I., Reichstein, M., Carvalhais, N., Ciais, P., Jiang, L., Lehmann, J., Wang, Y.P., Houlton, B.Z., Ahrens, B., Mishra, U., Hugelius, G., Hocking, T.D., Lu, X., Shi, Z., Viatkin, K., Vargas, R., Yigini, Y., Omuto, C., Malik, A.A., Peralta, G., Cuevas-Corona, R., Di Paolo, L.E., Luotto, I., Liao, C., Liang, Y.S., Saynes, V.S., Huang, X., Luo, Y., 2023. Microbial carbon use efficiency promotes global soil carbon storage. Nature 618, 981–985. doi:10.1038/s41586-023-06042-3

Taş, N., Prestat, E., Wang, S., Wu, Y., Ulrich, C., Kneafsey, T., Tringe, S.G., Torn, M.S., Hubbard, S.S., Jansson, J.K., 2018. Landscape topography structures the soil microbiome in arctic polygonal tundra. Nature Communications 9, 777. doi:10.1038/s41467-018-03089-z

Taylor, D.L., Hollingsworth, T.N., McFarland, J.W., Lennon, N.J., Nusbaum, C., Ruess, R.W., 2014. A first comprehensive census of fungi in soil reveals both hyperdiversity and fine-scale niche partitioning. Ecological Monographs 84, 3–20. doi:10.1890/12-1693.1

Tedersoo, L., Bahram, M., Põlme, S., Kõljalg, U., Yorou, N.S., Wijesundera, R., Ruiz, L.V., Vasco-Palacios, A.M., Thu, P.Q., Suija, A., Smith, M.E., Sharp, C., Saluveer, E., Saitta, A., Rosas, M., Riit, T., Ratkowsky, D., Pritsch, K., Põldmaa, K., Piepenbring, M., Phosri, C., Peterson, M., Parts, K., Pärtel, K., Otsing, E., Nouhra, E., Njouonkou, A.L., Nilsson, R.H., Morgado, L.N., Mayor, J., May, T.W., Majuakim, L., Lodge, D.J., Lee, S.S., Larsson, K.-H., Kohout, P., Hosaka, K., Hiiesalu, I., Henkel, T.W., Harend, H., Guo, L., Greslebin, A., Grelet, G., Geml, J., Gates, G., Dunstan, W., Dunk, C., Drenkhan, R., Dearnaley, J., De Kesel, A., Dang, T., Chen, X., Buegger, F., Brearley, F.Q., Bonito, G., Anslan, S., Abell, S., Abarenkov, K., 2014. Global diversity and geography of soil fungi. Science 346, 1052–1053. doi:10.1126/science.1256688

Thai, S., Pavlů, L., Tejnecký, V., Vokurková, P., Nozari, S., Borůvka, L., 2021. Comparison of soil organic matter composition under different land uses by DRIFT spectroscopy. Plant, Soil and Environment 67, 255–263. doi:10.17221/11/2021-PSE

Tian, Y., Schindlbacher, A., Malo, C.U., Shi, C., Heinzle, J., Kwatcho Kengdo, S., Inselsbacher, E., Borken, W., Wanek, W., 2023a. Long-term warming of a forest soil reduces microbial biomass and its carbon and nitrogen use efficiencies. Soil Biology and Biochemistry 184, 109109. doi:10.1016/j.soilbio.2023.109109

Tian, Y., Shi, C., Malo, C.U., Kwatcho Kengdo, S., Heinzle, J., Inselsbacher, E., Ottner, F., Borken, W., Michel, K., Schindlbacher, A., Wanek, W., 2023b. Long-term soil warming decreases microbial phosphorus utilization by increasing abiotic phosphorus sorption and phosphorus losses. Nature Communications 14. doi:10.1038/s41467-023-36527-8

Tolu, J., Gerber, L., Boily, J.F., Bindler, R., 2015. High-throughput characterization of sediment organic matter by pyrolysis-gas chromatography/mass spectrometry and multivariate curve resolution: A promising analytical tool in (paleo)limnology. Analytica Chimica Acta 880, 93–102. doi:10.1016/j.aca.2015.03.043

Tornocai, C., Canadell, J.G., Schuur, E.A.G., Kuhry, P., Mazhitova, G., Zimov, S., 2009. Soil organic carbon pools in the northern circumpolar permafrost region. Global Biogeochemical Cycles 23, 1–11. doi:10.1029/2008GB003327

Treat, C.C., Natali, S.M., Ernakovich, J., Iversen, C.M., Lupascu, M., Mcguire, A.D., Norby, R.J., Roy Chowdhury, T., Richter, A., Šantrůčková, H., Schädel, C., Schuur, E.A.G., Sloan, V.L., Turetsky, M.R., Waldrop, M.P., 2015. A pan-Arctic synthesis of CH4 and CO2 production from anoxic soil incubations. Global Change Biology 21, 2787–2803. doi:10.1111/gcb.12875

van't Hoff, J.H., 1884. Etudes de dynamique chimique. Frederik Muller & Co, Amsterdam.

van den Enden, L., Anthony, M.A., Frey, S.D., Simpson, M.J., 2021. Biogeochemical evolution of soil organic matter composition after a decade of warming and nitrogen addition. Biogeochemistry 156, 161–175. doi:10.1007/s10533-021-00837-0

Vancampenhout, K., Wouters, K., De Vos, B., Buurman, P., Swennen, R., Deckers, J., 2009. Differences in chemical composition of soil organic matter in natural ecosystems from different climatic regions - A pyrolysis-GC/MS study. Soil Biology and Biochemistry 41, 568–579. doi:10.1016/j.soilbio.2008.12.023

Vance, E.D., Brookes, P.C., Jenkinson, D.S., 1987. An extraction method for measuring soil microbial biomass C. Soil Biology and Biochemistry 19, 703–707. doi:10.1016/0038-0717(87)90052-6

Varsadiya, M., Urich, T., Hugelius, G., Bárta, J., 2021. Microbiome structure and functional potential in permafrost soils of the Western Canadian Arctic. FEMS Microbiology Ecology 97, 1–14. doi:10.1093/femsec/fiab008

Védère, C., Lebrun, M., Honvault, N., Aubertin, M.L., Girardin, C., Garnier, P., Dignac, M.F., Houben, D., Rumpel, C., 2022. How does soil water status influence the fate of soil organic matter? A review of processes across scales. Earth-Science Reviews 234. doi:10.1016/j.earscirev.2022.104214

Walker, D.A., Reynolds, M.K., Daniëls, F.J.A., Einarsson, E., Elvebakk, A., Gould, W.A., Katenin, A.E., Kholod, S.S., Markon, C.J., Melnikov, Evgeny S., Moskalenko, Natalia G., Talbot, S.S., Yurtsev, B.A., Bliss, L.C., Edlund, S.A., Zoltai, S.C., Wilhelm, M., Bay, C., Gudjónsson, G., Moskalenko, N. G., Ananjeva, G. V., Drozdov, D.S., Konchenko, L.A., Korostelev, Y. V., Melnikov, E. S., Ponomareva, O.E., Matveyeva, N. V., Safranova, I.N., Shelkunova, R., Polezhaev, A.N., Johansen, B.E., Maier, H.A., Murray, D.F., Fleming, M.D., Trahan, N.G., Charron, T.M., Lauritzen, S.M., Vairin, B.A., 2005. The Circumpolar Arctic vegetation map. Journal of Vegetation Science 16, 267–282. doi:10.1111/j.1654-1103.2005.tb02365.x

Walker, T.W.N., Kaiser, C., Strasser, F., Herbold, C.W., Leblans, N.I.W., Woebken, D., Janssens, I.A., Sigurdsson, B.D., Richter, A., 2018. Microbial temperature sensitivity and biomass change explain soil carbon loss with warming. Nature Climate Change 8, 885–889. doi:10.1038/s41558-018-0259-x

Walkup, J., Dang, C., Mau, R.L., Hayer, M., Schwartz, E., Stone, B.W., Hofmockel, K.S., Koch, B.J., Purcell, A.M., Pett-ridge, J., Wang, C., Hungate, B.A., Morrisseay, E.M., 2023. The predictive power of phylogeny on growth rates in soil bacterial communities. ISME Communications 3. doi:10.1038/s43705-023-00281-1

Wallenstein, M.D., Weintraub, M.N., 2008. Emerging tools for measuring and modeling the in situ activity of soil extracellular enzymes. Soil Biology and Biochemistry 40, 2098–2106. doi:10.1016/j.soilbio.2008.01.024

Wang, C., Morrissey, E.M., Mau, R.L., Hayer, M., Piñeiro, J., Mack, M.C., Marks, J.C., Bell, S.L., Miller, S.N., Schwartz, E., Dijkstra, P., Koch, B.J., Stone, B.W., Purcell, A.M., Blazewicz, S.J., Hofmockel, K.S., Pett-Ridge, J., Hungate, B.A., 2021. The temperature sensitivity of soil: microbial biodiversity, growth, and carbon mineralization. ISME Journal 15, 2738–2747. doi:10.1038/s41396-021-00959-1

Weedon, J.T., Bååth, E., Rijkers, R., Reischke, S., Sigurdsson, B.D., Oddsdottir, E., van Hal, J., Aerts, R., Janssens, I.A., van Bodegom, P.M., 2023. Community adaptation to temperature explains abrupt soil bacterial community shift along a geothermal gradient on Iceland. Soil Biology and Biochemistry 177, 108914. doi:10.1016/j.soilbio.2022.108914

Weiland-Bräuer, N., 2021. Friends or Foes - Microbial Interactions in Nature. Biology 10. doi:10.3390/biology10060496

Weissman, J.L., Hou, S., Fuhrman, J.A., 2021. Estimating maximal microbial growth rates from cultures, metagenomes, and single cells via codon usage patterns. Proceedings of the National Academy of Sciences of the United States of America 118, 1–10. doi:10.1073/pnas.2016810118

Werner, W.J., Sanderman, J., Melillo, J.M., 2020. Decreased Soil Organic Matter in a Long-Term Soil Warming Experiment Lowers Soil Water Holding Capacity and Affects Soil Thermal and Hydrological Buffering. Journal of Geophysical Research: Biogeosciences 125, 1–14. doi:10.1029/2019JG005158

White, T.J., Bruns, T.D., Lee, S.B., Taylor, J.W., 1990. Amplification and direct sequencing of fungal ribosomal RNA Genes for phylogenetics, in: Innis, M.A., Gelfand, D.H., Sninsky, J.J., White, T.J. (Eds.), PCR Protocols: A Guide to Methods and Applications. Academic Press, New York, pp. 315–322. doi:10.1016/B978-0-12-372180-8.50042-1

Wickham, H., 2016. ggplot2: Elegant Graphics for Data Analysis. Springer-Verlag, New York.

Wickham, H., Averick, M., Bryan, J., Chang, W., McGowan, L.D., François, R., Grolemund, G., Hayes, A., Henry, L., Hester, J., Kuhn, M., Pedersen, T.L., Miller, E., Bache, S.M., Müller, K., Ooms, J., Robinson, D., Seidel, D.P., Spinu, V., Takahashi, K., Vaughan, D., Wilke, C., Woo, K., Yutani, H., 2019. Welcome to the tidyverse. Journal of Open Source Software 43, 1686. doi:10.21105/joss.01686

Wickham, H., François, R., Henry, L., Müller, K., 2022. dplyr: A Grammar of Data Manipulation. R Package, Version 1.0.10.

Wild, B., Gentsch, N., Capek, P., Diáková, K., Alves, R.J.E., Bárta, J., Gittel, A., Hugelius, G., Knoltsch, A., Kuhry, P., Lashchinskiy, N., Mikutta, R., Palmtag, J., Schleper, C., Schnecker, J., Shibistova, O., Takriti, M., Torsvik, V.L., Urich, T., Watzka, M., Šantrūcková, H., Guggenberger, G., Richter, A., 2016. Plant-derived compounds stimulate the decomposition of organic matter in arctic permafrost soils. Scientific Reports 6, 1–11. doi:10.1038/srep25607

Wild, B., Schnecker, J., Bárta, J., Čapek, P., Guggenberger, G., Hofhansl, F., Kaiser, C., Lashchinsky, N., Mikutta, R., Mooshammer, M., Šantrůčková, H., Shibistova, O., Urich, T., Zimov, S.A., Richter, A., 2013. Nitrogen dynamics in Turbic Cryosols from Siberia and Greenland. Soil Biology and Biochemistry 67, 85–93. doi:10.1016/j.soilbio.2013.08.004

Wolter, J., Lantuit, H., Fritz, M., Macias-Fauria, M., Myers-Smith, I., Herzschuh, U., 2016. Vegetation composition and shrub extent on the Yukon coast, Canada, are strongly linked to ice-wedge polygon degradation. Polar Research 35, 1–13. doi:10.3402/polar.v35.27489

Wolter, J., Lantuit, H., Wetterich, S., Rethemeyer, J., Fritz, M., 2018. Climatic, geomorphologic and hydrologic perturbations as drivers for mid- to late Holocene development of ice-wedge polygons in the western Canadian Arctic. Permafrost and Periglacial Processes 29, 164–181. doi:10.1002/PPP.1977

Xia, Q., Rufty, T., Shi, W., 2020. Soil microbial diversity and composition: Links to soil texture and associated properties. Soil Biology and Biochemistry 149, 107953. doi:10.1016/j.soilbio.2020.107953

Yang, Z., Yang, S., Van Nostrand, J.D., Zhou, J., Fang, W., Qi, Q., Liu, Y., Wullschleger, S.D., Liang, L., Graham, D.E., Yang, Y., Gu, B., 2017. Microbial community and functional gene changes in Arctic tundra soils in a microcosm warming experiment. Frontiers in Microbiology 8, 1–11. doi:10.3389/fmicb.2017.01741

Zechmeister-Boltenstern, S., Keiblinger, K.M., Mooshammer, M., Peñuelas, J., Richter, A., Sardans, J., Wanek, W., 2015. The application of ecological stoichiometry to plant-microbial-soil organic matter transformations. Ecological Monographs 85, 133–155. doi:10.1890/14-0777.1

Zona, D., Lafleur, P.M., Hufkens, K., Bailey, B., Gioli, B., Burba, G., Goodrich, J.P., Liljedahl, A.K., Euskirchen, E.S., Watts, J.D., Farina, M., Kimball, J.S., Heimann, M., Göckede, M., Pallandt, M., Christensen, T.R., Mastepanov, M., López-Blanco, E., Jackowicz-Korczynski, M., Dolman, A.J., Marchesini, L.B., Commane, R., Wofsy, S.C., Miller, C.E., Lipson, D.A., Hashemi, J., Arndt, K.A., Kutzbach, L., Holl, D., Boike, J., Wille, C., Sachs, T., Kalhori, A., Song, X., Xu, X., Humphreys, E.R., Koven, C.D., Sonnentag, O., Meyer, G., Gosselin, G.H., Marsh, P., Oechel, W.C., 2022. Earlier snowmelt may lead to late season declines in plant productivity and carbon sequestration in Arctic tundra ecosystems. Scientific Reports 12, 1–10. doi:10.1038/s41598-022-07561-1